PEPTIDE-ANTIBIOTIC CONJUGATES AS NOVEL DEVELOPMENTS FOR INCREASED ANTIMICROBIAL TRANSPORT AND EFFICIENCY

Belina Sithole

MSc by Research

University of York

Chemistry

December 2015

Abstract

The emergence of bacterial strains with resistance to most known antibiotics has raised an urgent need for the development of new antimicrobial agents in order to avoid a serious threat to public health and return to the pre-antibiotic era. The 'Trojan Horse' strategy is one of the approaches that has been explored to evade membrane – based resistance mechanisms by smuggling the antibiotic in through the bacterial cell membrane(s).

The 'Trojan Horse' strategy involves conjugating a siderophore, sugar or an amino acid moiety to an antimicrobial agent to allow more effective antimicrobial transport. They can be conjugated through a non-biolabile or a biolabile linker; both types of the 'Trojan Horse' conjugates were prepared based on the antibiotic ciprofloxacin and alanine (Ala) and di-alanine (Ala-Ala). The conjugates were screened against wild type *E. coli* to compare the minimum inhibitory concentrations (MIC)/minimum bacterial concentrations with those of the free parent drug ciprofloxacin.

The conjugate coupled through a non-biolabile linker, Ala-Ala-ciprofloxacin, was found to have a very significant reduced antimicrobial activity compared to the parent drug with no evidence of active transport by peptide transporters. A DNA gyrase assay revealed that the conjugate was no longer an effective DNA gyrase-inhibitor.

The conjugates coupled through the biolabile disulfide linker, ciprofloxacin-disulfide-Ala and ciprofloxacin-disulfide-Ala-Ala, were found to have retained some antimicrobial activity although lower than that of the parent drug. The conjugates reached a peak OD_{650} of 3.0 at 0.1 µM whereas ciprofloxacin reached a peak OD_{650} of 1.0 at the same concentration. No evidence of transport by peptide transporters was observed. The retained antimicrobial activity suggested that intracellular cleavage of the disulfide linker occurred releasing free ciprofloxacin however the reduced antimicrobial activity could be due to inefficient cleavage of the disulfide bond or inefficient intracellular release of ciprofloxacin due to slow formation of the thiirane ring allowing re-formation of a disulfide bond.

Table of contents

List of Figures

List of Schemes

List of Tables

Acknowledgements

Firstly I wish to thank my supervisor Dr Anne Routledge for supervising me throughout the year and the continued support during my write up period. I would also like to thank Dr Gavin Thomas for his helpful suggestions and ideas during the screening of my compounds.

I would also like to thank Professor Anne Duhme-Klair for her support during my supervisor's absence, Ms. Heather Fish for her assistance with NMR experiments and Dr Karl Heaton for mass spectrometry experiments. I wish to thank my colleagues in the lab in particular Thomas Sanderson for all his help from the start to the end of the year, Sophie Rugg for her guidance with the biological procedures, Daniel Raines, Ellis Wilde and Aurelien Ducrot.

Last but not least, special thanks to my mother (Sipiwe Sithole), my aunt (Joyce Sithole) for funding this research and my family for believing in me and their continued support throughout the year. Thank you!

Declaration

I declare that this work is original except where specifically acknowledged with references made to authors. Mass spectrometric analysis was performed by Dr Karl Heaton. This work has not been submitted for any other academic award at, or any other institution.

Chapter 1. Introduction

1.1. Antibiotics

The first antibiotics were discovered in the early 20th century and these included sulphonamides **1** (1930s), penicillin **2** (1940s), and towards the latter half of the 20th century quinolones **3** (1960s) were discovered.[1] During the early period of antibiotic usage, antibiotics were being used to treat potentially lethal bacterial infections and as a result these infections were no-longer life-threating.[2]

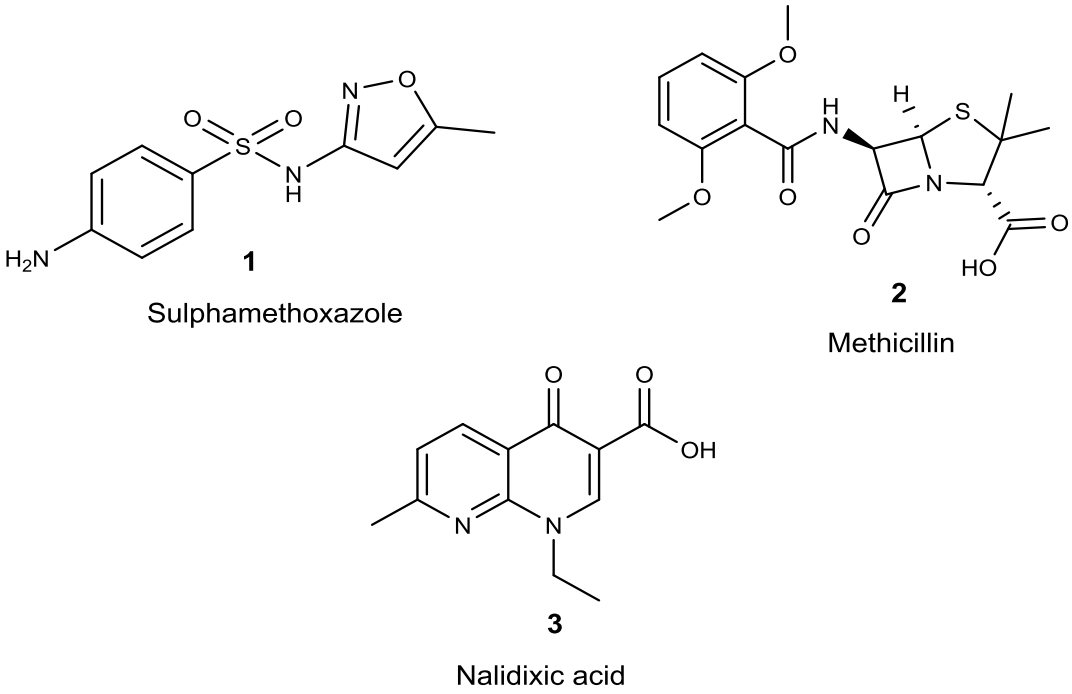

Figure 1: Members of classes of antibiotics; sulphonamides, penicillin and quinolones

Until the latter part of the 20th century, infections derived from most bacterial strains could be treated.[1] However, the widespread use/misuse of antibiotics has promoted the emergence of more antibiotic-resistant organisms including multi-drug resistant (MDR) strains.[2]

1.1.1. Antibacterial resistance

Bacterial organisms can share resistance genes if they come in close contact, resistance genes are either carried on the chromosomes of Wild-type (WT) bacteria or on elements of extrachromosomal DNA such as resistance (R) plasmids.[2]

There are various mechanisms through which antimicrobial resistant organisms express resistance; alteration/modification of the intracellular target site, chemical/enzymatic degradation/inactivation of the antibiotic molecule, decreased permeability of the bacterial outer membrane and active antibiotic efflux[2] (**Figure 2**).

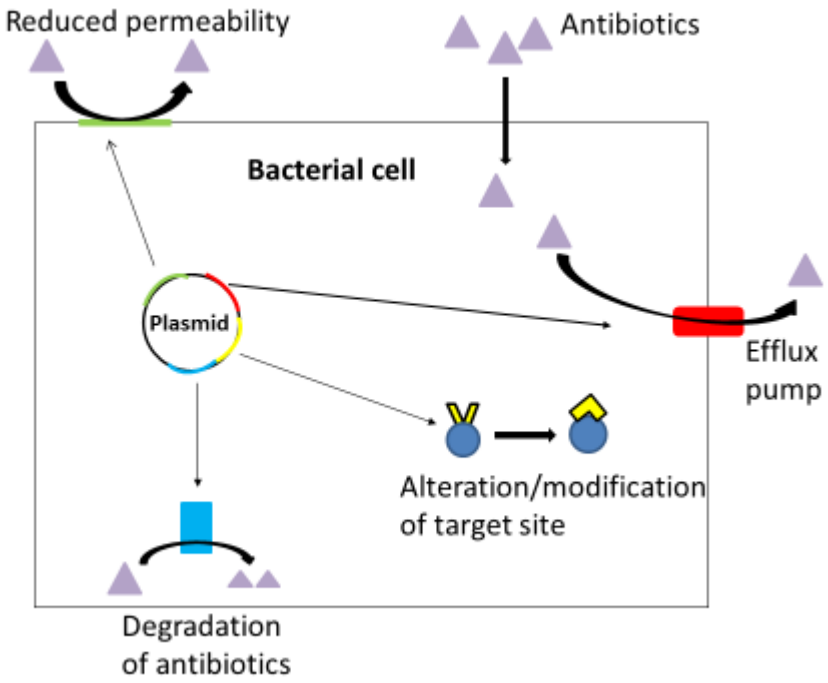

Figure 2: Schematic diagram of a plasmid containing antibacterial resistant genes illustrating the resistant mechanisms drawn based on Levy and Marshall[3]

1.1.2. Alteration/modification of the intracellular target site

A variety of intracellular processes play an essential role in the growth and survival of bacterial organisms. Therefore, inhibition of these processes either leads to cell death or cell growth inhibition.[4] In order to evade antimicrobial action, bacterial organisms develop mutational changes in the target site which reduces susceptibility whilst retaining cellular function.[4] This type of mutation occurs, for example, in RNA polymerase resulting in resistance to rifamycins **4** and in DNA gyrase leading to resistance to quinolones **3** respectively.[4]

Mutations in RNA polymerase and DNA gyrase reduces antimicrobial action whilst retaining cellular function. However, mutations of Mec A in *S. aureus,* which imparts resistance to methicillin **2** and most β-lactam antibiotics, requires other changes in the cell to compensate for the mutations in order to retain cellular function.[4]

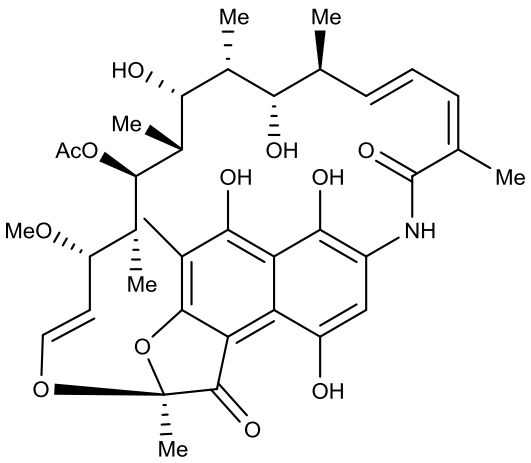

4

Figure 3: Structure of a rifamycin

1.1.3. Antibiotic inactivation/degradation

The chemical modification of antibiotics catalysed by enzymes results in covalent modification of the antibiotic preventing strong interaction with the intracellular target.[5] An example of antibiotic chemical modification is the degradation of β-lactam antibiotics. The activity of β-lactam antibiotics is based on the strained electrophilic lactam ring which binds to penicillin binding proteins (PBPs) blocking the active site therefore impairing cell growth and division.[5] β-lactam antibiotics are inactivated by the enzyme β-lactamase which hydrolyses the β-lactam ring to yield a ring opened structure[5] as shown in **Figure 4**.

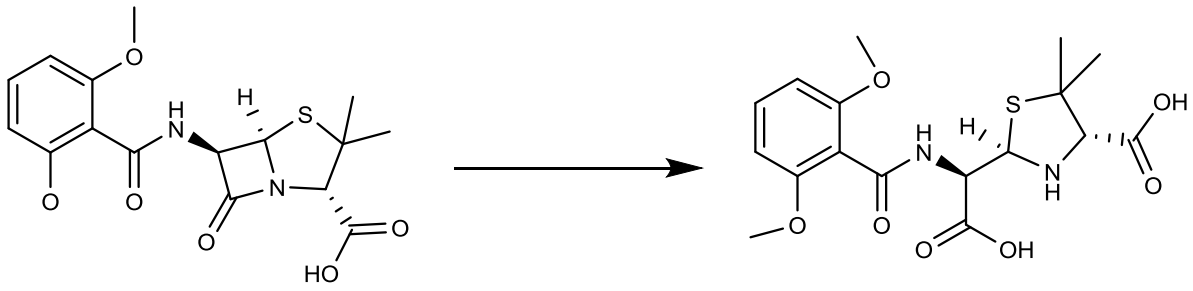

Figure 4: The hydrolysis of a β-lactam antibiotic (methicillin) by β-lactamase

1.1.4. Efflux pumps

Both Gram-positive and Gram-negative bacteria have efflux pumps to remove toxic compounds from the cell. However Gram-negative bacteria have the more complex efflux system due to the two cell-envelope membrane and their most important efflux systems are the resistance, nodulation and division (RND) systems.[6] According to studies carried out by Hancock *et al.* efflux systems are co-determinant resistance mechanisms, however, overexpression of certain pumps can result in resistance to a variety of antibiotics.[6]

1.1.5. Reduced Permeability

The outer membrane of Gram-negative bacteria consists of porin proteins, a transport channel through which hydrophilic compounds such as fluoroquinolones and β-lactams enter the periplasm.[6] Bacteria exhibit resistance to these compounds by down regulation of porins and/or mutation of a porin gene.[6] Mutations of the porin gene could lead to the porin's single-channel conductance being lowered and lack of voltage sensitivity as observed for the porin from the resistant strain of *Enterobacter aerogenes.*[7]

The outer membrane of Gram-negative bacteria also consists of a bilayer which has lipopolysaccharides (LPS) on the outer leaflet of the membrane.[6] LPS are highly anionic due to the phosphate groups within their structure. This anionic nature promotes the cross-bridging of the core region of the LPS with divalent cations such as Mg^{2+} and Ca^{2+} cations.[6] The cross-bridging stabilises the polyanionic external surface of the outer membrane and according to Hancock *et al*. this surface stabilisation is thought to inhibit the partitioning of hydrophobic antibiotics into the hydrophobic bilayer leading to the slow uptake of hydrophobic antibiotics.[6]

1.1.6. Overcoming bacterial resistance

In order to overcome bacterial resistance, new antibiotics need to be developed; antibiotics that either block or circumvent resistance mechanisms or that attack new targets.[3] Currently there has been a lack of development of new antibiotics as genomics has not delivered the anticipated novel therapeutics and also pharmaceutical industry has reduced its research efforts in infections.[1] The pharmaceutical industry has reduced antibiotic research and development due to a number of reasons including poor return

on investment, increasing cost of drug development and the increasing demand for more safety data.[1]

1.1.6.1 Combination therapy

Various strategies have been developed to overcome bacterial resistance including combination therapy and the chemical modification of antibiotics to target resistance mechanisms. Oxazolidinone-quinolone hybrids **5** are an example of combination therapy with potent antibacterial activity higher than that of the free parent drugs, the hybrids simultaneously act on two different cellular functions; with the oxazolidinone acting on protein synthesis and the quinolone on DNA replication.[8]

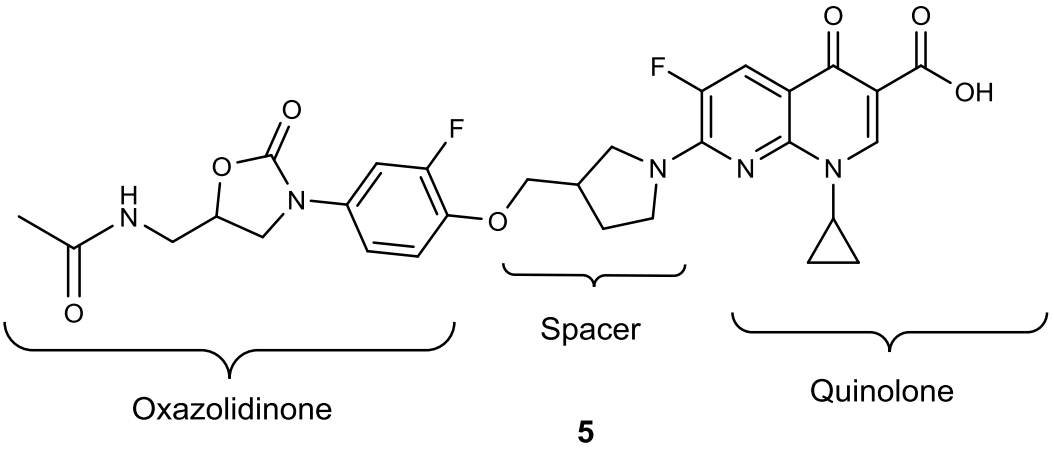

5

Figure 5: Structure of an oxazolidinone-quinolone hybrid

1.1.6.2 Overcoming membrane-based resistance

Chemical modification of existing antibiotics by conjugating the antibiotic to a biologically essential nutrient such as iron has been observed to bypass membrane-based resistance mechanisms, this is known as the 'Trojan Horse' strategy.[9] Permeabilizing agents like antimicrobial polycationic compounds have been investigated, polycationic antimicrobials interact with LPS on the surface of the outer membrane through electrostatic bonding as the LPS are highly anionic.[6]

Hancock *et al*. states that polycationic antimicrobials have higher affinity for the LPS than divalent cations, therefore the polycationic antimicrobials competitively displace divalent cations on the surface of LPS leading to distortion of the outer membrane structure and the membrane becomes permeable to various antibiotics as well as the polycationic antimicrobials.[6]

1.2. Introduction to fluoroquinolones

The first quinolone antibiotics were discovered in 1962 by George Lesher and co-workers as by-products in chloroquine synthesis.[10] Chloroquine **6** is a drug used in the treatment or prevention of malaria. The by-product **7** showed anti Gram-negative activity but its potency and antimicrobial spectrum was not significant enough to be used as a therapy.[11] Nalidixic acid **3** was found to have excellent activity against Gram-negative bacteria such as *E. coli* and *A. aerobacte*r and it was used for the treatment of urinary tract infections, however it was generally inactive against Gram-positive bacteria such as *S. aureus.*[10]

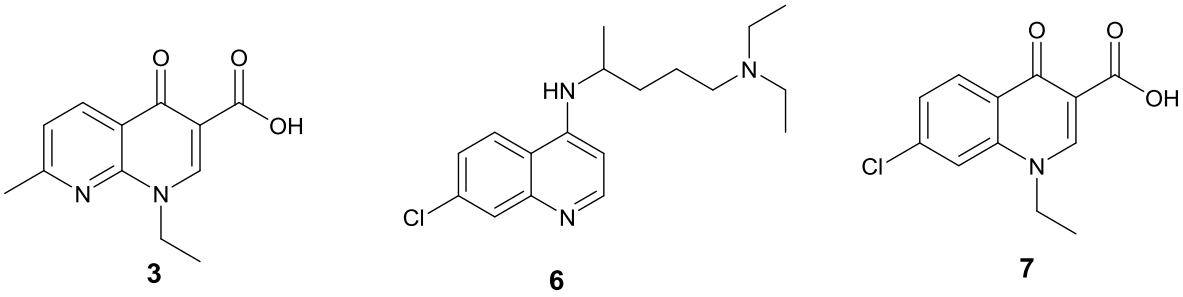

Figure 6: Structures of nalidixic acid **3**, chloroquine **6** and chloroquine by-product **7**

Other first generation quinolones such as oxolinic acid and cinoxacin (**Figure 7**) were introduced but their limited activity against Gram-negative bacteria and poor systemic distribution led to the introduction of fluoroquinolones.[12] The fluoroquinolones, ciprofloxacin and norfloxacin (**Figure 7**), were developed in the 1980s and they have an extended spectrum of activity and improved pharmacokinetics with increased activity against *Enterobacteriaceae* and many Gram-positive organisms.[13]

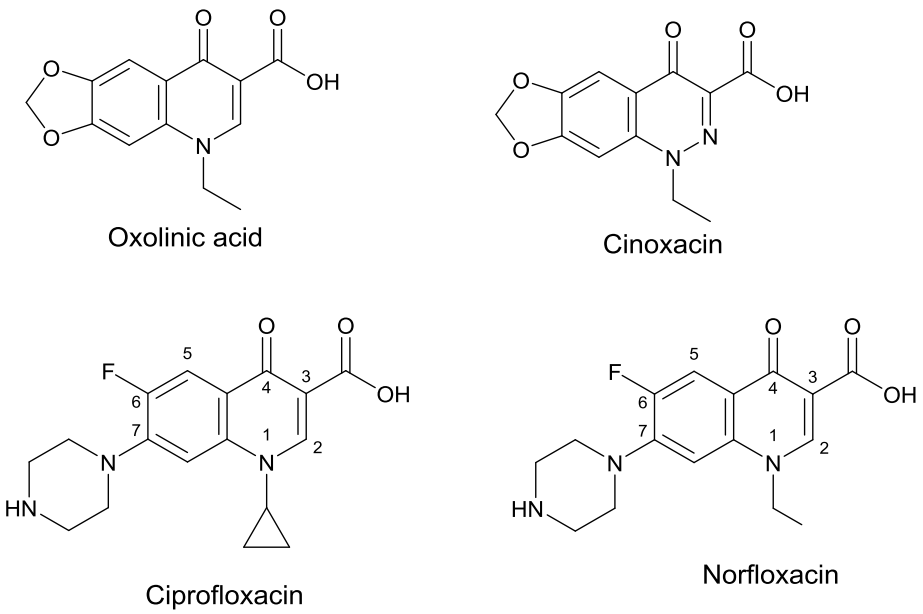

Figure 7: First and second generation quinolone antibiotics

This significant improvement was due to critical changes of the quinolone skeleton with the introduction of a fluorine at position C6 and a piperazine at position C7 [13] hence the name "fluoroquinolones". The piperazine is believed to enhance potency and favourable pharmacokinetics whilst the fluorine at C6 broadens the spectrum of activity.[11]

Ciprofloxacin was the first fluoroquinolone to show significant activity outside of the urinary tract and it is the most widely used antibacterial drug against Gram-negative bacteria strains.[14] Ciprofloxacin is chemically related to norfloxacin, – with modification of the ethyl group on N1 position to a cyclopropane. This modification improved both oral absorption and systemic distribution of the fluoroquinolone, therefore, allowing the use of ciprofloxacin for a variety of tissue infections including the lower respiratory tract in addition to urinary tract infections.[15]

Although the second generation fluoroquinolones have a broad spectrum of activity they have moderate activity against many but not all Gram-positive strains. Therefore, fluoroquinolone research has been aimed at developing fluoroquinolones with improved activity against Gram-positive strains whilst maintaining the activity against Gram-negative organisms.

1.2.1. Development of fluoroquinolones

A third generation fluoroquinolones was developed (**Figure 8**). These fluoroquinolones; moxifloxacin, levofloxacin and trovafloxacin have enhanced activity against Gram-positive organisms whilst retaining excellent activity against Gram-negative organism.[13] Trovafloxacin was found to be more active than ciprofloxacin, showing activity against the Gram-positive penicillin-resistant *S. pneumoniae* and anaerobe infections whilst retaining activity against Gram-negative strains.[15] However trovafloxacin has been withdrawn due to serious hepatotoxicity.[16]

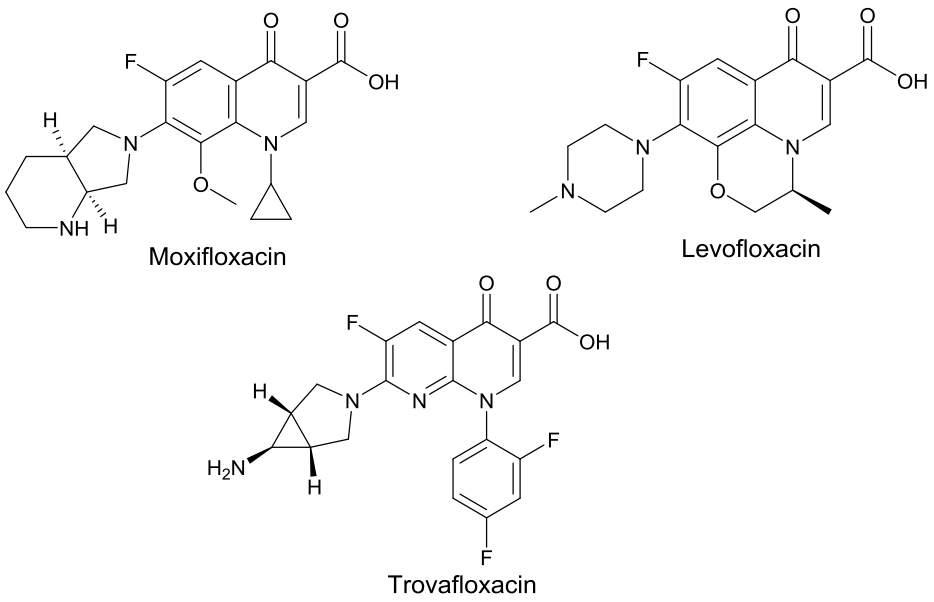

Figure 8: Structures of the third generation of fluoroquinolones

Modifications to the basic chemical structure of the quinolone has produced compounds with an extended spectrum of activity and improved pharmacokinetics therefore there is hope for 'newer' generations of fluoroquinolones. It is important to retain certain groups in the fluoroquinolone core structure when designing new compounds as some of the functional groups are essential for antimicrobial activity.

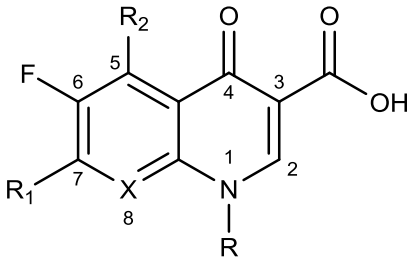

Figure 9: Fluoroquinolone pharmacophore showing sites that can be modified (R, R_1 and R_2)

Positions N1, C2, C3, C4 and C6 (**Figure 9**) are indispensable for activity of the fluoroquinolone therefore modifications at these sites are not favourable.[11] Substitutions at C5 are tolerated if the substituents are small (methyl) and preferably polar (amine) groups.[11] C7 is the most adaptable position, usually cyclic systems containing a secondary or tertiary amino moiety are introduced.[11] Successful C8 substituents have been found to be nitrogen. C8 halogens have been found to enhance the likelihood of phototoxicity.[11] Substituents on the N1 nitrogen have been mainly cyclopropyl and aryl groups.

Recently a new fluoroquinolone, ABT-492, (Delafloxacin) was synthesised.[17]The drug is still under investigation and has been designated as a Qualified Infectious Disease Product (QIDP) by the U.S Food and Administration (FDA).

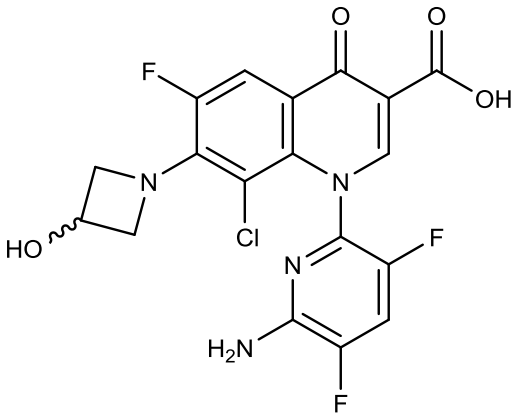

Delafloxacin

Figure 10: Structure of delafloxacin

The intracellular target for all quinolone antibiotics is DNA gyrase or topoisomerase IV; DNA gyrase is the primary target of quinolones in Gram-negative bacteria whereas topoisomerase IV is mainly targeted in Gram-positive bacteria.

1.2.2. Mode of action of DNA gyrase

Bacteria express two related type II topoisomerases which are essential for bacterial growth; DNA gyrase and topoisomerase IV. DNA gyrase is an A_2B_2 tetrameric complex that catalyses the negative supercoiling of circular chromosomal DNA using free energy derived from ATP hydrolysis[18,19] (**Figure 11**) and topoisomerase IV which mediates topological unlinking of catenated daughter chromosomes.[19]

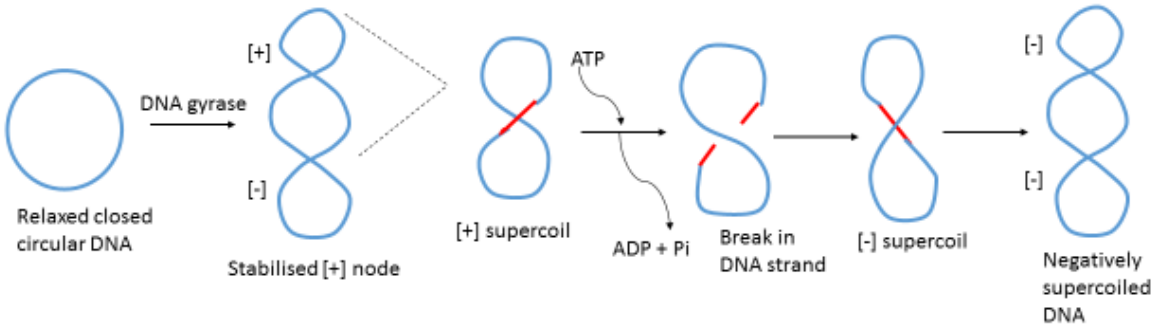

Figure 11: Schematic diagram of DNA gyrase mechanism of action, drawn using information obtained from Gmunder *et al*

1.2.3. Mode of action of quinolones

Quinolones have been found to bind poorly to relaxed double-stranded DNA, they preferentially bind to single-stranded DNA by forming hydrogen bonds with the unpaired bases.[20] However, they were found to have enhanced drug binding to relaxed DNA in the presence of the enzyme DNA gyrase and ATP, therefore, it was suggested that bound DNA gyrase induces a binding site for quinolones in the relaxed DNA which in turn inhibits the enzyme.[20]

DNA gyrase induces this binding site by forming a single-stranded DNA pocket where the drug binds and locks DNA and enzyme in place[20] (**Figure 12**).The drug-stabilized gyrase complex then acts as a physical block to ligation of the break leading to cell apoptosis.[14]

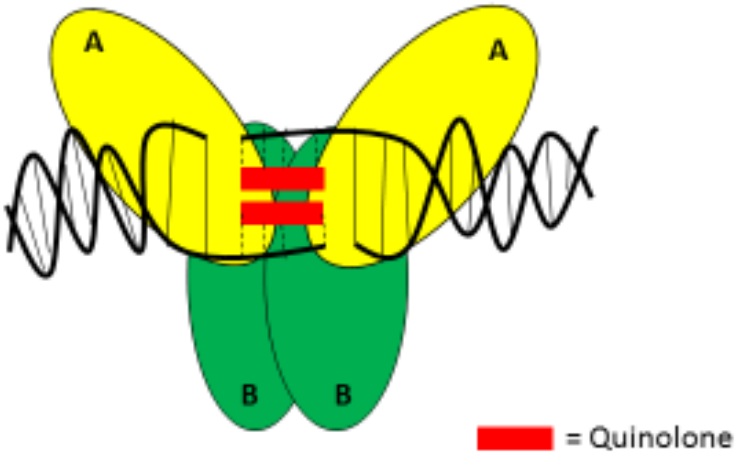

Figure 12: Diagram drawn from an adaptation of Shen *et al.* Quinolone-DNA stabilised complex inhibiting DNA gyrase (an A_2B_2 complex) with the dotted lines representing hydrogen bonding between the DNA strands and the quinolone molecules[20]

Shen *et al.* hypothesised that the drug self-associates within the pocket through hydrogen bonds between the DNA bases (N-H groups) and the hydrogen bond acceptors on the quinolone rings (C=O groups).[20] The drugs also interact through (i) π-π ring stacking of adjacent quinolone rings (ii) tail-to-tail hydrophobic interactions between N1 hydrophobic groups of drug molecules bonded to two opposite DNA strands.[20]

Shen *et al.* suggested that the number of drug molecules that can bind depends on the size and the configuration of the binding site with the proposed model having

four quinolone molecules bound per complex.[20] However Laponogov *et al.* established that only two quinolone molecules are present in the drug-stabilised complex[19](**Figure 13**).

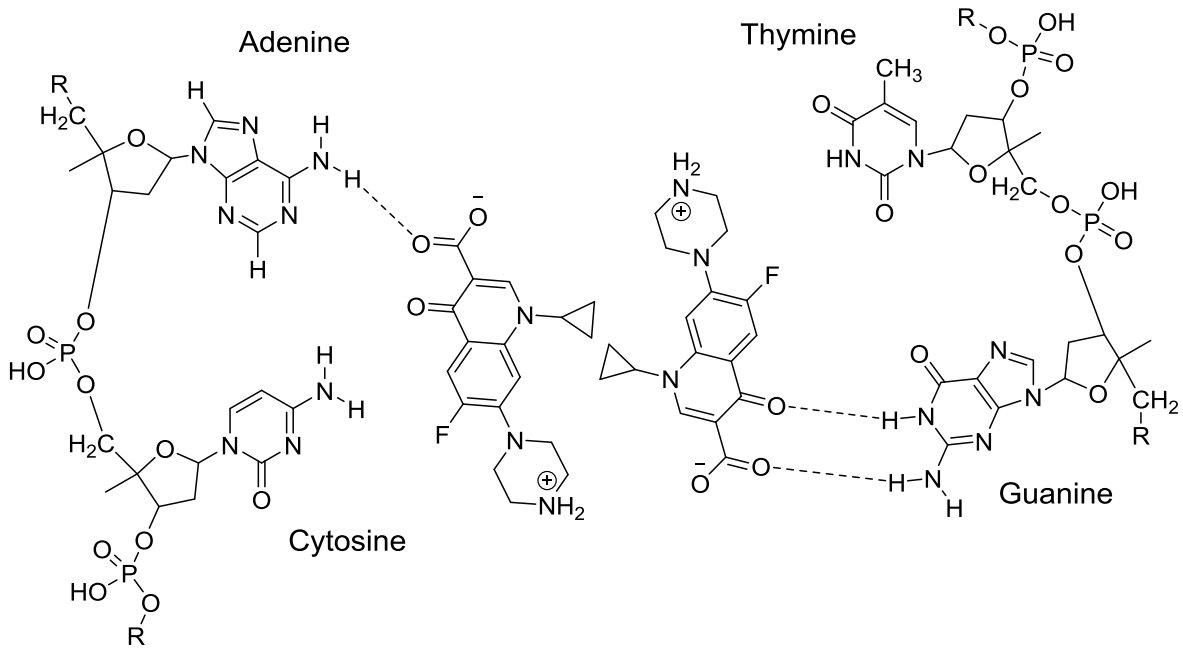

Figure 13: Diagram showing self-association of fluoroquinolones (ciprofloxacin) in the DNA binding pocket showing hydrogen bonding between the DNA bases and ciprofloxacin (represented by dashed lines) and tail-to-tail hydrophobic Interactions between the cyclopropane rings of ciprofloxacin. Interaction of DNA gyrase is not shown for clarity[20]

1.2.4. Plasmid-mediated resistance

There are three families of genes that cause plasmid-mediated quinolone resistance; Qnr genes, aac(6')-Ib-cr proteins and efflux pumps.

Qnr genes protect DNA gyrase and topoisomerase IV from quinolone inhibition by two mechanisms: (i) Qnr proteins act as DNA mimics and compete with DNA for binding to the enzyme therefore lowering the number of enzyme-DNA complexes available for quinolone binding, (ii) they inhibit quinolones from entering the binding pocket on enzyme-DNA complex.[21]

Aac(6')-Ib-cr enzyme is a variant of an aminoglycoside acetyltransferase that includes two mutations which reduce aminoglycoside resistance but confer resistance to ciprofloxacin and norfloxacin.[22] This enzyme acetylates the unsubstituted nitrogen of the

C7 piperazine ring reducing drug activity. Acquisition of aa(6')-Ib-cr was found to increase ciprofloxacin MICs 2- to 4-fold.[22]

Only three plasmid-encoded efflux pumps have been identified so far; QepA1 and QepA2 found in human bacterial infections and OqxAB found in animal infections.[14]

1.2.5. Chromosome-mediated resistance

Quinolone intracellular concentration is controlled by the opposing actions of diffusion-mediated drug uptake and pump-mediated efflux. Therefore, overexpression of chromosome-encoded efflux pumps reduces the intracellular concentration of quinolone in bacterial cell.[14] In Gram-negative bacteria quinolone resistance can also be regulated by altering expression of outer membrane porin proteins (OmpF and OmpC in *E. coli*) that form channels for passive diffusion.[23] Both Gram-positive and Gram-negative bacteria have non-specific, energy-dependent efflux systems.[23]

1.2.6. Overcoming quinolone resistance

Most common cause of high-level quinolone resistance is mutations in DNA gyrase and/or topoisomerase IV therefore an ideal fluoroquinolone would be one that retains activity against these mutated enzymes, however no such drug has been reported.[14] In theory, designing a fluoroquinolone-like drug that does not depend on the water-metal ion bridge for primary interaction with gyrase or topoisomerase IV would overcome target-mediated resistance.[14]

Membrane-based resistance such as permeability resistance can be overcome by conjugation of the antibiotic to an actively transported bacterial nutrient as this will allow the exploitation of bacterial cell nutrient transport mechanisms.[9]

1.3. Overview of 'Trojan Horse' strategy

The main concept of the 'Trojan Horse' strategy involves conjugation of an antibacterial moiety to a nutrient molecule (or nutrient-binding molecule) that is required for bacterial growth. This is done in order to bypass membrane-based resistance mechanisms. Nutrients that can be used include iron-(III), carbohydrates or peptides with bacterial iron transport being the ideal target due to the delicate balance of iron homeostasis in all organisms.[9]

A general nutrient (or nutrient-binding molecule)-drug conjugate system (**Figure 14**) consist of three components, (i) Nutrient- to increase uptake of the drug (ii) linker which connects the drug moiety to the nutrient (iii) the drug.

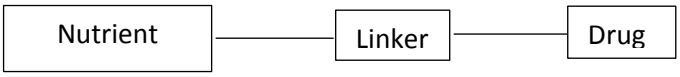

Figure 14: An illustration of a general nutrient-drug conjugate system

Naturally occurring 'Trojan Horse' conjugates have been isolated from various microorganisms, some of the conjugates are albomycins[24] and salmycin[25] (**Figure 15**) which both contain a siderophore (iron binder) component that chelates the iron nutrient and an antimicrobial component.

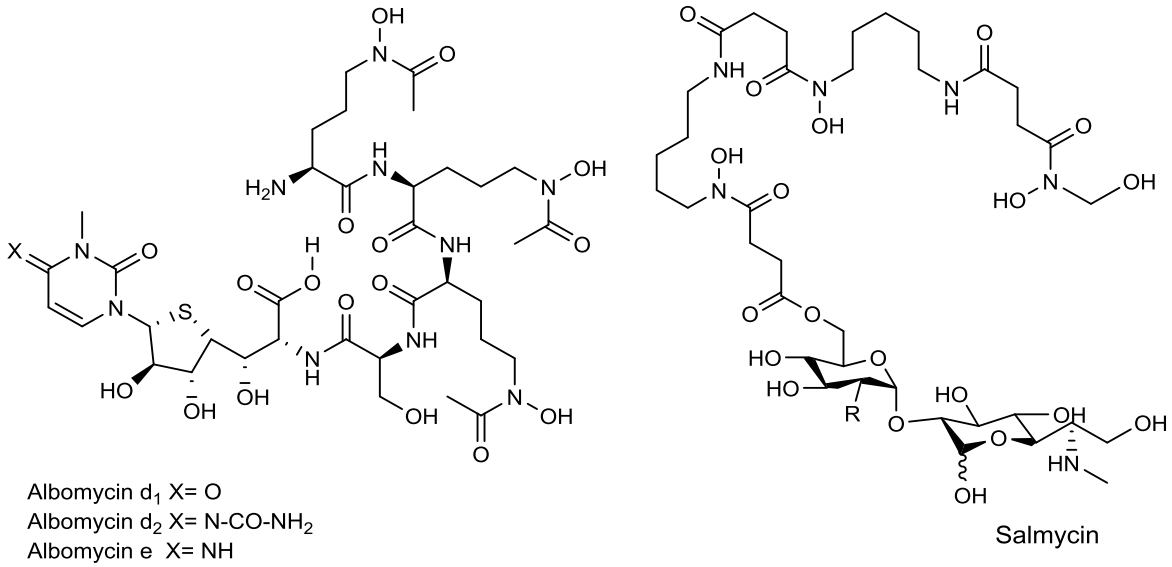

Figure 15: Structures of the natural 'Trojan Horse' conjugates; albomycins and salmycin

The natural design of 'Trojan Horse' conjugates was applied to synthesise artificial siderophore conjugates. The first synthetic 'Trojan Horse' conjugate **8** was synthesised in 1977 by Zähner *et al.* using hydroxamate siderophores.[26]

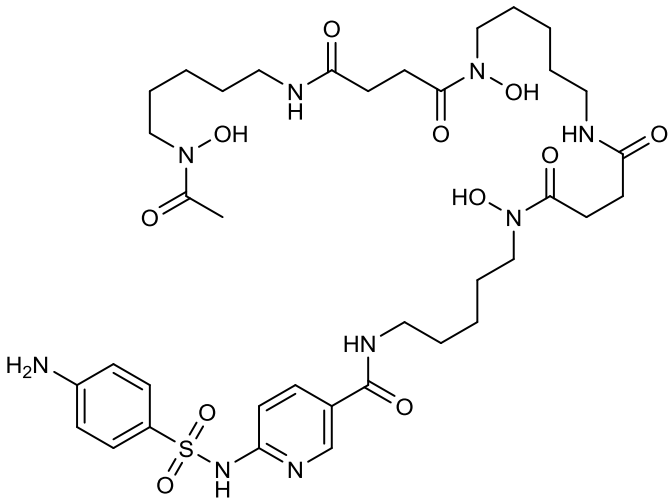

8

Figure 16: Structure of one of the first synthetic siderophore conjugate with a sulphonamide as the antibiotic moiety

The concept of using synthetic siderophores has developed and a clear benefit of using β-lactam antibiotics as a drug moiety, many examples have been reported of potent antimicrobial activity including siderophore aminopenicillin **9** conjugates,[9] ampicillin and amoxicillin **10** conjugates[27] (**Figure 17**) . β-lactam antibiotics target penicillin binding proteins (PBPs) which are located in the periplasm therefore only need to cross the bacterial outer membrane to gain access.[9] Also compared to most other antibiotics, β-lactam drugs have two separate sites for target attachment therefore the entire conjugate is capable of binding to the target without releasing the siderophore moiety.[9]

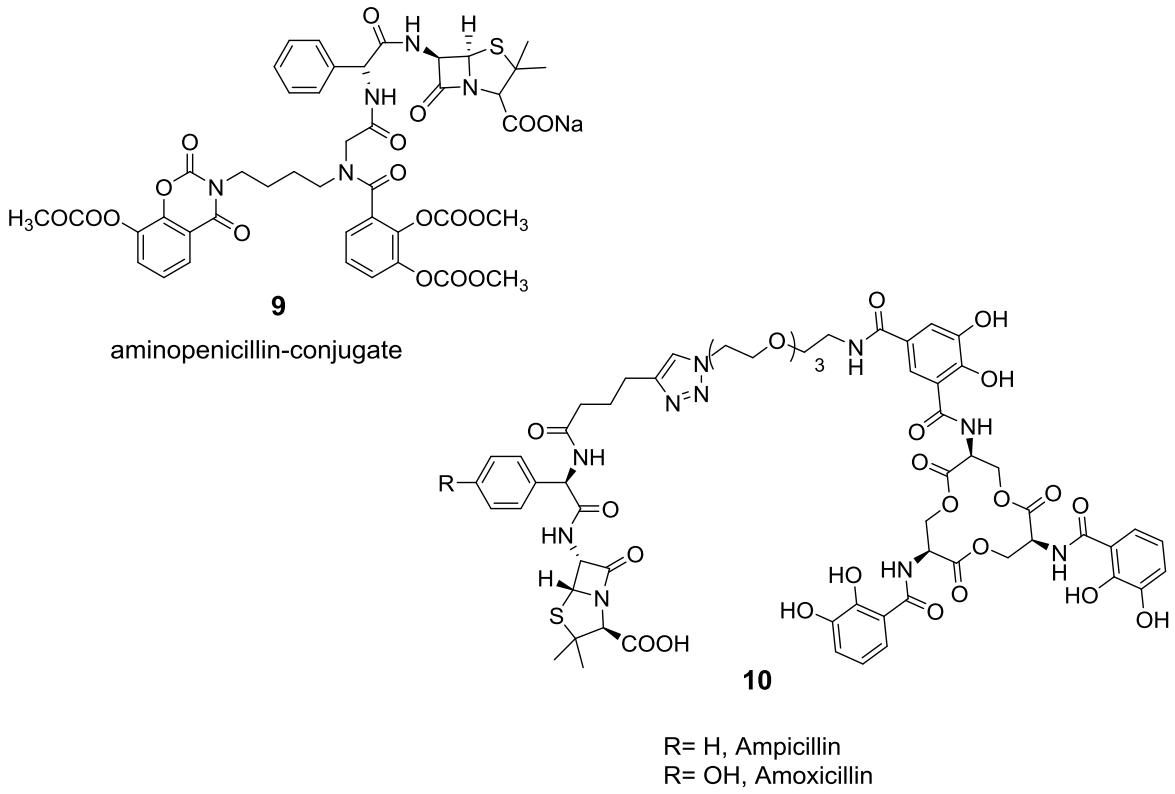

Figure 17: Synthetic siderophores using β-lactam antibiotic as the drug moiety

Although the β-lactam siderophore conjugates proved to be successful, nearly all other siderophore-drug conjugates with an antibiotic component that have a cytoplasmic target have shown decreased activity compared to the free drug alone.[28] This posed a question of whether drug release is essential for antimicrobial activity of siderophore-drug conjugates.

Wencewicz *et al.* and colleagues conducted a study of desferridanoxamine-antibiotic conjugates (**Figure 18**) to understand the role of drug release in siderophore-mediated drug delivery.[28] Desferridanoxamine (Dan) is an effective growth promoter for Gram-negative and Gram-positive bacteria; the antibiotics used for the study included Lorabid® (Lor), ciprofloxacin (Cip) and trisclosan (Tri). Wencewicz *et al.* concluded that for siderophore-drug conjugates with intracellular targets, an active drug release process is needed for antimicrobial activity as all conjugates linked with a non-labile amide linker (Dan-Lor **11** and Dan-Cip **12** conjugates) were less active than the free drug while Dan-Tri **13** conjugate which was linked through a bio-labile ester linker had equal or greater activity compared to the free drug alone.[28]

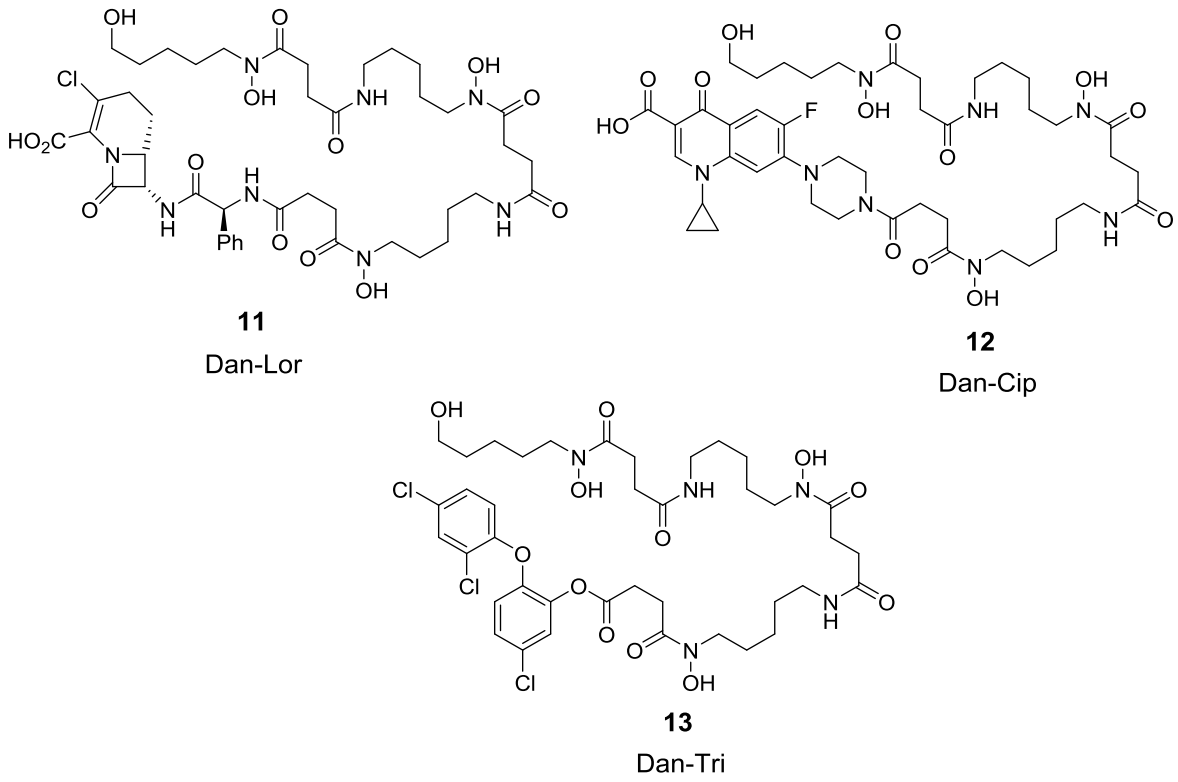

Figure 18: Desferridanoxamine-antibiotic conjugates; Dan-Lorabid (Dan-Lor), Dan-ciprofloxacin (Dan-cip) and Dan-Trisclosan (Dan-Tri)

The 'Trojan Horse' strategy has also been applied to other fluoroquinolone antibiotics using different nutrients to synthesise alternative 'Trojan Horse' conjugates; siderophore-fluoroquinolone conjugates[9] and glycosylated-fluoroquinolone conjugates.[29]

1.3.1. Siderophore-fluoroquinolone conjugates

Mislin *et al.* carried out a study of pyochelin-norfloxacin conjugates (**Figure 19**) to test the conjugates and the effect of the linker on antimicrobial activity of the antibiotic.[30] Pyochelin is a siderophore of *Pseudomonas aeruginosa* pathogen and the researchers observed that only conjugates with a labile linker **14** showed antibacterial activity whereas conjugate **15**, with non-labile linker, had no activity. Therefore it was suggested that the presence of the siderophore may prevent the antibiotic from interacting with its target (DNA gyrase) due to steric hindrance.[30]

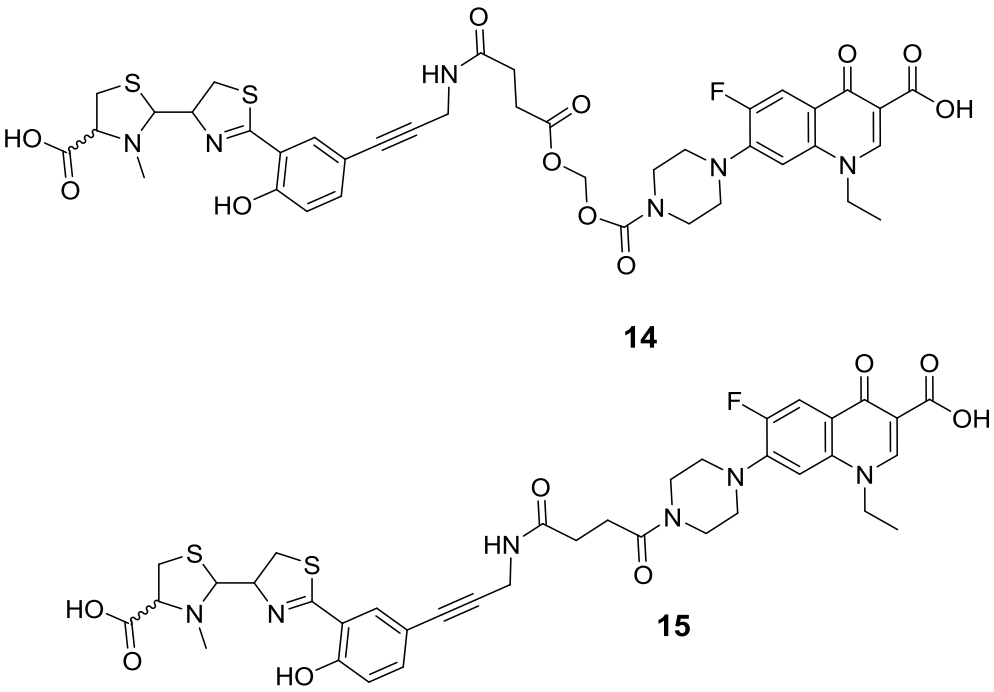

Figure 19: Structures of pyochelin-norfloxacin conjugates with a labile linker **14** and with a non-labile linker **15**

Citrate-ciprofloxacin conjugates **16** and **17** (**Figure 20**)[31] were reported by Duhme-Klair/Routledge research groups, they observed that the conjugates retained some antimicrobial activity, however activity was significantly reduced compared to that of free ciprofloxacin. The effect of the length of the linker on antimicrobial activity was also investigated by introducing a glycine **18** and aminovaleric acid spacer **19**.[31] The insertion of a spacer was found to cause a significant reduction in activity especially with conjugate **19** therefore it was suggested that a non-biolabile spacer should not contain more than 1-2 atoms.[31] The reduction in activity was proposed to be due to less stable binding to DNA gyrase.

A study of staphyloferrin-ciprofloxacin conjugates (**Figure 21**) was also carried out to assess whether the modification of ciprofloxacin with racemic staphyloferrin altered the antimicrobial activity of ciprofloxacin.[32] Both conjugates displayed a significant reduction in activity against strains that were susceptible to ciprofloxacin, this reduction in activity was thought to be due to incomplete inhibition of the DNA gyrase potentially due to steric clashes of the modified drug and/or electrostatic repulsions.[32]

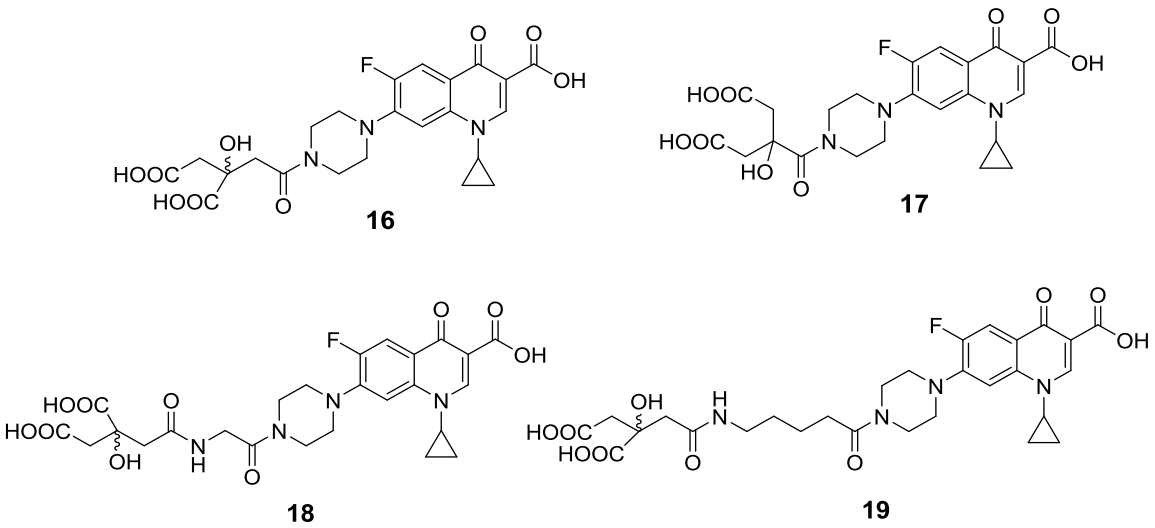

Figure 20: Structures of citrate-ciprofloxacin conjugates

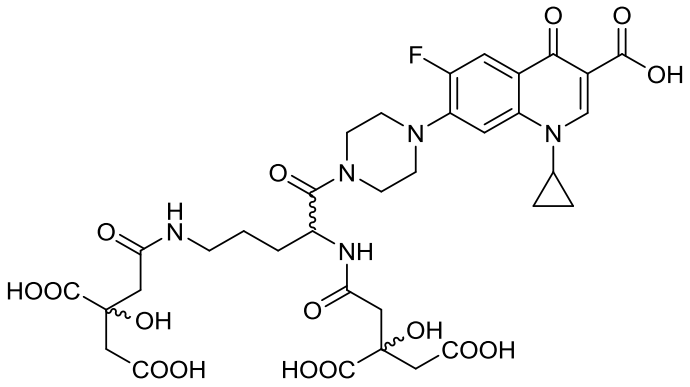

Figure 21: Structure of ornithine-based staphyloferrin ciprofloxacin conjugates

1.3.2. Glycosylated-fluoroquinolone conjugates

Although detailed investigations in the use of iron bacterial transport systems in 'Trojan Horse' antibiotics have been conducted, bacterial carbohydrate transporters have been studied to a much lesser extent with the first carbohydrate based 'Trojan Horse' conjugates reported in 1999 by Jung *et al.*[33]

Monosaccharides glucose and galactose were conjugated to ciprofloxacin[33] and norfloxacin.[34] In bacteria, glucose and galactose monosaccharides can be transported through proton symport[35] and the phosphoenolpyruvate-dependent sugar: phosphotransferase system (PEP-PTS).[36] The monosaccharide-ciprofloxacin conjugates were tested for their antimicrobial activity as well as the effect of adding a linker to the conjugate.

The monosaccharide-ciprofloxacin conjugates with no linker, **20** and **21** were found to retain antimicrobial activity comparable to free ciprofloxacin however conjugates with a linker, **22** and **23** had significantly reduced activity compared to the free ciprofloxacin but the glucose conjugate **22** displayed higher activity than the galactose conjugate **23**.[33] It was suggested that the conjugates were being actively transported but no definite evidence was provided.

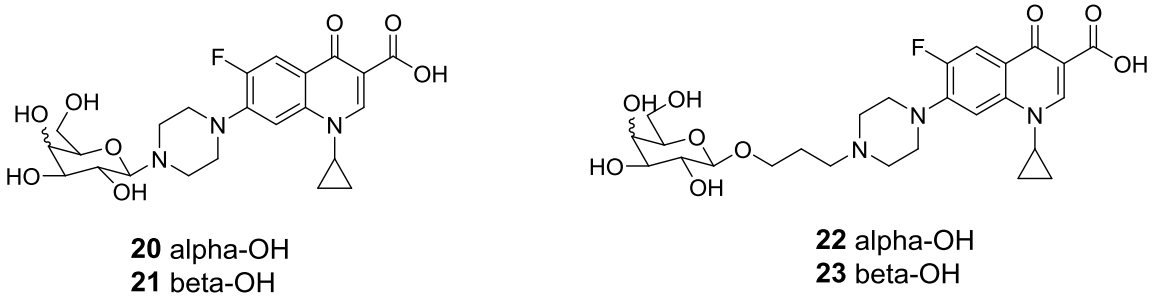

20 alpha-OH
21 beta-OH

22 alpha-OH
23 beta-OH

Figure 22: Glucose and galactose-ciprofloxacin conjugates with no linker, **20** and **21**, and with linker, **22** and **23**

A further investigation of the monosaccharide-ciprofloxacin conjugates was carried out by Routledge/ Duhme-Klair research groups to determine if these conjugates were being actively transported or being transported through fluoroquinolone uptake mechanisms and/or passive diffusion.[29] Glucose-ciprofloxacin conjugate **22**, galactose-ciprofloxacin conjugate **23** and lactose-ciprofloxacin conjugate **24** were synthesised with propyl linkers. Conjugates **22** and **23** retained antimicrobial activity but lower than that of free ciprofloxacin and **24** showed no activity. It was suggested that adding lactose to ciprofloxacin has a significant effect on the ability of ciprofloxacin to inhibit DNA gyrase compared the effect observed following addition of galactose and glucose.

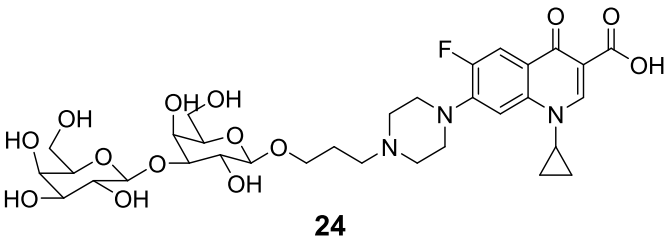

24

Figure 23: Structure of lactose-ciprofloxacin conjugate with a biostable linker

No evidence was found to support the active transport of the monosaccharide-ciprofloxacin conjugates across the cytoplasmic membrane but there was evidence which suggested that the conjugates were diffusing through porins to penetrate the

outer membrane then probably diffusing at a lower rate through the inner membrane to reach their target.[29] Therefore, it was concluded that the use of carbohydrate based 'Trojan Horse' conjugates to exploit the carbohydrate transport system could essentially be flawed.

1.3.3. Peptide-drug conjugates

In order to improve the absorption of drugs with low oral bioavailability, peptide-'Trojan Horse' conjugates have been synthesised to target specific carrier proteins. Mitra *et al.* conducted a study on lopinavir; a protease inhibitor used for the treatment of HIV infection.[37] Lopinavir has low bioavailability which is thought to be due to extensive metabolism by CYP3A4[38] and lopinavir is also a substrate for the efflux transporters P-glycoprotein (P-gp) and Multidrug Resistance Protein (MRP2).[39]

Lopinavir-valine-valine **25** and Lopinavir-glycine-valine **26** conjugates were synthesised to study their uptake and transport across the MDCKII-MDR1 and MDCKII-MRP2 cell membrane. Both conjugates were found to be substrates of peptide transporters expressed on the intestinal barrier as they displayed better solubility, metabolism and internal permeability profiles compared to the parent drug lopinavir.[37] This indicates that the conjugates were able to circumvent P-gp and MRP2 mediated efflux.

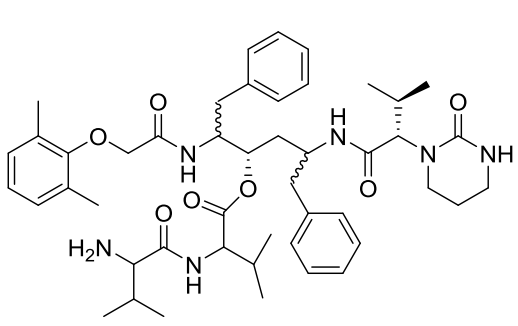

25

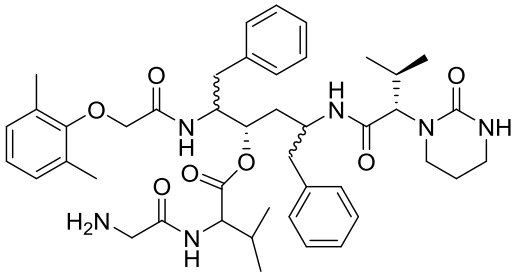

26

Figure 24: Structures of Lopinavir-valine-valine **25** and Lopinavir-glycine-valine **26**

Peptide based conjugates were also applied to target other peptide transporters, Foley *et al.* synthesised two peptide based conjugates using nabumetone linked through a hydrolysable linker to a thiodipeptide.[40] The conjugates were designed to target transport via PepT1, an intestinal peptide transporter.

1.3.4. Peptide Trojan Horse conjugates

Routledge/Duhme-Klair research groups synthesised peptide based conjugates; ciprofloxacin-Gly-Gly **27** (a control that should not be actively transported) and ciprofloxacin-L-Ala **28** to investigate their transport in bacteria. These conjugates were designed to target the ABC transporters and proton symporters (PTRs) in *E. coli*, which is explained in detail in section (1.4). Tests were conducted using mutated *E. coli* species with ABC transporters knocked out or PTR knocked out and wild type *E.* coli as a control organism.

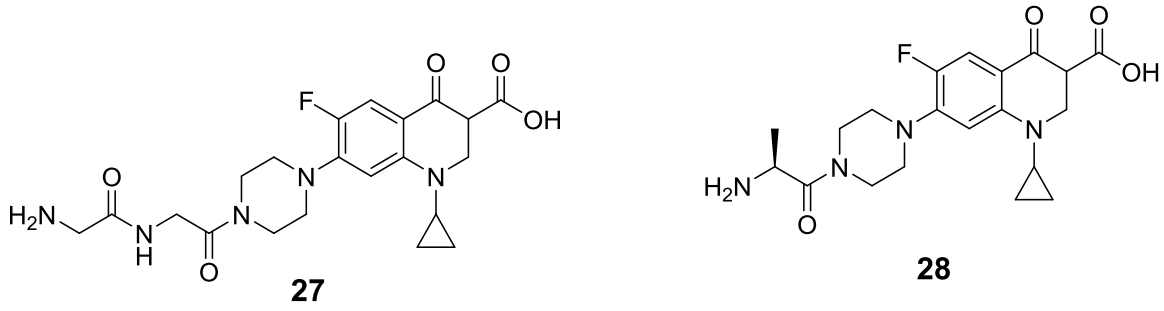

Figure 25: Structures of glycine-glycine-ciprofloxacin **27** and L-alanine-ciprofloxacin **28**

Although both conjugates retained antimicrobial activity, the activity was significantly lower than that of free ciprofloxacin and no growth advantage was observed for the ABC or PTR knock outs. This suggests that **28** was not being transported via peptide transporters (unpublished results). However this conclusion was not conclusive and further investigations are described in this thesis.

1.4. Peptide Transporters

1.4.1. ABC transporters

ABC transporters are associated with many important biological processes in both prokaryotes and eukaryotes and they are characterised by their highly conserved ATP-binding cassette.[41] ABC transporters utilize the energy of ATP hydrolysis to pump substrates across the membrane against a concentration gradient.[41] Typical ABC transporters consists of four membrane-associated domains (i) two highly hydrophobic transmembrane domains which form the pathway for substrates to cross through the membrane and these domains are thought to be the substrate specificity domains (ii) two ATP binding domains which are highly hydrophilic, these are located at the

cytoplasmic face of the membrane, they bind ATP and couple ATP hydrolysis to the transport process.[41]

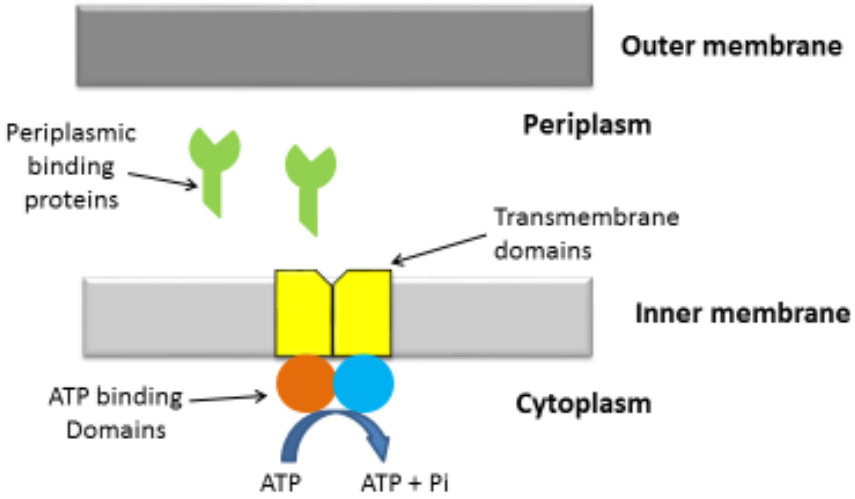

Figure 26: A diagram drawn based on *Higgins et al* showing the domains of a typical bacterial ABC transporter and where the domains are located within a bacterial cell[41]

In addition to the four core domains, all bacterial ABC transporters require a substrate-binding protein in the periplasmic space.[41] These periplasmic proteins (also known as oligopeptide-binding proteins) are essential for the function of the transport system; they are made up of two globular domains and a cleft that forms the substrate-binding site. They serve as the initial receptor for transport therefore play a role in determining substrate specificity.[41] Although periplasmic-binding proteins are involved in determining substrate specificity, transmembrane domains are the primary determinants.[41]

1.4.1.2. Substrate specificity

Study of the oligopeptide-binding protein OppA from *E. coli* was carried out to investigate the peptide substrates.[42] The binding protein was found to have little or no affinity for free amino acids and dipeptides but high affinity for tripeptides, it also demonstrated preference for peptides with unmodified amino termini, although it was still able to transport peptides with modified C-termini the binding protein requires peptide substrates to possess free amino termini.[42] Tripeptides with hydrophobic or

polar side chains such as alanine and serine had higher affinity for the binding site compared to peptides with ionic side chains like glutamic acid.[42]

1.4.2. Overview of POT family transporters

Proton-dependent oligopeptide (POT/PTR) transporters, PepT1 and PepT2, belong to the major facilitator superfamily (MFS) of secondary active transporters; they actively transport di-and tri-peptides across membranes.[43] PepT1 and PepT2 also transport a number of drugs and amino acid-conjugates prodrugs across the cell membrane. Therefore, a detailed understanding of substrate recognition could allow the modification of pharmacologically active compounds into substrates for PepT1 and PepT2 transport therefore improving bioavailability and distribution.[44]

PepT1 and PepT2 are proton (H^+)-driven symporters that use the inwardly directed proton electrochemical gradient to drive uptake of peptides across membranes through a transport mechanism known as the rocking bundle mechanism.[43] The rocking bundle mechanism is a transport mechanism which MFS use; MFS transporters consist of two 6 trans-membranes bundles that assemble together in the membrane to form a 'V'-shaped transporter with a central binding site formed between the two bundles.[43] $PepT_{so}$ (*Shewanella oneidensis*) crystal structure was the first crystal structure of a POT transporter to be determined which revealed a novel asymmetrical occluded conformation and a conserved intracellular gate.[45]

1.4.2.2. Mode of action

Structural and conformational studies of a POT family transporter from the bacterium *S. thermophiles*, $PepT_{st}$, was carried out.[43] It was concluded that the N-terminal domain of the binding site dictates peptide binding and affinity characteristics while the C-terminal domain is more dynamic and facilitates the opening and closing of the peptide-binding site; alternating salt bridge interactions that form and break during transportation at both the extracellular and intracellular ends of the peptide-binding site were also proposed.[43] The proposed salt bridge networks have been suggested to have an important role in many secondary active transporters; they are suggested to be important for orchestrating structural re-arrangements during transport.[46]

The mechanism of transport of $PepT_{st}$ was proposed to be through three conformations; outward-facing, occluded and inward-facing.[43] In the outward-facing

state, the central binding site is accessible to the extracellular side of the membrane to allow peptides to enter the binding site but closed to the intracellular end by a salt bridge formed between Lys126 of helix 4 (H4) and Glu400 of (H10).[43] The $PepT_{st}$ then transitions to the occluded state after proton and peptide binding.

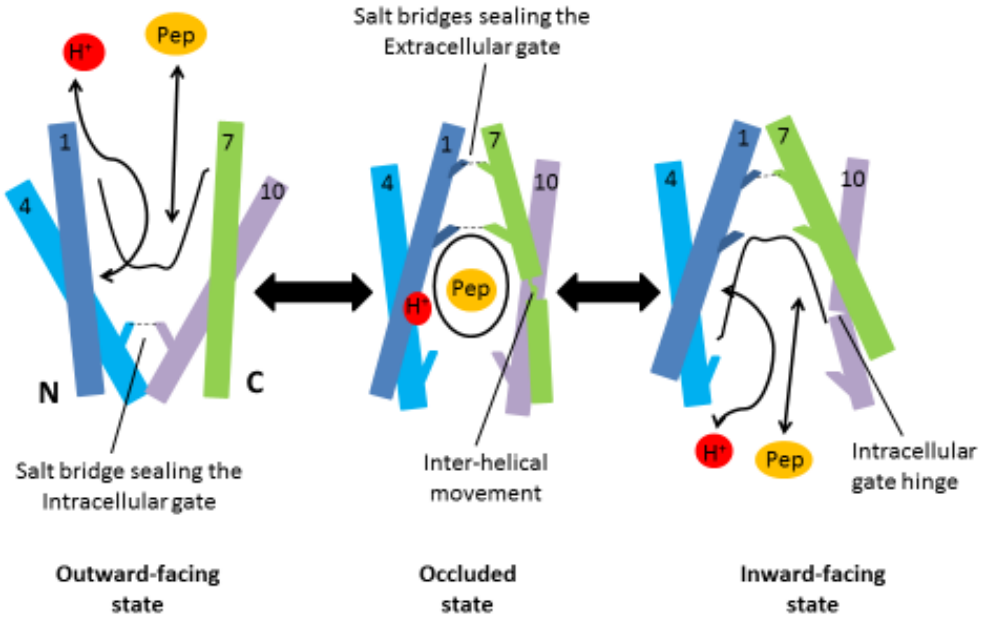

Figure 27: Schematic diagram drawn based on *Solcan et al* showing the mode of action of PepTst transporter through three states; outward-facing, occluded and inward-facing states[43]

The occluded state is closed to both the exterior and the interior of the cell with the peptide occluded within the binding site. Transition of extracellular state to occluded state is facilitated by the substantial inter-helical movement within the C-terminal half of the transporter. This allows salt bridge interactions at two sites, Arg53 (H1)-Glu312 (H7) and Arg33 (H1)-Glu300 (H7), therefore allowing the closure of the extracellular gate.[43]

The $PepT_{st}$ then transforms from the occluded state to the inward-facing state which weakens one of the salt bridges, Lys126-Glu400.[43] This transition occurs as a result of localised hinge-like bending in H10 helix which is in parallel to the movement of H7 helix. Within the intracellular state the central cavity is accessible to the interior of the cell to enable the release of the bound peptide and proton.[43] Once the peptide and the proton have been released the transport cycle then recycles back through an empty occluded state in-order to complete the cycle.[43]

1.4.2.3. Selectivity mechanism

The structure of a PepT transporter from *S. oneidensis* ($PepT_{so2}$) crystallised with three different peptides was studied so as to gain an understanding of the structural information on peptide binding to PepT transporters.[44] This study demonstrated that the PepT binding site prefers di-and tripeptides over single amino acids and also that the binding-site pockets (Pocket 1, 2 and 3) are tolerant of small-and medium-sized hydrophobic and aromatic side chains.[44] It was also suggested that the PepT binding site has a highly conserved peptide backbone within the PepT family and this peptide backbone plays a large part in the recognition and affinity of substrates.[44]

L-valyl prodrug of zanamivir **29** (a treatment for influenza A and B infections) is an example of a successful prodrug that has been generated by linking the pharmaceutically active drug to the carboxylate group of a small amino acid.[47]

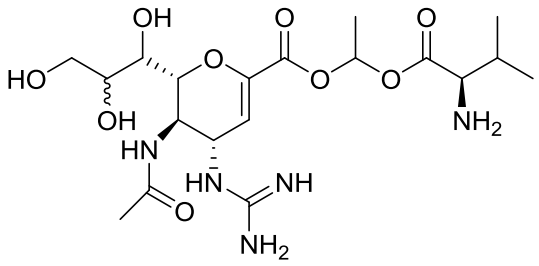

29

L-Val-Zanamivir

Figure 28: Structure of L-valyl prodrug of zanamivir

The use of peptides as a nutrient of the 'Trojan Horse' strategy was adapted within this thesis (**Figure 29**) to exploit these peptide transport mechanism to actively transport the drug moiety across the bacterial inner membrane.

Figure 29: An illustration of a peptide conjugated to a drug moiety through a linker

In the 'Trojan Horse' strategy studies have shown that the use of stable, non-labile linkers compromises the activity of the pharmaceutically active drug, the nutrient or nutrient binding molecule may be sterically hindering therefore inhibiting the drug from interacting with its target. This was observed in a study carried out by Mislin *et al*.

of pyochelin-norfloxacin conjugates (**Figure 19**) which showed that only conjugates with a labile linker had antibacterial activity comparable to that of the parent drug, norfloxacin.[30]

1.5. Biolabile linkers

An ester linkage is an example of commonly used labile linker, Godtfredsen *et al*. synthesised linked esters of ampicillin (β-lactam antibiotic) and penicillanic acid sulfone (β-lactamase inhibitor) **30** so as to increase the oral absorption of β-lactam antibiotics as well protecting the lactam antibiotic from inactivation by β-lactamase.[48]

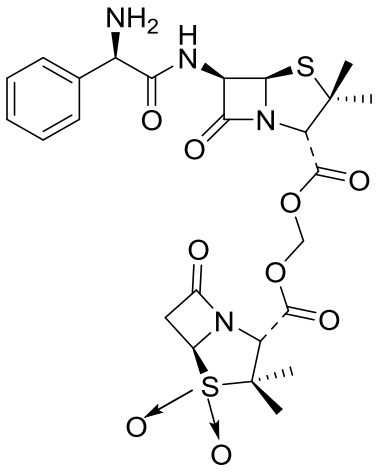

30

Figure 30: Structure of a linked ester of ampicillin and penicillanic acid sulfone

1.5.1. Disulfide linkers

The disulfide moiety has been applied in the development of many compounds including prodrugs.[49] Glutathione disulfide (GSSG) **32** is one of the major biological disulfide compounds and is produced on oxidation of free glutathione (GSH) **31**. A disulfide bond is relatively stable in mildly oxidising and physiological pH conditions but readily susceptible to the reductive disulfide cleavage reaction to generate two thiols, GSSG can be reduced back to GSH in the presence of the NADPH-dependent enzyme (**Figure 31**).[49]

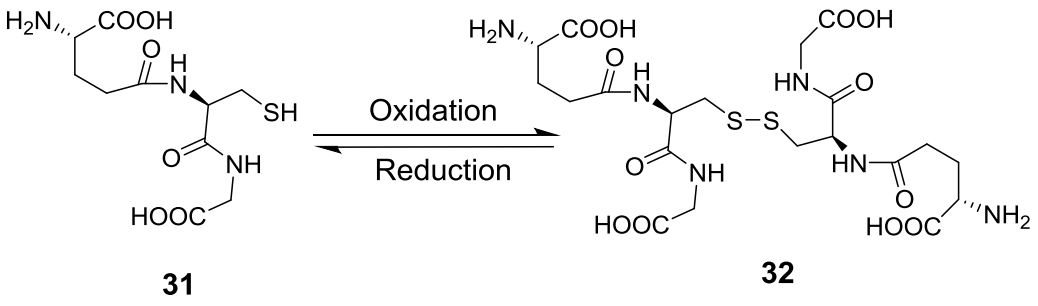

31 32

Figure 31: Reversible changes between glutathione and glutathione disulfide

Disulfides have been incorporated in drug delivery strategies as they have demonstrated high biocompatibility, stability in the bloodstream and cleavage by disulfide reductase or metabolic thiols allowing the drug molecule to be released at the target site with high efficiency.[49] All these properties makes a disulfide bond a suitable bio-labile linker as it can also accommodate various types of chemicals such as cytotoxic agents (Nitric oxide-Diclofenac prodrug **33**) [50] and tumour-targeting molecules (RGD peptide-appended naphthalimide camptothecin **34**).[51]

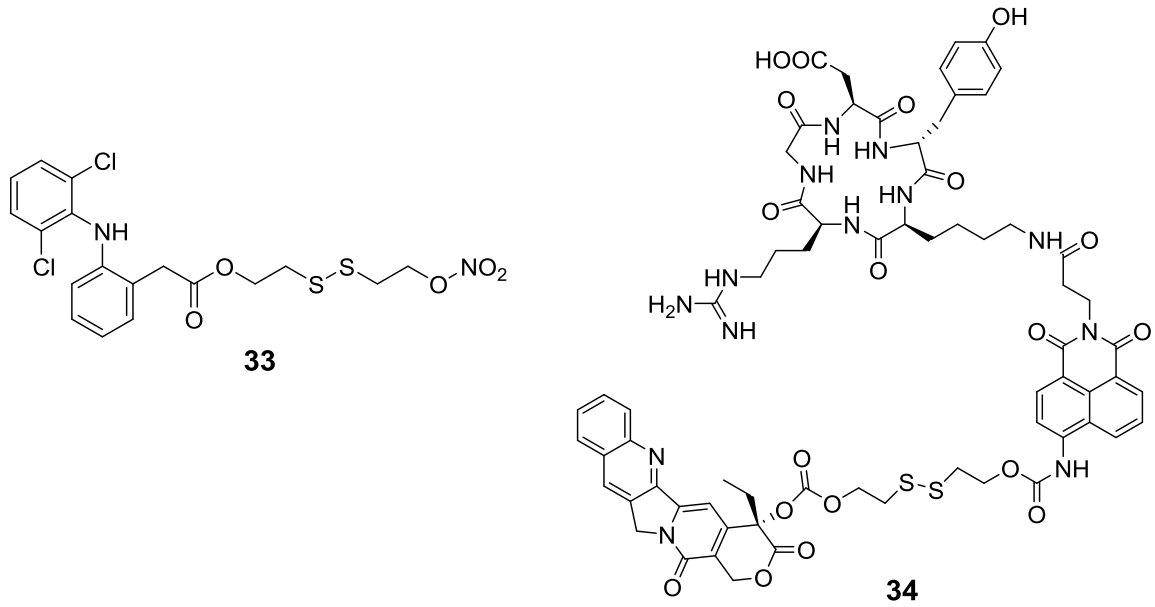

33 34

Figure 32: Structures of Nitric Oxide-Diclofenac prodrug **33** and RGD peptide-appended naphthalimide camptothecin **34**

Disulfide bonds have been utilized as linkers between constituent drugs in a mutual prodrug. A mutual prodrug is a form of prodrug which consists of two pharmacologically active agents attached to each other in a synergistic or additional way with one drug acting as a promoiety/carrier for the other drug.[52] Synergistic association is when the carrier shows the same biological action as the parent drug and additional

association is when the carrier shows new pharmacological action which the parent does not have.[52]

1.5.1.2. Release of disulfide-based prodrugs

Jain and co-workers designed and synthesised several novel mutual prodrugs containing drug-releasable disulfide linkers and proposed a plausible mechanism of drug release from the mutual prodrugs.[53] It is proposed that *in vivo* Intracellular attack of the disulfide bond by sulfhydryl-containing species such as glutathione, at biological pH will lead to the release of the drug conjugates, ethylene monothiolcarbonate **35**, ethylene sulfide **36**, and the RS-S containing conjugate **37** which can be excreted.[53] The active-drug is released in the cytoplasm because the cytoplasm is maintained under reducing conditions by free thiols such as glutathione whereas the periplasm is maintained in an oxidative state, the free thiols cleave the disulfide bond allowing the release of the active drug.[54]

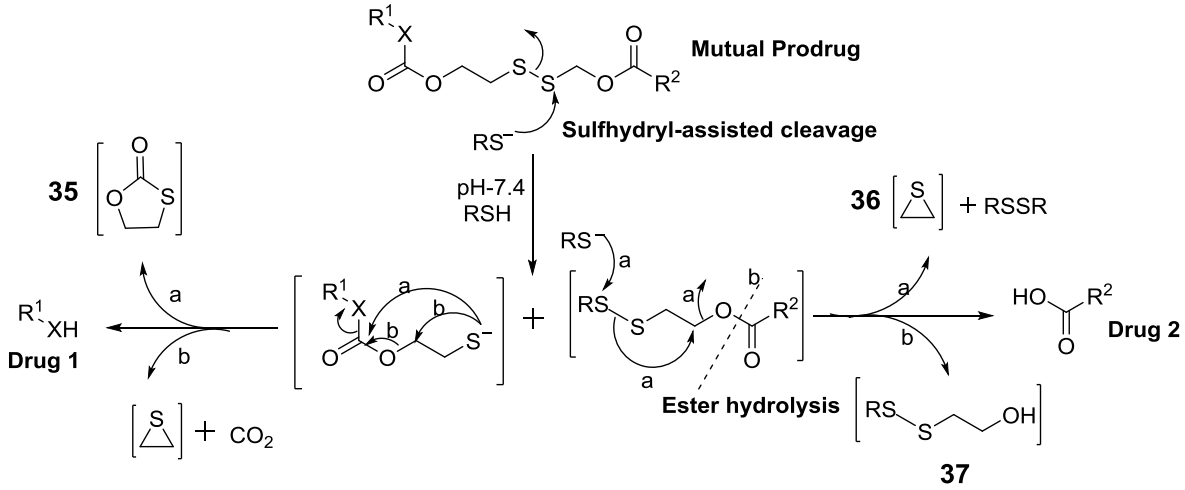

Scheme 1: Mechanism of in vivo mutual prodrug release via ester hydrolysis and /or sulfhydryl-assisted cleavage. Where X =O, N and RSH and RSSR = reduced cellular Cysteine or Glutathione. Scheme adapted from Jain et al.[53]

The proposed drug release mechanism was supported by the mechanistic study which was carried out on the reported prodrugs. This study confirmed the formation of some important metabolites, ethylene monothiolcarbonate **35** and ethylene sulfide **36**, therefore proving the mechanism to be plausible.[53] A disulfide linker was proposed in the synthesis of conjugates described in this thesis to link the peptide nutrient to the drug; ciprofloxacin.

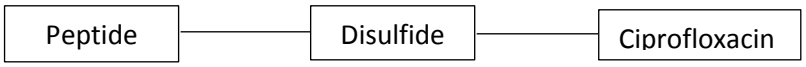

Figure 33: An illustration of a peptide conjugated to ciprofloxacin through a disulfide linker

The hypothesis of the thesis being that the conjugate diffuses across the bacterial outer membrane into the periplasm where it will be actively transported by the peptide transporters across the inner membrane into the reducing environment of the cytoplasm where the disulfide bond is cleaved by free thiols to release free ciprofloxacin (**Scheme 2**).

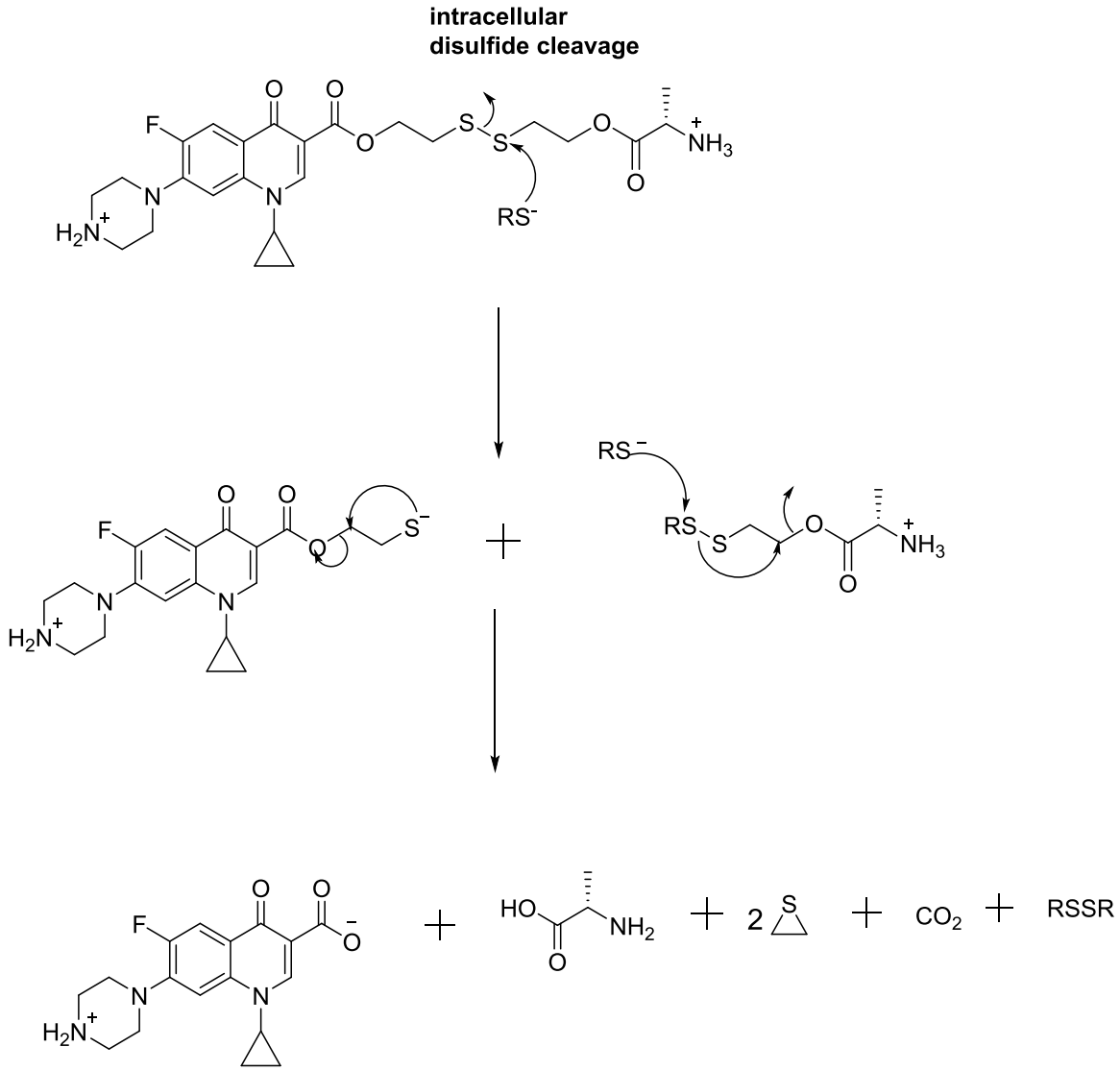

Scheme 2: The proposed intracellular cleavage of ciprofloxacin-Ala conjugate

1.6. Project Overview

The synthetic aim of the project is to synthesise a 'Trojan Horse' conjugate with ciprofloxacin as the drug moiety (**Figure 7**) and an amino acid (Ala) and dipeptide (Ala-Ala) as the nutrient conjugated to the carboxylic acid group of ciprofloxacin via an intracellular, reductively activated disulfide bond. Ala-Ala-ciprofloxacin conjugate **38** with a non biolabile linker will also be synthesised to allow comparison with a previously synthesised Ala-ciprofloxacin conjugate **28** which was found to retain antimicrobial activity but lower than that of free ciprofloxacin (unpublished results). Ciprofloxacin acts as an amino acid mimic as it is zwitterionic with a nitrogen and carbonyl end which can be considered analogous to the N and C termini of amino acids. Therefore the conjugation of Ala-Ala through the peptide's C termini to the nitrogen of the piperazine ring of ciprofloxacin will generate a pseudo tripeptide **38** which could potentially be recognised by bacterial peptide transporters.

Once ciprofloxacin-disulfide-Ala **39** and ciprofloxacin-disulfide-Ala-Ala **40** are synthesised, they will be used to investigate bacterial homologs of peptide transporters PepT1, PepT2 and ABC to actively transport the conjugate in *E. coli*. Once delivered in the cytoplasm the conjugate can be reduced by intracellular sulfhydryl-containing species releasing free ciprofloxacin. All synthesised conjugates (**Figure 34**) will be screened against wild type *E. coli* to compare the minimum inhibitory concentrations (MIC)/minimum bacterial concentrations with those of the free parent drug ciprofloxacin.

The key objectives of the project are;

- To synthesis ciprofloxacin 'Trojan Horse' conjugates with amino acids Ala and Ala-Ala conjugated via a biolabile disulfide bond or a non biolabile amide bond
- Synthesised conjugates will be screened against wild type E. coli to compare the MIC/minimum bacterial concentrations with that of ciprofloxacin

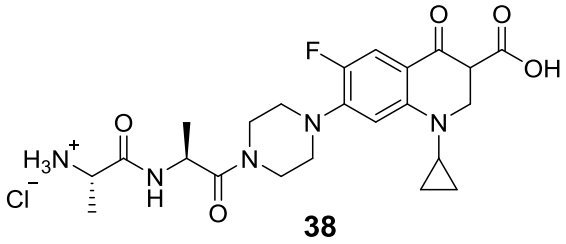

38

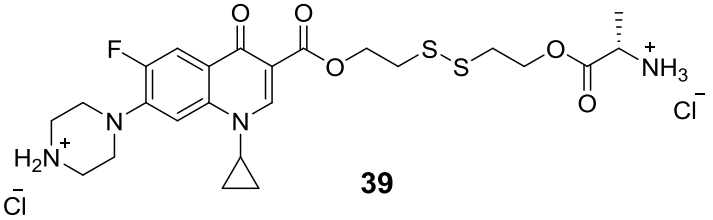

39

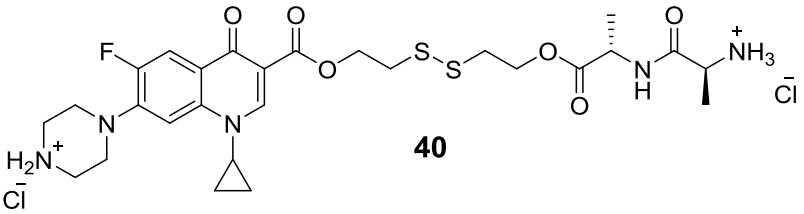

40

Figure 34: Structures of peptide-ciprofloxacin conjugates conjugated via a non-biolabile linker **38** and a bio-labile disulfide linker **39** and **40**

Chapter 2. Results and Discussions

2.1. Synthesis of Ala-Ala-ciprofloxacin conjugate 38 via a non-biolabile amide

L-alanine is a hydrophobic amino acid and ABC transporters have higher affinity for peptides with hydrophobic side chains,[41] however, they have little affinity for dipeptides compared to tripeptides.[42] PTR secondary active transporters (PepT1 and PepT2) are known to transport a number of amino acid prodrugs across the cell membrane[43] with higher affinity for di-and tri-peptides over single amino acids,[44] therefore, the pseudo tripeptide Ala-Ala-ciprofloxacin conjugate **38** was synthesised to target these transporters. The peptide was directly attached to the nitrogen of the piperazine ring of ciprofloxacin as this is not part of the pharmacophore.[11] The proposed synthesis of conjugate **38** is outlined in **Scheme 3**.

2.1.1. Methylation of ciprofloxacin

The first step towards the synthesis of **38** was the methylation of ciprofloxacin to protect the carboxylic acid group and remove the zwitterionic character of ciprofloxacin, improving its solubility profile in organic solvents.[23]

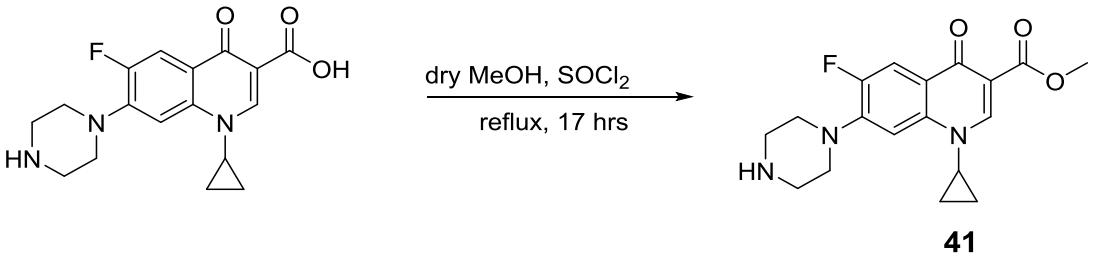

41

Scheme 4: Methylation of ciprofloxacin

Ciprofloxacin methanoate **41** was successfully synthesised from commercially available ciprofloxacin, in 94% yield. The successful synthesis was supported by mass spectrometric analysis with a peak at m/z 346.15 present in the spectrum corresponding to $[M+H]^+$ $C_{18}H_{21}FN_3O_3$. In addition ^1H NMR spectroscopic analysis showed a singlet at 3.84 ppm with a relative integration of three corresponding to the methyl group, the ^{13}C NMR spectrum showed a peak at 51.63 ppm confirming the presence of an added methyl group on **41**.

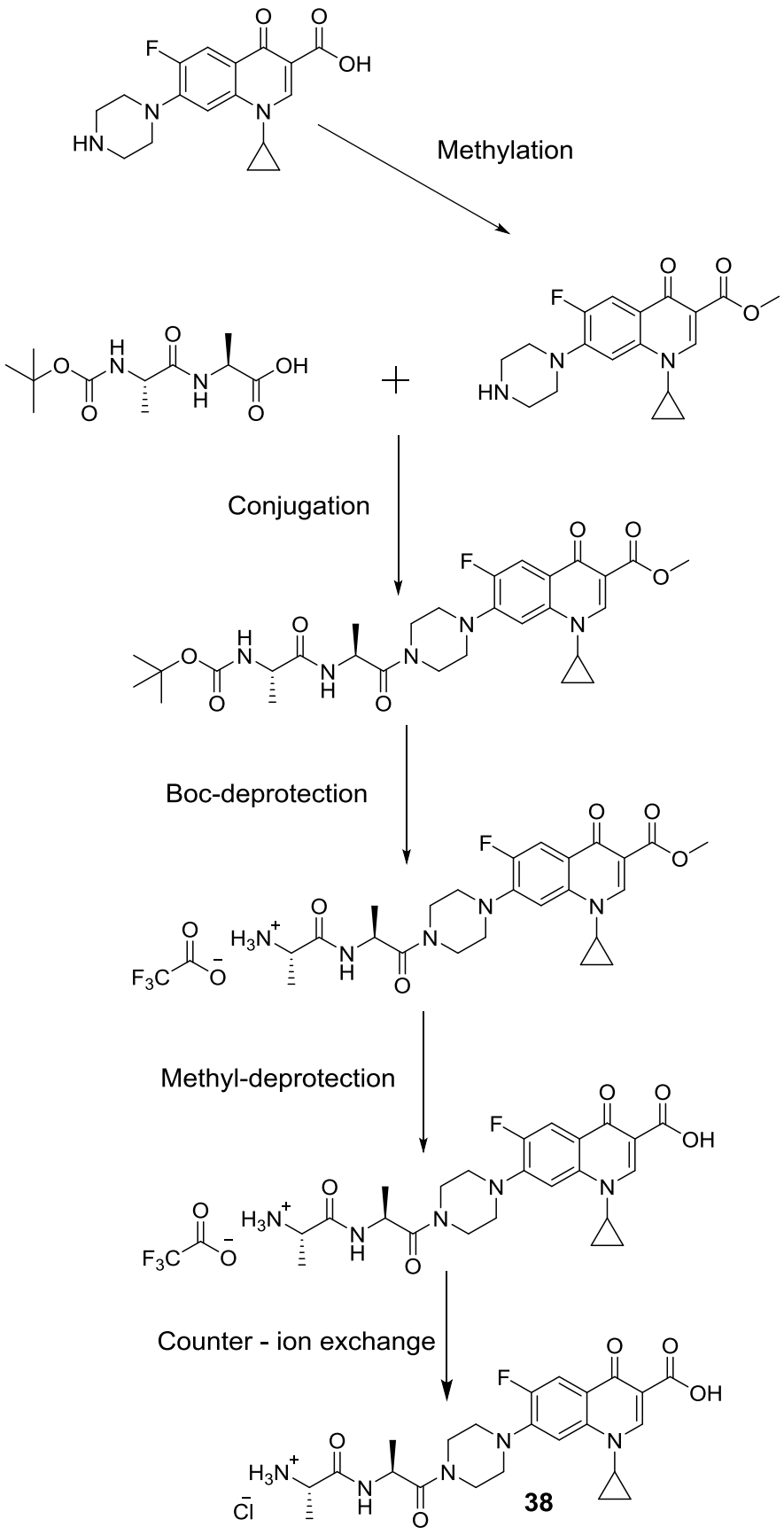

Scheme 3: The proposed synthesis of conjugate **38**

2.1.2. Conjugation of Boc-Ala-Ala-OH to methyl-ciprofloxacin 41

Methyl-ciprofloxacin **41** was coupled to Boc-protected di-alanine (Boc-Ala-Ala-OH) **42** using EDC-mediated coupling (**Scheme 5**).[55,56]

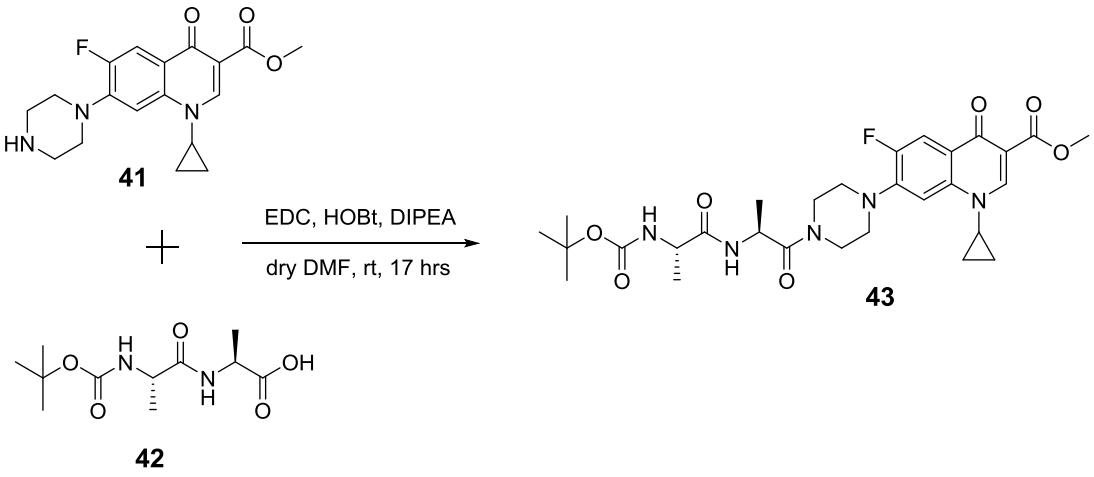

Scheme 5: Coupling of Boc-Ala-Ala-OH to **41**

Conjugate **43** was isolated in 43% yield by column chromatography. The successful synthesis of **43** was supported by mass spectrometric analysis with a peak at m/z 588.28 present in the spectra corresponding to $[M+H]^+$ $C_{29}H_{39}FN_5O_7$. ^1H NMR spectroscopy showed a singlet at 3.83 ppm (s, 3H relative integration) in the spectrum which corresponds to the ester methyl group of ciprofloxacin and an additional singlet at 1.38 ppm (s, 9H relative integration) corresponding to the methyl group of the t-butyl group. In addition, the spectrum revealed peaks at 1.32 ppm (m, 6H relative integration) corresponding to the two methyl side chains on Ala-Ala , 4.90 ppm (m, 1H relative integration) and 4.18 ppm (m, 1H relative integration) these correspond to the two α – CH groups of the peptide. The assignment of the two peaks (4.90 ppm and 4.18 ppm) was supported by homonuclear correlation spectroscopy COSY below (**Figure 35**) showing the coupling of the α – CH protons with side chain methyl group. This coupling and the presence of ciprofloxacin protons in the spectrum strongly supports the structure of **43**.

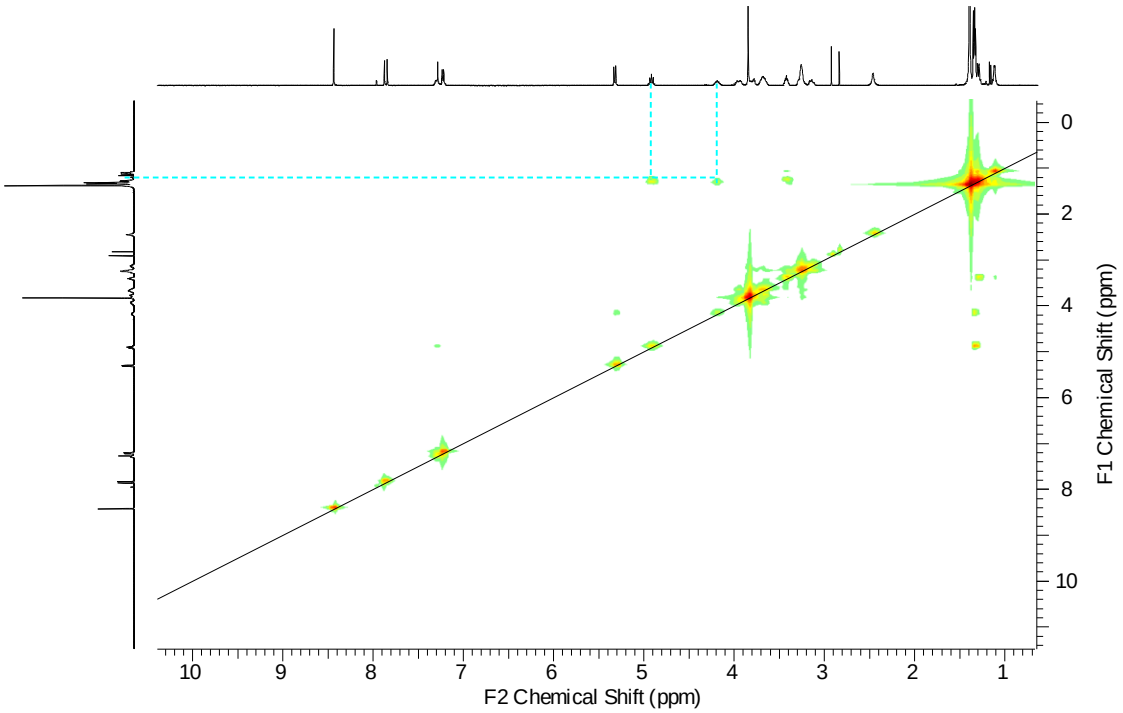

Figure 35: COSY spectrum showing coupling of Ala-Ala protons of **43**

The successful synthesis of **43** was also supported by ^{13}C NMR spectroscopy in which the spectrum showed peaks at 18.52 ppm corresponding to the two CH_3 side chain groups of the peptide, 28.13 ppm corresponding to the methyl groups of the t-butyl and a peak at 51.81 ppm corresponding to the methyl ester of ciprofloxacin.

2.1.3. Deprotection of conjugate 43

Removal of the t-butyloxycarbonyl protecting group was performed first (**Scheme 6**) because it was discovered during synthesis of **28** that performing methyl-deprotection first leads to solubility issues (unpublished results). Conjugate **43** was hydrolysed to the TFA salt using 20% TFA in dry DCM[57].

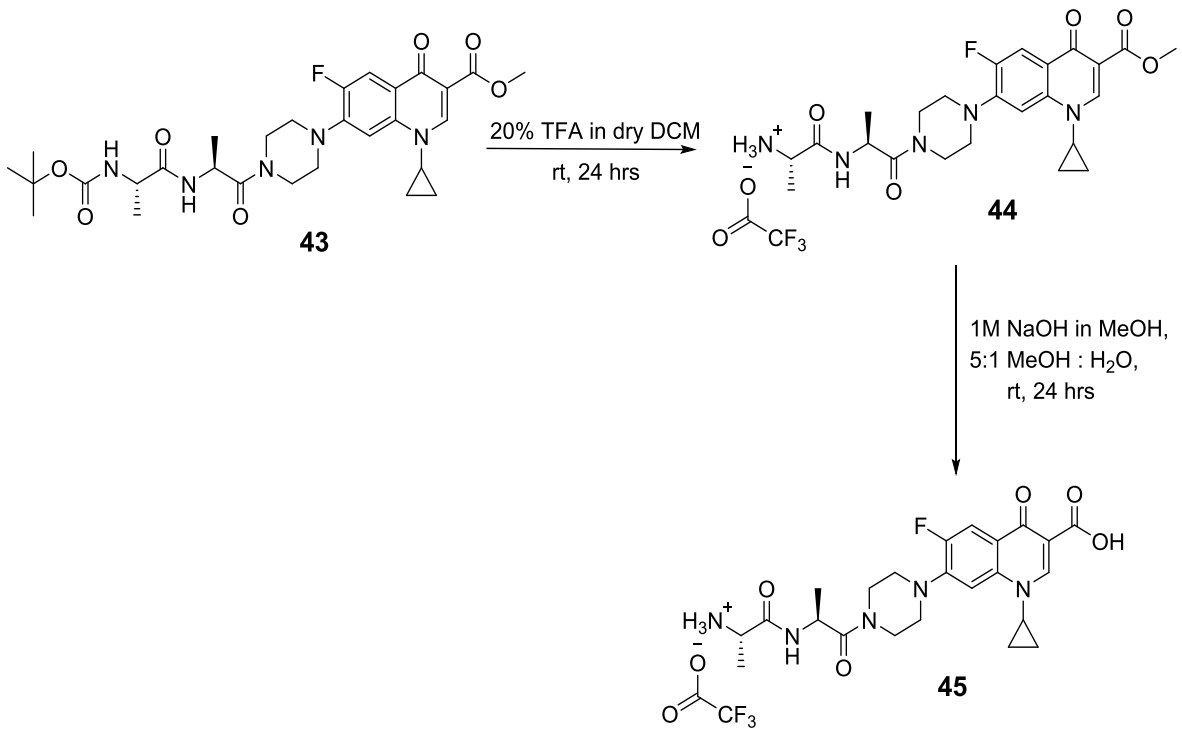

Scheme 6: Deprotection of **43**

The successful deprotection of **43** to give **44** was supported by mass spectrometric analysis with a peak at m/z 488.23 corresponding to $[M+H]^+$ $C_{24}H_{31}FN_5O_5$ present in the spectrum. ^{1}H NMR spectroscopic analysis also supported the successful synthesis of **44** as the singlet at 1.38 ppm (s, 9H relative integration) which corresponds to the t-butyloxycarbonyl group protons absent from the spectrum. The ^{13}C NMR spectrum also showed the absence of the three CH_3 groups of the t-butyloxycarbonyl at 28.13 ppm.

The deprotection of the methyl ester by base hydrolysis was done with 1M HCl to neutralise the sodium carboxylate and reveal the carboxylic acid in **45**. Successful synthesis of **45** was supported by ^{1}H NMR spectroscopy which showed the absence of the singlet at 3.83 ppm (s, 3H relative integration) in the spectrum. In addition the ^{13}C NMR spectrum showed the absence of a peak at 51.81 ppm and mass spectrometric analysis gave a spectrum with a peak at m/z 464. 21 corresponding to $[M+H]^+$ $C_{23}H_{29}FN_5O_5$. The ^{19}F NMR spectroscopy showed a peak at -76.76 ppm corresponding to the trifluroacetate and a peak at -126.76 ppm corresponding to the aromatic fluorine of ciprofloxacin.

2.1.4. Counter-ion exchange

Trifluoroacetate salts are known to perturb *in vivo* studies,[58] therefore counter-ion exchange of trifluroacetate by another acid is desirable. The procedure of freeze-drying the peptide several times in the presence of HCl to directly replace the trifluroacetate counter ion with chloride ion[59] was applied to conjugate **45** and **28.**

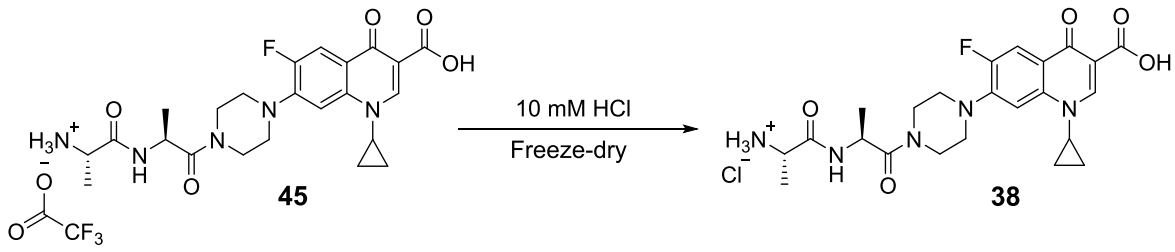

Scheme 7: Counter ion exchange of conjugate **45**

The successful synthesis of **38** was supported by ^{19}F NMR which showed only one peak at -126.78 ppm corresponding to the aromatic fluorine of ciprofloxacin and the fluorine trifluroacetate peak at -76.76 ppm was not observed in the spectrum.

Successful synthesis was also supported by mass spectrometric analysis with the product peak at m/z 464.21 corresponding to $[M+H]^+$ $C_{23}H_{29}FN_5O_5$ present in the mass spectrum.

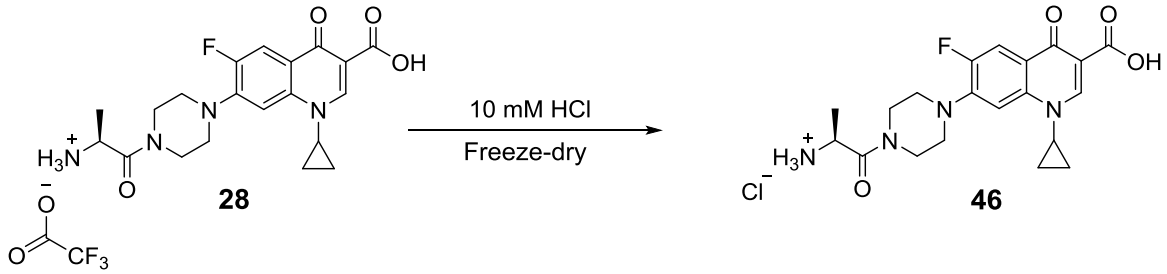

Scheme 8: Counter ion exchange of conjugate **28**

Compound **28** was subjected to the same counter ion exchange and the successful synthesis of conjugate **46** was supported by ^{19}F NMR spectroscopic analysis showed one peak at -126.76 ppm corresponding to the ciprofloxacin fluorine and no peak observed at -76.76 ppm in the spectrum indicating the successful removal of trifluroacetate. The mass spectrometric analysis showed a peak at m/z 403.18 which corresponds to $[M+H]^+$ $C_{20}H_{24}FN_4O_4$ present in the spectrum.

2.2. Synthesis of ciprofloxacin-disulfide-Ala conjugate 39

In the design of the biolabile ciprofloxacin conjugates, 2,2'-dithiodiethanol **48** was used in order to release ciprofloxacin in the bacterial cytoplasm. Disulfide **48** was conjugated to the carboxylic group of ciprofloxacin, although this functional group is essential for antimicrobial activity[11] cleavage of the biolabile linker within the cytoplasm will reveal the ciprofloxacin carboxylic group (**Scheme 2**). Conjugation to the carboxylic acid group also results in a conjugate/-prodrug with a net positive charge allowing favourable interaction with highly anionic LPS on the surface of the bacterial outer membrane.[6]

Alanine (Ala) was used as a control for the synthetic approach allowing testing the chemistry. It was unlikely that conjugation of a single amino acid would allow the conjugate to be actively transported as it has been reported that PTR secondary active transporters have higher affinity for di-and tri-peptides over single amino acids.[44] The proposed synthesis of ciprofloxacin-disulfide-Ala **39** is shown in **Scheme 9**.

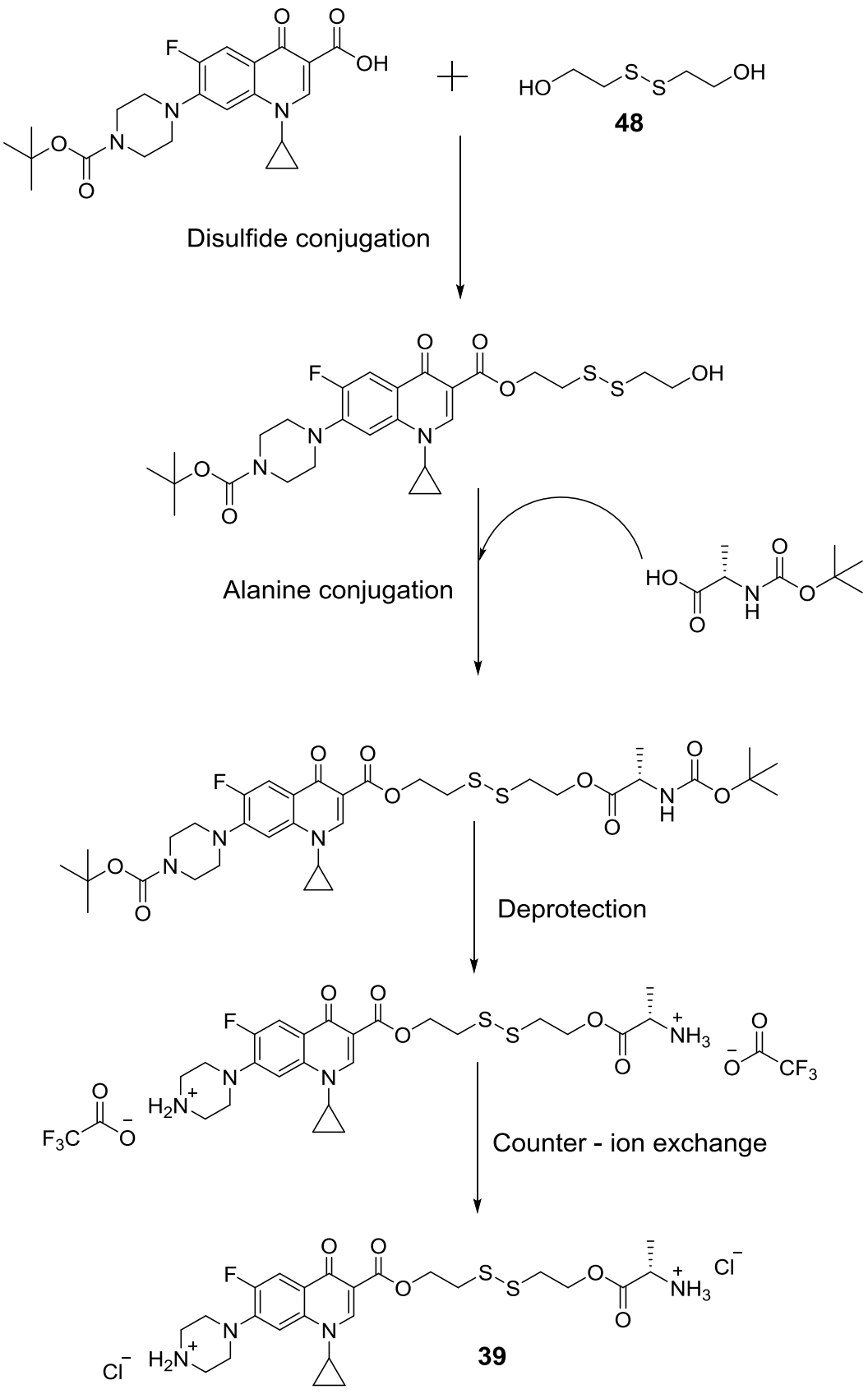

Scheme 9: Proposed synthesis of ciprofloxacin-disulfide-Ala **39**

2.2.1. Disulfide conjugation

The conjugation of 2,2'-dithiodiethanol **48** to commercially available ciprofloxacin was initially attempted using thionyl chloride to make acid chloride **47** (**Scheme 10**).[60] A solubility scan of ciprofloxacin in a range of solvents was carried out and it was found to be insoluble in all solvents tested; polar and non-polar, however, it was slightly soluble in DCM therefore DCM was used in the synthesis (**Scheme 10**). It was noted that previous successful esterification reactions of ciprofloxacin in the presence of thionyl chloride were possible when the alcohol used for esterification was also used as the reaction solvent.[60] This approach was discounted in the synthesis of **49** as 2,2'-dithiodiethanol would be required as the solvent, with considerable waste and expense.

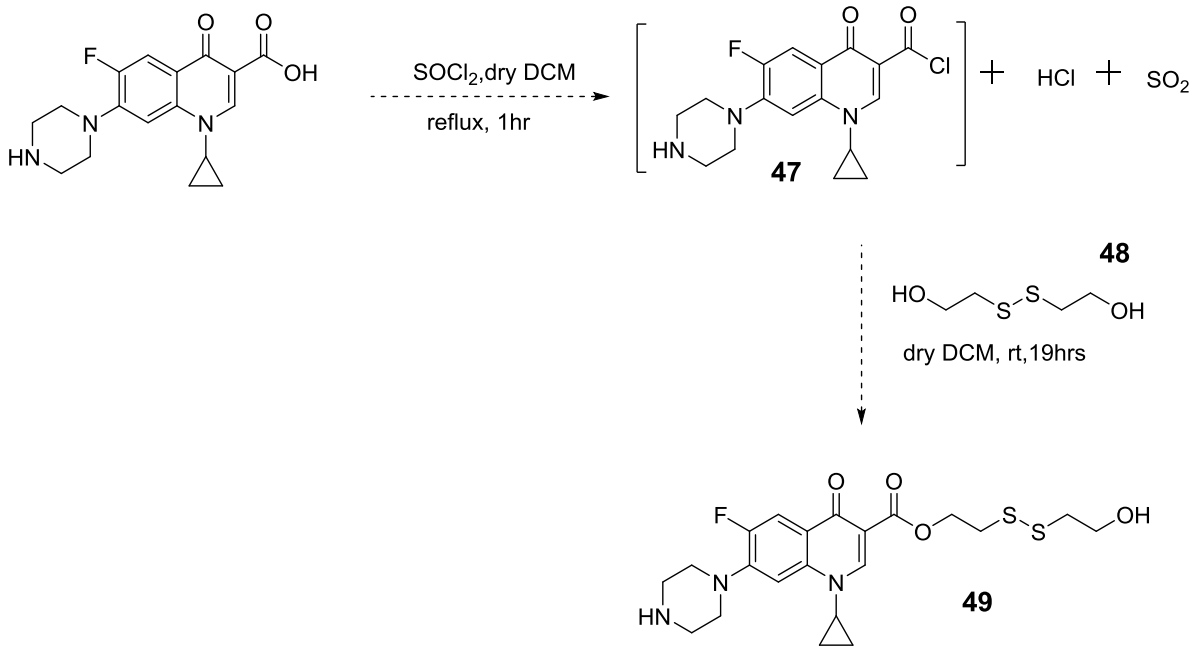

Scheme 10: The esterification of ciprofloxacin in the presence of thionyl chloride

The synthesis of **49** was found to be unsuccessful, by both mass spectrometric and ^{1}H NMR spectroscopic analysis of the crude reaction in spite of the reaction being carried out under anhydrous conditions as the reactive intermediate **47** is moisture sensitive.[61] However, as the acid chloride **47** was not isolated, the synthesis of the acid chloride intermediate could not be confirmed.

A second synthesis of **49** was attempted with the addition of DMF (1.29mM) as a catalyst was carried out. The use of DMF as a catalyst in the presence of thionyl chloride

was adapted from the preparation of an acid chloride using oxalyl chloride and DMF.[53,62] It is believed that DMF reacts with thionyl chloride to give the Vilsmeier-Haack reagent which will then react with the carboxylic acid forming the reactive acid chloride[63] (**Scheme 11**). However no evidence of the desired product **49** was observed by mass spectrometric or ^{1}H NMR spectroscopic analysis.

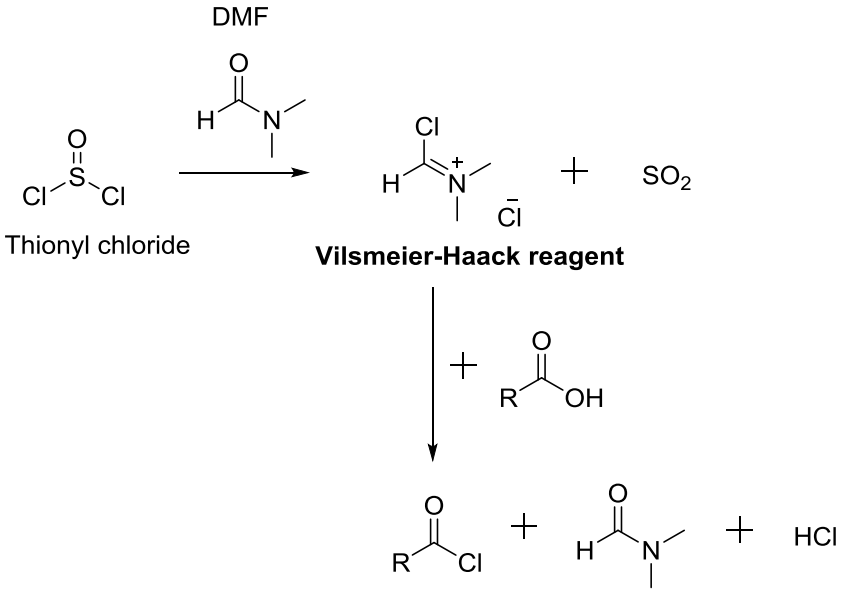

Scheme 11: DMF-catalysed synthesis of carboxylic chloride in the presence of thionyl chloride

As the solubility of ciprofloxacin was limited in organic solvents. One approach to enhance reactivity was to increase the solubility profile of ciprofloxacin; therefore the piperazinyl nitrogen group was Boc-protected removing the zwitterionic character of ciprofloxacin as shown in scheme **12**.

2.2.1.1. Boc-protection of ciprofloxacin

Commercially available ciprofloxacin (1eqv) was reacted with Boc anhydride (2eqv) in the presence of 1M NaOH dissolved in a solution of dioxane:water (1:1) (**Scheme 12**).

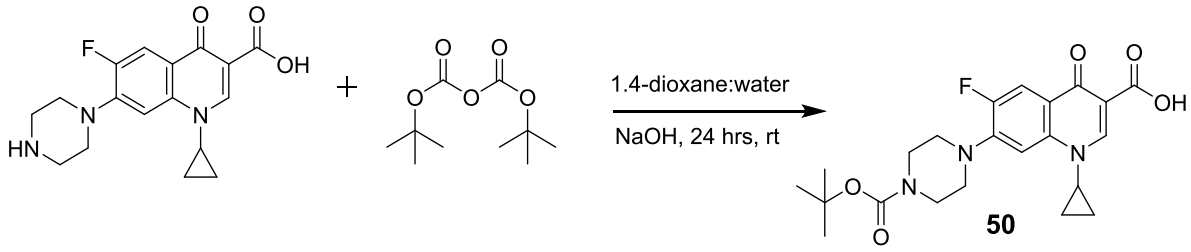

Scheme 12: Synthesis of Boc-protected ciprofloxacin **50**

Protected ciprofloxacin **50** was isolated in 94% yield and the successful synthesis of **50** was supported by mass spectrometric analysis with a peak at m/z 454.17 evident in the spectrum corresponding to $[M+Na]^+$ $C_{22}H_{26}FN_3NaO_5$ and also by ^1H NMR spectroscopic analysis as the spectrum showed a signal at 1.48 (s, 9H) corresponding to the three methyl groups on the t-butyloxycarbonyl protecting group.

Although the Boc-group enhances the solubility of ciprofloxacin it also prohibits the esterification of **50** using thionyl chloride because an acid, HCl, is produced as a by-product of the reaction and the Boc-protected amine is acid labile.[62] As a result of this incompatibility alternative esterification methods were explored.

2.2.1.2. Dicyclohexylcarbodiimide (DCC) – mediated esterification

DCC has frequently and successfully been used for the synthesis of amino acid derivatives and has also been adopted as a method for the preparation of esters.[62] The addition of 4-dimethylaminopyridine (DMAP) has been proved to significantly accelerate DCC-activated esterification of carboxylic acids with alcohols.[64] Therefore DCC/DMAP mediated esterification was carried out in order to synthesise Boc-protected ciprofloxacin – 2,2'-dithiodiethanol conjugate **51** (**Scheme 13**).

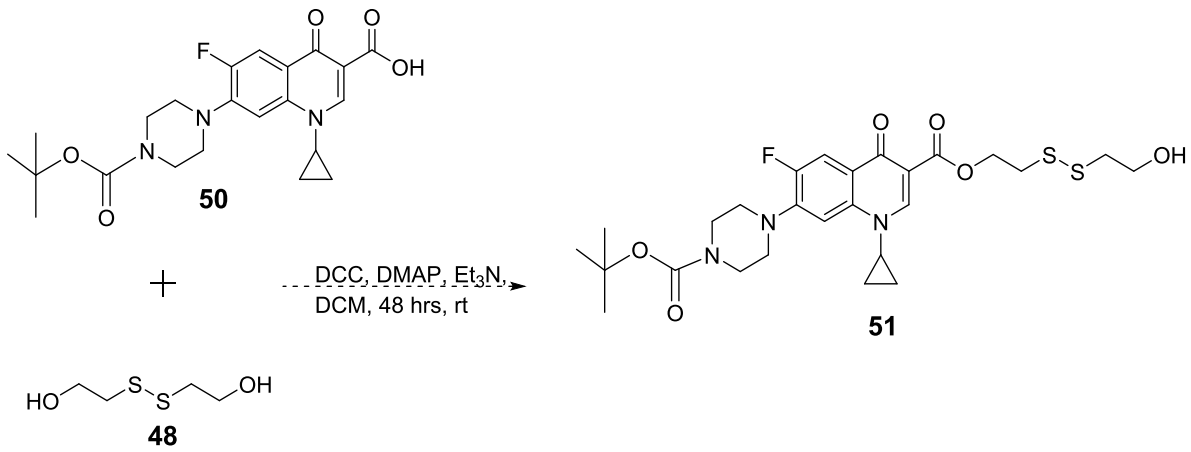

Scheme 13: Synthesis of boc-protected ciprofloxacin-2,2'-dithiodiethanol **51**

The attempted synthesis of **51** using DCC/DMAP method was repeated several times with no evidence of the coupled product. A few modifications were applied to the experimental procedure on each repeat, with the original procedure being based on the method adapted from Jain *et al.*[53] Some modifications included incremental changes in the molar ratios of DCC and DMAP in order to facilitate the activation of **50** and also carrying out the reaction under anhydrous conditions so as to avoid any side reactions with water.

Run Number	Boc-cip **50** / mmol	DCC / mmol	DMAP / mmol	Other Reaction Modification
1	0.36	0.36	0.36	THF
2	0.46	0.46	0.46	DMF
3	0.46	0.60	0.60	dry DCM
4	0.46	0.60	0.60	dry DCM, stepwise

Table 1: Table showing the modifications of the reaction conditions for the esterification of Boc-protected ciprofloxacin **50** using DCC/DMAP method

Another modification whereby reagents were added stepwise (run 4) to allow analysis of the activated intermediates was carried out. The active O-acylisourea intermediate often undergoes acetyl transfer forming the unreactive N-acylurea.[62] This competes with the forward esterification reaction which is catalysed by DMAP as shown in **Scheme 14**.

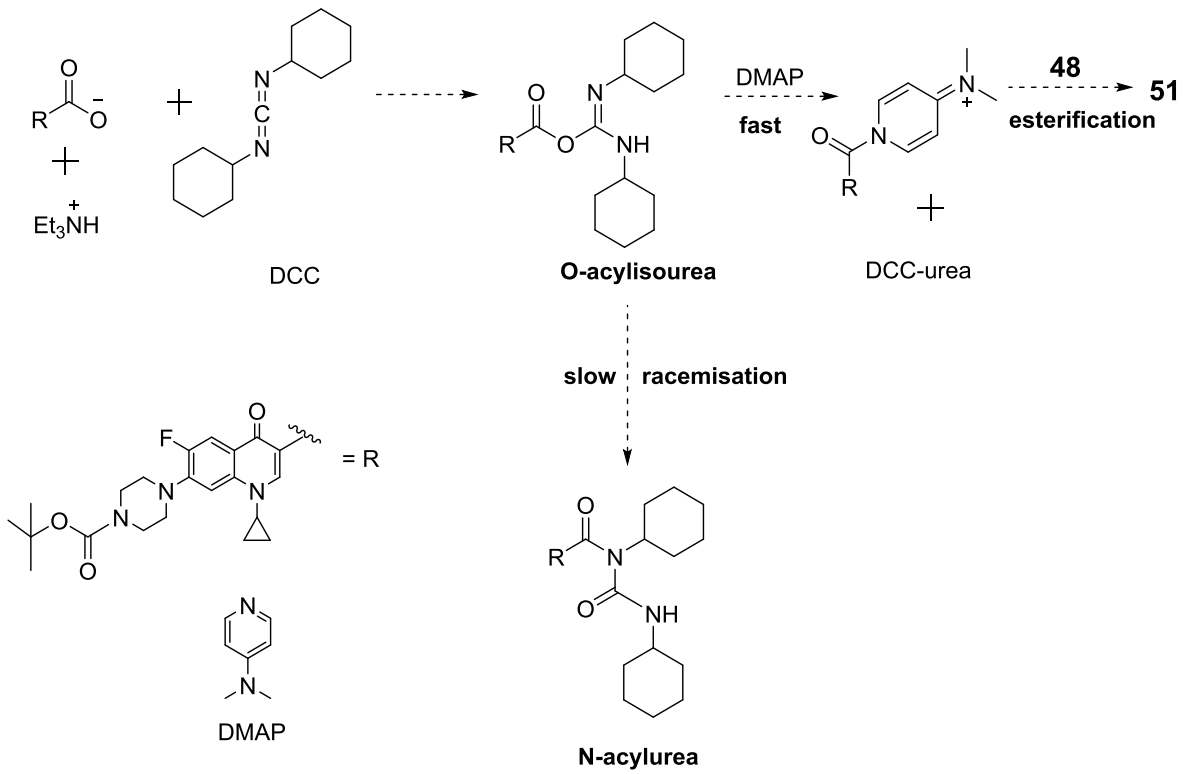

Scheme 14: Rearrangement and esterification of O-acylisourea

The unsuccessful esterification of **50** was thought to be due to rearrangement of O-acylisourea to unreactive N-acylurea. However this was found to be not the case as no evidence of either the O-acylisourea or N-acylurea was found by mass spectrometric analysis of the crude reaction mixture. A peak at m/z of 454.17 was evident in the spectrum, this corresponds to unreacted **50** ($C_{22}H_{26}FN_3NaO_5$). Therefore it was concluded that there was no activation of **50** using the DCC/DMAP method and alternative methods were explored.

2.2.1.3. NHS/DCC – mediated esterification

An alternative activation method was explored using N-hydroxysuccinimide (NHS) and DCC as an activating agents.[65]

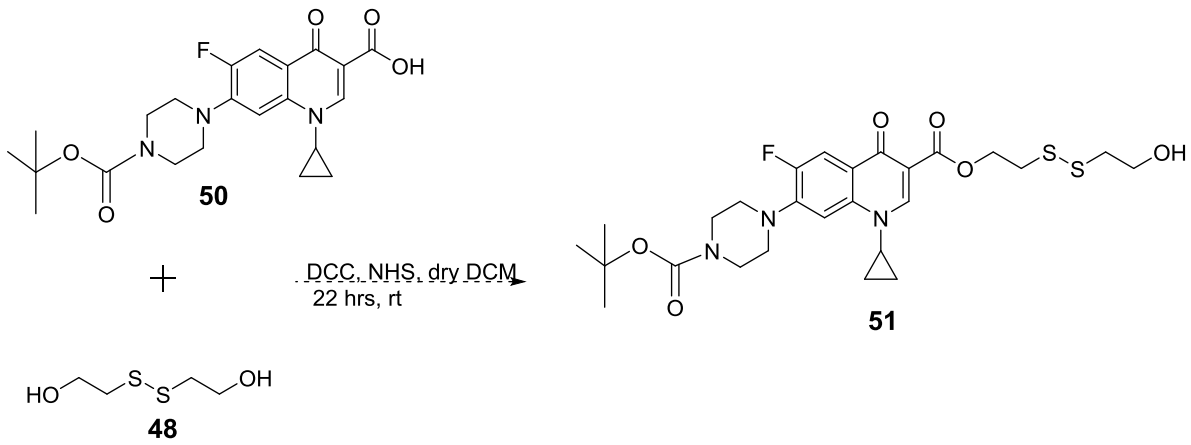

Scheme 15: Synthesis of **51** using DCC and NHS as activating agents

However, the synthesis was not successful as no evidence for the coupled product was observed either by mass spectrometric analysis or ^{1}H NMR spectroscopy of the crude reaction mixture. It was then decided to change the reactant ratios to 1:1.5:1.5 (Boc-ciprofloxacin: NHS: DCC) so as to increase the chances of the activation of **50**. The reaction was also carried out stepwise to allow isolation and analysis of the ciprofloxacin-NHS ester as shown below (**Scheme 16**).

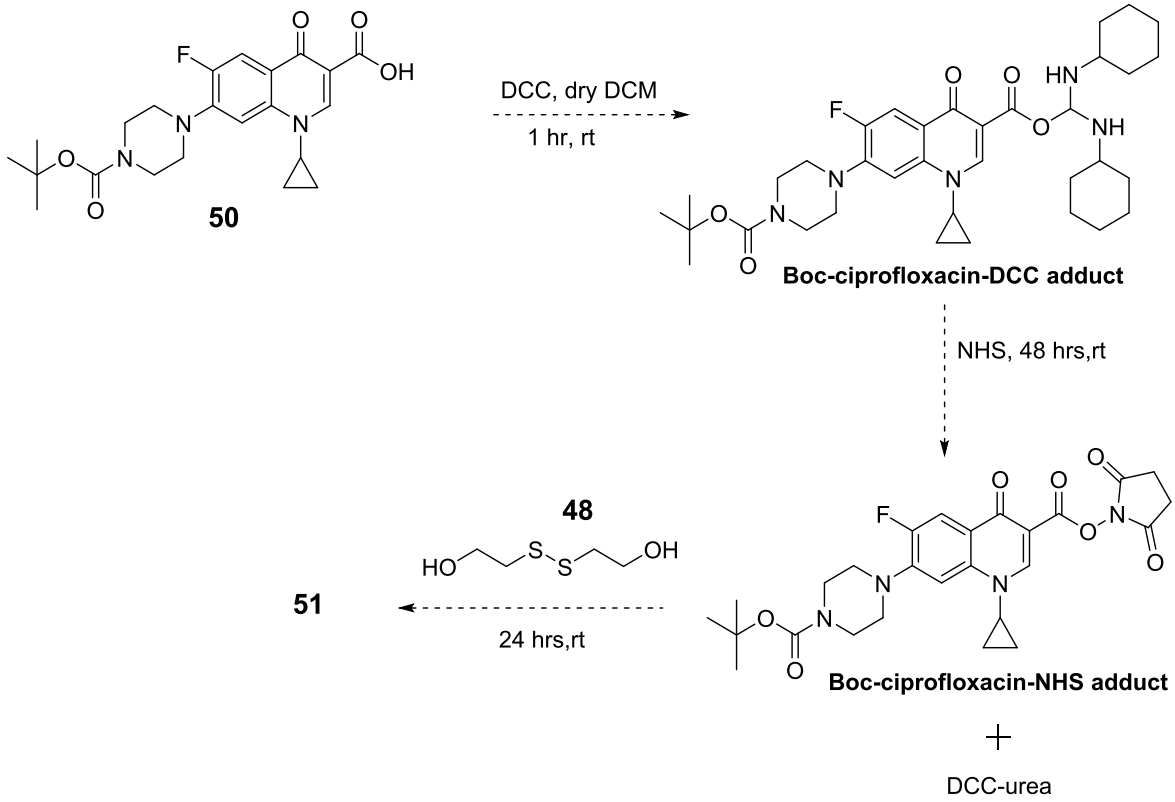

Scheme 16: Stepwise activation of Boc-ciprofloxacin with DCC and NHS

There was no visible change to the reaction mixture by observation or by TLC analysis and also mass spectrometric analysis did not show peaks relating to successful

product formation. Regardless of the unsuccessful isolation of the intermediates the reaction was continued by adding the 2,2'-dithiodiethanol **48** to the reaction mixture as the intermediates might not be stable enough to be isolated. However there was no evidence of **51** either by mass spectrometric or ^{1}H NMR spectroscopic analysis.

A control experiment was carried out in order to test the DCC/DMAP chemistry. Nicotinic acid **52** and 2,2'-dithiodiethanol **48** were used in the synthesis of nicotinic acid-2,2'-dithiodiethanol **53** using an experimental procedure adapted from Jain *et al*[53] (**Scheme 17**).

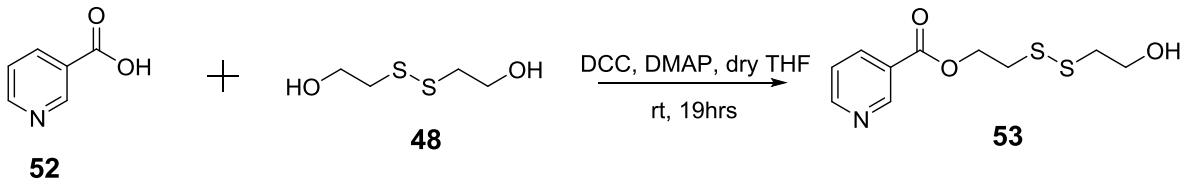

52 **48** **53**

Scheme 17: Synthesis of nicotinic acid-2,2'-dithiodiethanol **53**

The synthesis of **53** was successful by mass spectrometric analysis of the crude product. Peaks at m/z 260.04 and m/z 365.06 were observed in the mass spectrum, corresponding to $[M+H]^+$ $C_{10}H_{14}NO_3S_2$ and $[2M+H]^+$ $C_{16}H_{17}N_2O_4S_2$ respectively. This indicated the DCC/DMAP method is a viable method for esterification but it had proved unsuccessful with Boc-protected ciprofloxacin **50**.

It was then decided to explore alternative coupling reagents. Uronium salts such as HBTU and HATU have been found to be efficient peptide coupling reagents[66] therefore these agents were used in the esterification of Boc-protected ciprofloxacin **50** with disulfide **48**.

2.2.1.4. HBTU and HATU – mediated esterification

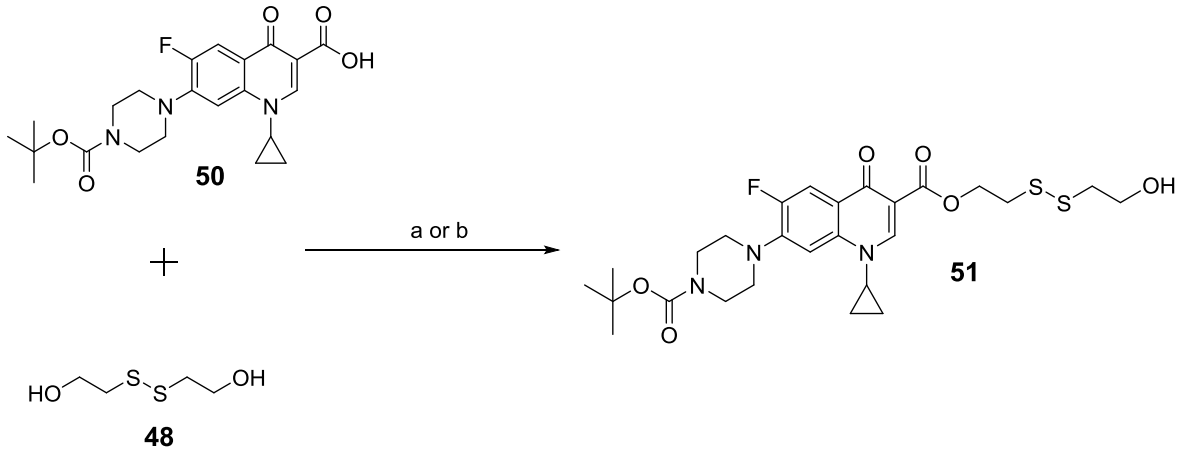

Scheme 18: Synthesis of **51**. Reagents and conditions: (a) HBTU, DMAP, DIPEA, dry DCM; (b) HATU, DMAP, DIPEA, dry DCM

The successful synthesis of **51** using either reagents a or b was supported by mass spectrometric analysis of the crude reaction mixture, in both reactions the mass spectra showed peaks for both the monomer and dimer at m/z 590.17 and 1003.35 which correspond to $[M+Na]^+$ and $[2M+Na]^+$ respectively. However the purification process was problematic due to co-elution with possibly the dimer during column chromatography and **51** was unable to be isolated to allow further characterisation.

Although both HBTU and HATU proved to be successful in performing the coupling between **50** and **48**, HATU was found to be more efficient of the two as the reaction time was significantly shorter although the yields were not evaluated at this stage due to problematic isolation. Looking at peptide coupling with HATU and HBTU, HATU shows enhanced reactivity towards amines relative to that of HBTU[66]. This is thought to be due to the effect of the neighbouring group on the intermediate as shown in **Figure 36**, with HATU an active ester intermediate is formed which is not possible when HBTU is used[66] therefore this could potentially be the reason for the observed faster reaction time with HATU.

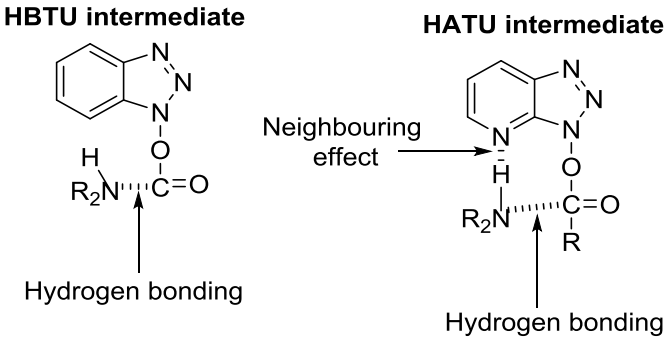

Figure 36. Intermediate structures of HBTU and HATU during peptide coupling

Since the purification of **51** was problematic it was decided to couple Boc-ciprofloxacin with a protected 2,2'-dithiodiethanol **54** (**Scheme 19**) aiming to change the polarity of the desired product **55** in order to obtain a better separation when using column chromatography.

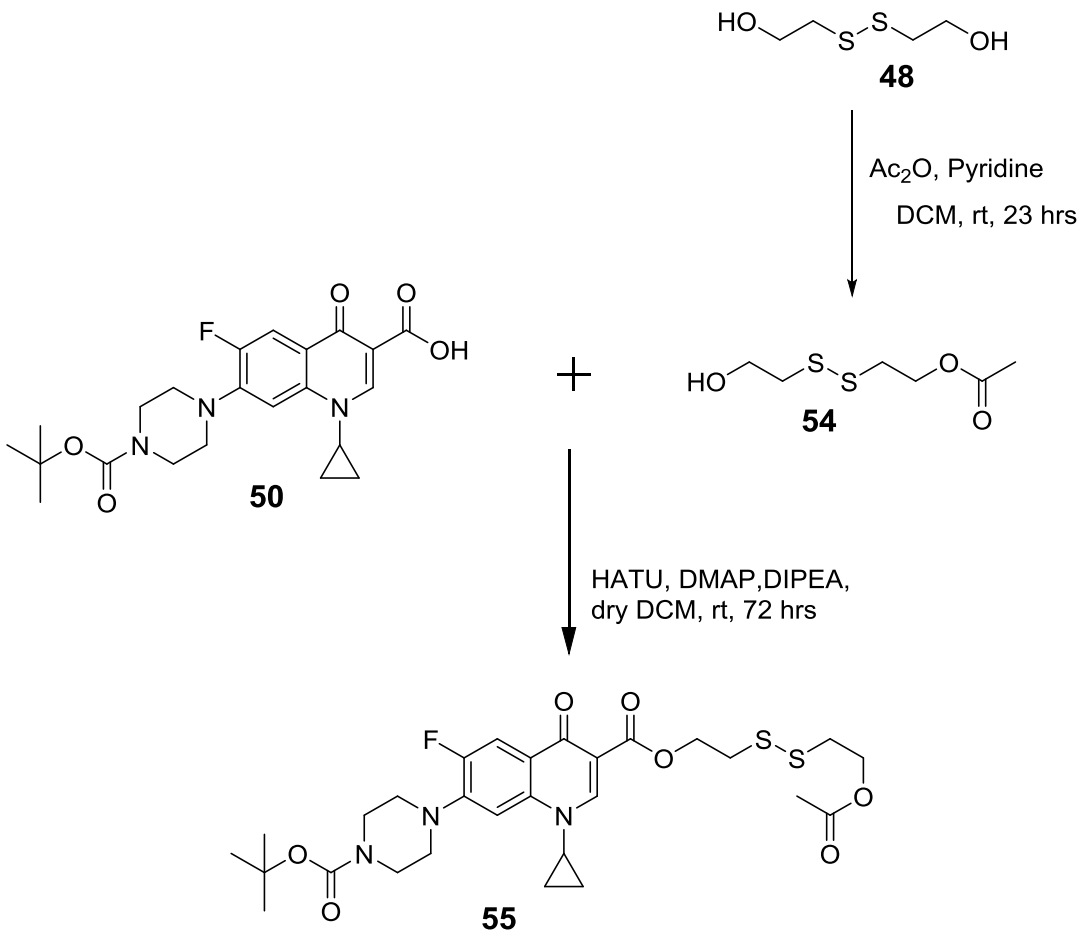

Scheme 19: The synthesis of conjugate **55**

Mono ester protected 2,2'-dithiodiethanol was synthesised and although the isolated yield of **54** was poor,26% , the successful synthesis of **54** was supported by mass

spectrometric analysis with a peak of m/z 219.01 corresponding to $[M+Na]^+$ present in the spectrum, ^1H NMR spectroscopic analysis showed the presence of a signal at 2.09 ppm (s, 3H) corresponding to the methyl group.

The protected disulfide **54** was then used in the HATU-mediated coupling with Boc-protected ciprofloxacin **50.** The successful synthesis of conjugate **55** was supported by mass spectrometric analysis with inspection of the spectrum revealing a peak at m/z of 632.19 $[M+Na]^+$, ^1H NMR spectroscopic analysis showed signals corresponding to the product; 1.41 ppm (s, 9H relative integration) of the Boc-protecting group and 1.98 ppm (s, 3H relative integration) corresponding to the acetate protecting group. ^{13}C NMR spectroscopic analysis showed the presence of three quaternary carbon signals at 170.28 ppm, 165.21ppm, and 164.17ppm. Analysis of the crude mixture strongly suggested that **55** was the main component of the reaction. However purification still proved to be problematic resulting in a poor 34% isolated yield of **55**.

Although conjugate **55** was synthesised successfully albeit in low yield, there was an additional problem, the removal of the methyl ester could result in the hydrolysis of the ester bond between **50** and **54**. Therefore it was decided that crude **51** could be further elaborated without purification, delaying a purification step to later in the synthesis.

2.2.2. Conjugation of alanine

Commercially available Boc-Ala **56** was coupled to crude **51** using a method adapted from Dhaon *et al*. for the esterification of N-protected α-amino acids.[67] The successful synthesis of **57** was supported by mass spectrometric analysis, ^{1}H NMR, ^{13}C NMR spectroscopy and IR analysis.

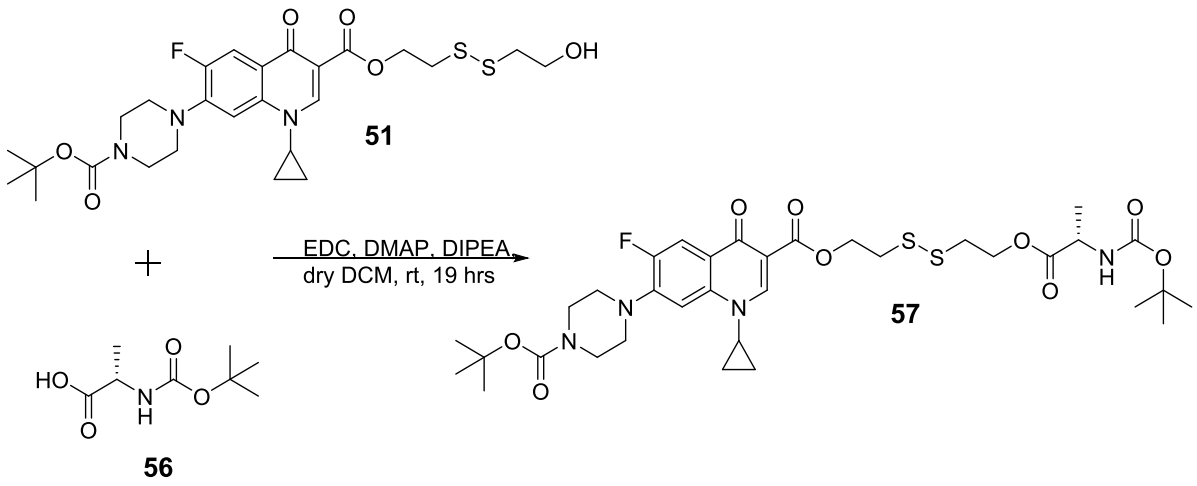

Scheme 20: The synthesis of conjugate **57** using EDC

The mass spectrum showed a peak at m/z of 761.27 which corresponds to $[M+Na]^{+}$, the ^{1}H NMR spectrum showed the presence of two Boc-groups with signals at 1.48 ppm (s, 9H relative integration), 1.42 ppm (s, 9H relative integration) and also multiplets corresponding to the disulfide backbone 2.82 ppm (m, 2H relative integration), 2.90 ppm (m, 2H relative integration) and 4.29 – 4.36 ppm (m, 4H relative integration). The connectivity was probed by two dimensional NMR spectroscopy.

The homonuclear correlation spectroscopy (COSY) shown below showed the expected coupling between the alanine methyl side chain and the α – hydrogen and the disulfide backbone protons strongly supporting the structure of **57** (**Figure 37**). ^{13}C NMR showed three quaternary carbon signals at 172.69 ppm, 172.15 ppm and 164.02 ppm also two signals at 27.87 ppm and 27.94 ppm corresponding to the Boc-groups, in addition IR spectroscopy showed the presence of N-H amide stretch at 3301 cm^{-1}.

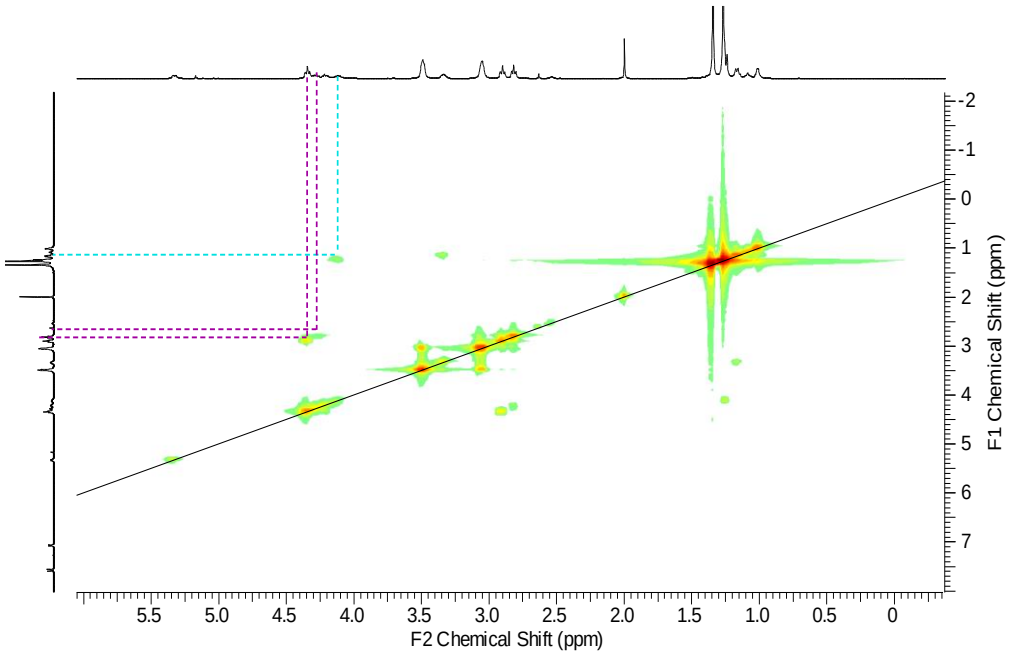

Figure 37: COSY NMR spectrum of **57** showing the coupling between the disulfide backbone protons (purple dotted lines) and coupling between the side chain methyl group and the α – CH (green dotted lines)

2.2.3. Deprotection of conjugate 57

Conjugate **57** has Boc protecting groups at both ends of the conjugate, therefore a global Boc-deprotection using 20%TFA in dry DCM to produce conjugate **58** was undertaken as shown in **Scheme 21**.

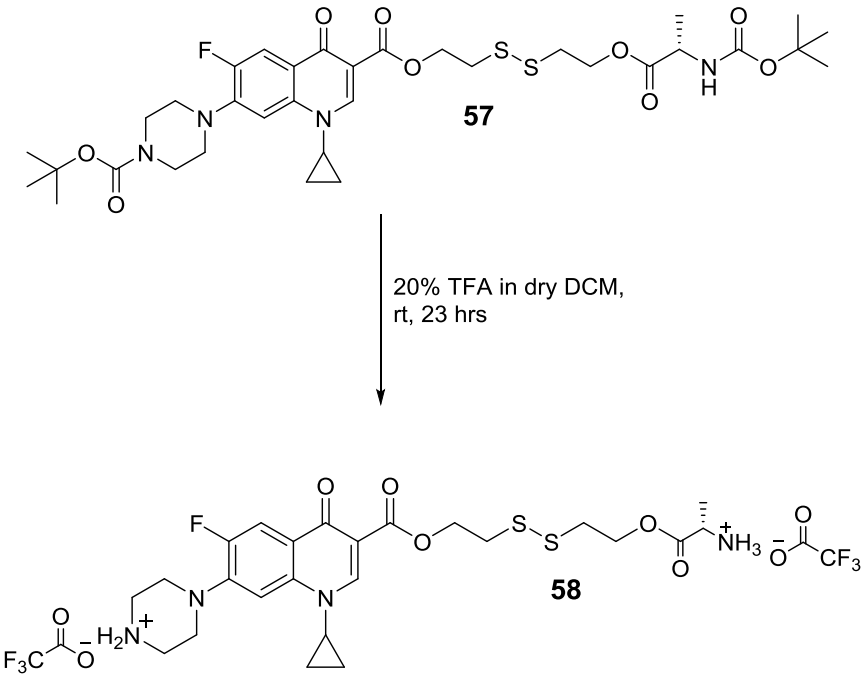

Scheme 21: The deprotection of conjugate **57**

The successful synthesis of conjugate **58** was supported by; mass spectrometric analysis which showed a peak with an m/z of 270.09 $[M]^{2+}$ $C_{24}H_{33}FN_4O_5S_2$ present in the spectrum, ^{1}H NMR spectrum supported the successful deprotection as signals at 1.42 ppm and 1.48 ppm corresponding to the t-butyloxycarbonyl group protons were not present in the spectrum and ^{13}C NMR spectrum showed only two quaternary carbon signals at 171.10 ppm and 167.35 ppm with no signals for the t-butyloxycarbonyl groups.

2.2.4. Counter - ion exchange of 58

As mentioned in **Section 2.1.4.** TFA salts are known to perturb *in vivo* studies[58] therefore the trifluroacetate was exchanged with a more bio-compatible ion, chloride.

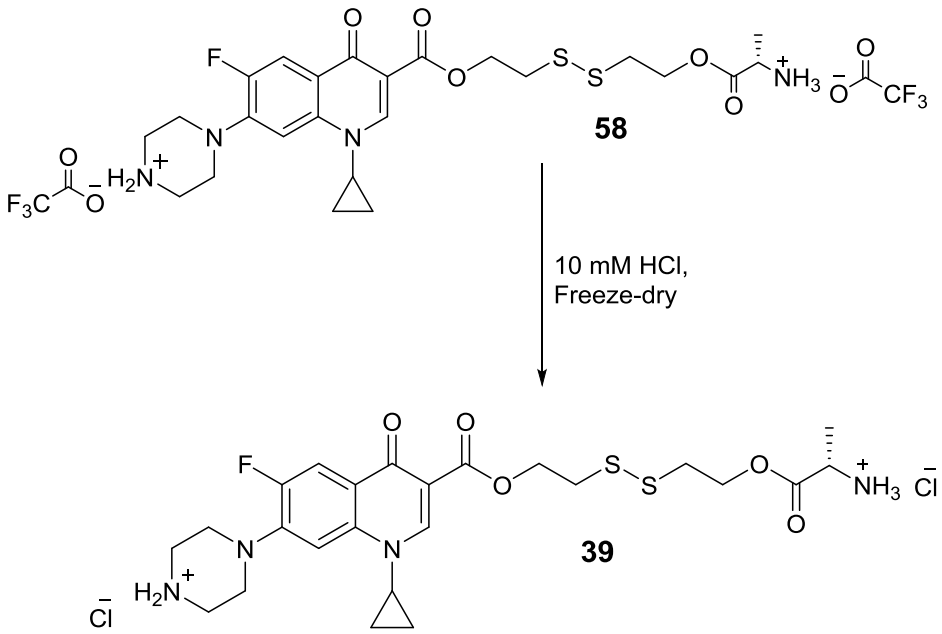

Scheme 22: Counter ion exchange of conjugate **58**

The successful synthesis of **39** was supported by ^{19}F NMR spectroscopic analysis which showed one peak at -122.29 ppm corresponding to the ciprofloxacin fluorine and no peak was observed at -76.76 ppm confirming the successful removal of trifluroacetate. The mass spectrometric analysis showed a peak at m/z 270.09 corresponding to $[M]^{2+}$ $C_{24}H_{33}FN_4O_5S_2$ present in the spectrum.

The successful synthesis of **39** showed the chemistry to be reliable therefore ciprofloxacin-disulfide-diAla **40** was synthesised using the same synthetic procedures developed in **Section 2.3.**

2.3. Synthesis of ciprofloxacin-disulfide-diAla conjugate 40

The dipeptide Ala-Ala was used a nutrient as it has been observed that the PTR secondary active transporters have higher affinity for di-and tri-peptides over single amino acids.[44] Therefore, ciprofloxacin-disulfide-diAla **40** was synthesised to exploit the PTR secondary active transporters so as to actively transport the conjugate across the bacterial inner membrane. The proposed synthesis of **40** is shown **Scheme 23**.

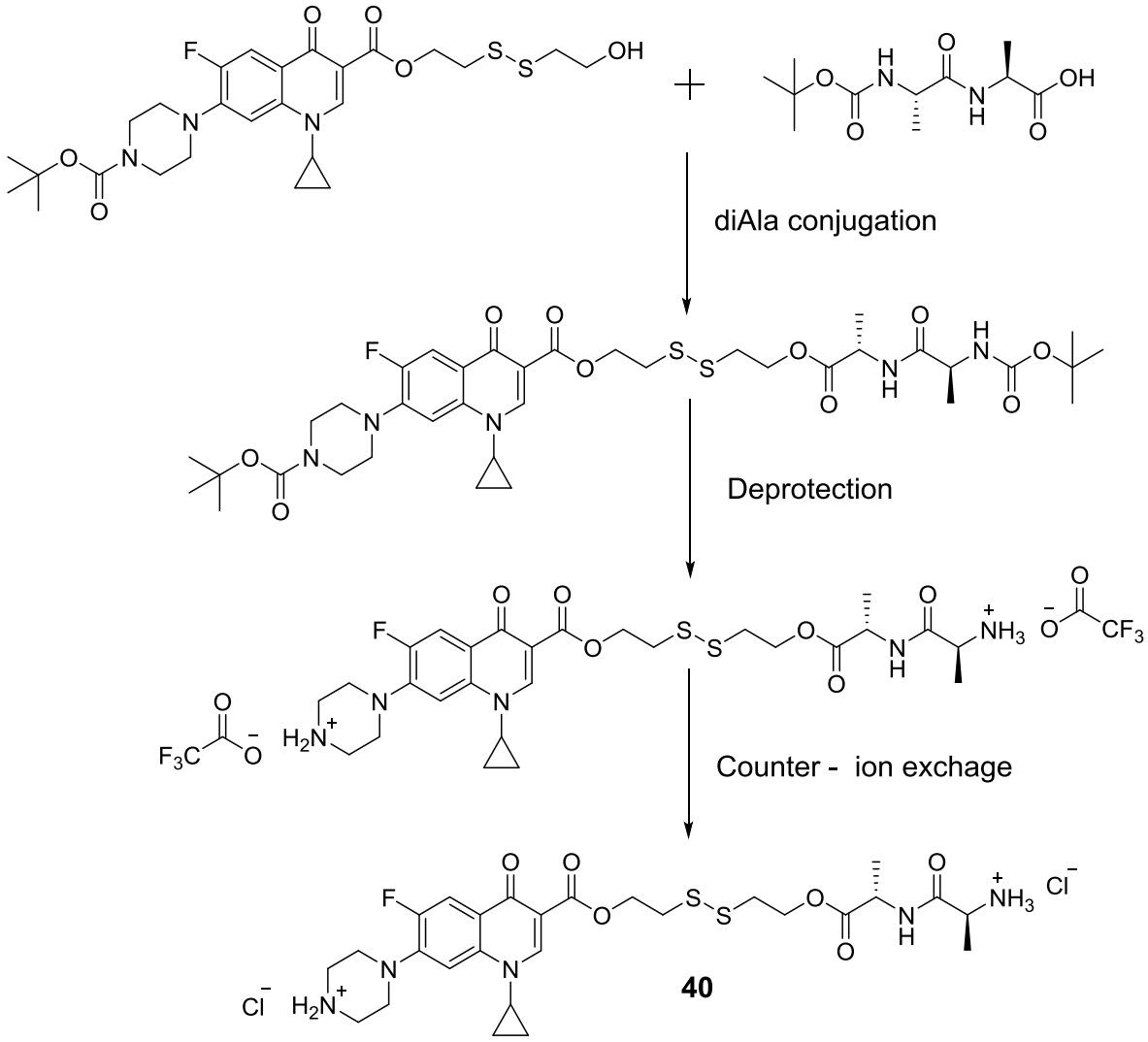

Scheme 23: The proposed synthesis of **40**

2.3.1. Conjugation of boc-diAla 59 to boc-ciprofloxacin-2,2'-dithiodiethanol 52

Boc-diAla **59** was coupled to crude Boc-ciprofloxacin-2,2'-dithiodiethanol **52** using the same synthetic procedure in **Section 2.2.1.5.** adapted from Dhaon *et al.*[67]

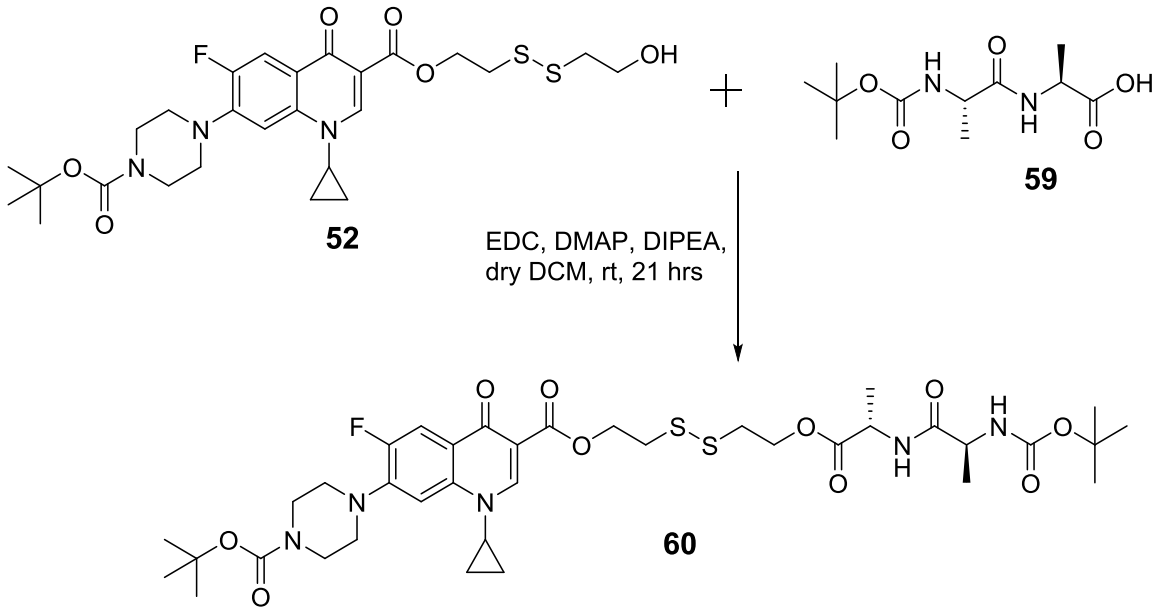

Scheme 24: The synthesis of **60** using EDC and DMAP coupling agents

The successful synthesis of **60** was supported by mass spectrometric, ^{1}H NMR spectroscopic and ^{13}C NMR spectroscopic analysis. Mass spectrometric analysis showed a peak with an m/z of 832.31 corresponding to $[M+Na]^{+}$, the ^{1}H NMR spectrum showed a multiplet at 1.33 ppm (5H relative integration) corresponding to 5H of the two CH_3 side chains of the dipeptide with the remaining proton incooperated into the peak at 1.41 ppm (10H relative integration) which corresponds to the 9H of one of the t-butyloxycarbonyl groups. A peak for the other t-butyloxycarbonyl group was observed at 1.47 ppm (9H relative integration). Disulfide backbone protons were also observed at 2.94 ppm (m, 2H relative integration), 3.04 ppm (m, 2H relative integration), 4.35-4.54 ppm (m, 5H relative integration) which incooperated one of the α – CH protons with the other α – CH observed at 4.21 ppm (m, 1H). COSY spectroscopy (**Figure 38**) showed the expected coupling in the peptide and disulfide therefore the structure of **60** was strongly supported by the ^{1}H spectroscopic evidence.

^{13}C NMR spectrum showed the presence of two t-butyloxycarbonyl with peaks at 27.91 ppm and 28.01 ppm corresponding to the methyl groups and peaks for the

peptide CH_3 side chain groups were also observed at 17.63 ppm, In addition four quaternary carbon signals were also observed.

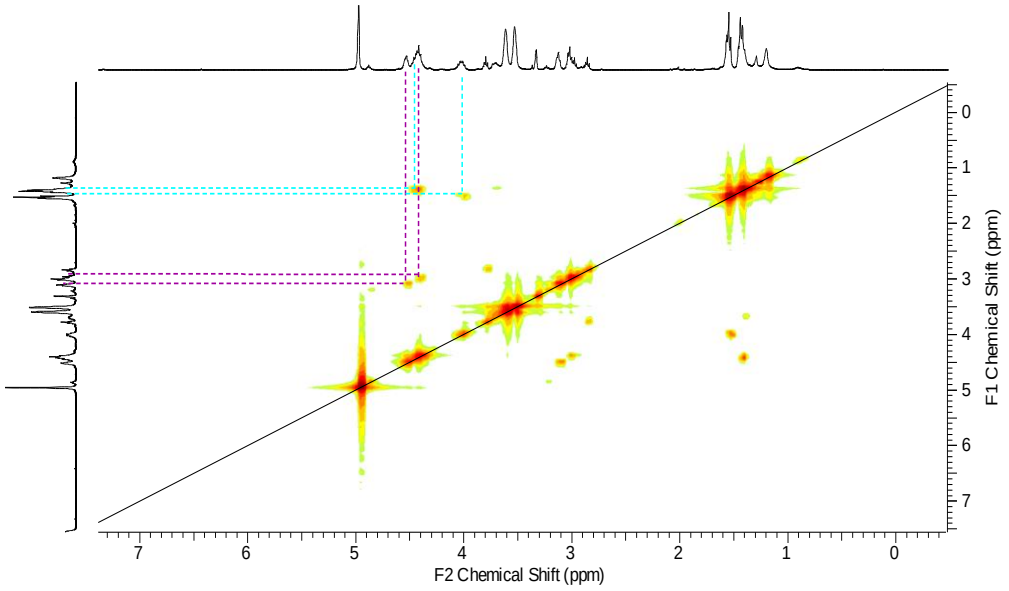

Figure 38: COSY NMR of **60** showing the coupling between disulfide backbone protons (purple dotted lines) and coupling between the side chain methyl groups and the α – CH (green dotted lines)

2.3.2. Deprotection of 60

The t-butyloxycarbonyl protecting groups on conjugate **60** were removed using the 20%TFA in dry DCM to produce **61**.

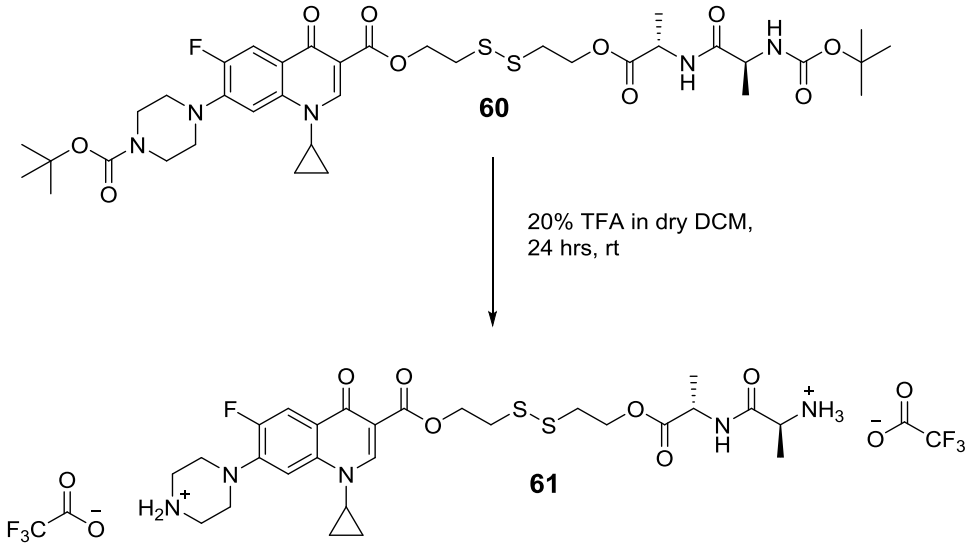

Scheme 25: Deprotection of conjugate **60**

The successful synthesis of conjugate **61** was supported by; mass spectrometric analysis which showed a peak with an m/z of 305.61 $[M]^{2+}$ $C_{27}H_{38}FN_5O_6S_2$ present in the spectrum. In addition, ^{1}H NMR spectroscopic analysis showed the signals at 1.41 ppm and 1.47 ppm corresponding to the t-butyloxycarbonyl group protons were not absent from the spectrum. In addition the ^{13}C NMR spectrum showed only three quaternary carbon signals at 174.06 ppm, 170.60 ppm and 163.23 ppm with no signals for the t-butyloxycarbonyl groups observed.

2.3.3. Counter - ion exchange of 61

Trifluroacetate was exchanged with a more bio-compatible ion, chloride, by freeze-drying conjugate **61** with 10 mM HCl.

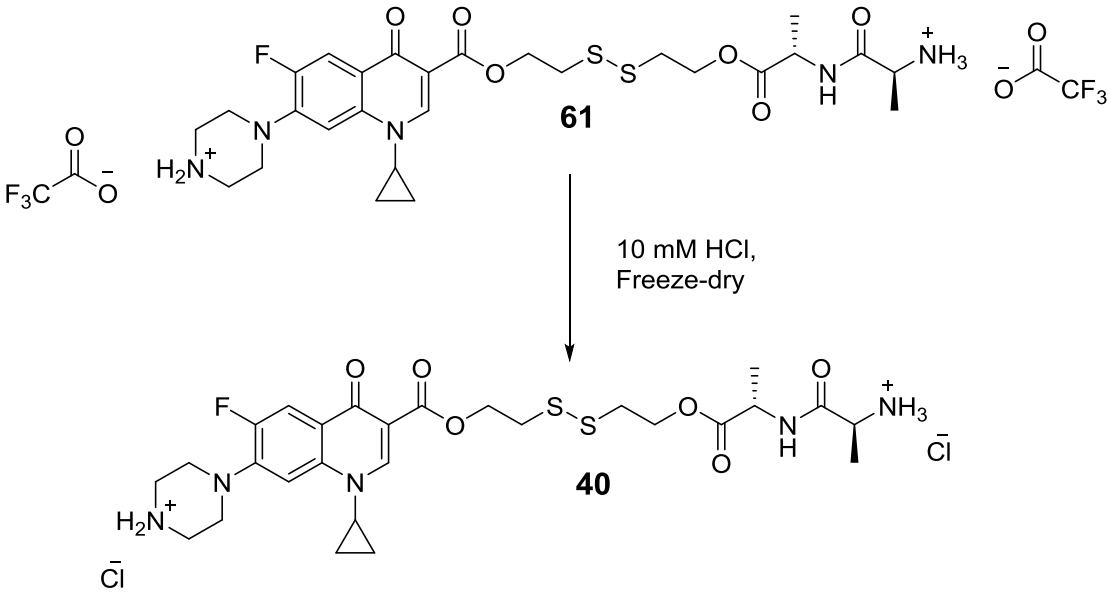

Scheme 26: Counter - ion exchange of conjugate **61**

The successful ion exchange in **40** was supported by ^{19}F NMR spectroscopic analysis which showed one peak at -122.82 ppm corresponding to the ciprofloxacin fluorine and no peak was observed at -76.75 ppm confirming the successful removal of trifluroacetate. The mass spectrometric analysis showed a peak at m/z 305.61 $[M]^{2+}$ $C_{27}H_{38}FN_5O_6S_2$ present in the spectrum.

2.4. Biological screening of conjugate 38 and 46

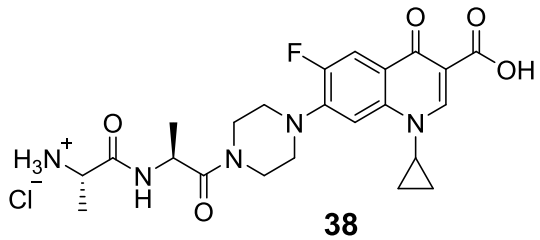

38

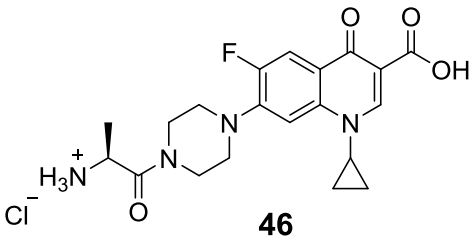

46

Figure 39: Structures of conjugate **38** and **46**

Conjugate **38** was tested for antibacterial activity against *E. coli* with a direct comparison to **46** since **28** (in its non-counter ion exchanged form) was shown to retain antimicrobial activity but at a lower level than ciprofloxacin (unpublished results). TFA acetate was used as a control in-order to determine if antimicrobial activity observed for conjugate **28** was due to the trifluroacetate.[58]

In vivo assays were carried out at different concentrations in lysogenic broth (LB) using sterile techniques to prepare a 96 well plate with the layout outlined in **Table 2**.

1	2	3	4	5	6	7	8	9	10	11	12
A											
B	TFA(1)	TFA(2)	TFA(3)	Cip-Ala(1)	Cip-Ala(2)	Cip-Ala(3)	Cip-diAla(1)	Cip-diAla(2)	Cip-diAla(3)	Blank	
C	TFA(1)	TFA(2)	TFA(3)	Cip-Ala(1)	Cip-Ala(2)	Cip-Ala(3)	Cip-diAla(1)	Cip-diAla(2)	Cip-diAla(3)	Blank	
D	TFA(1)	TFA(2)	TFA(3)	Cip-Ala(1)	Cip-Ala(2)	Cip-Ala(3)	Cip-diAla(1)	Cip-diAla(2)	Cip-diAla(3)	Blank	
E	TFA(1)	TFA(2)	TFA(3)	Cip-Ala(1)	Cip-Ala(2)	Cip-Ala(3)	Cip-diAla(1)	Cip-diAla(2)	Cip-diAla(3)	Blank	
F	TFA(1)	TFA(2)	TFA(3)	Cip-Ala(1)	Cip-Ala(2)	Cip-Ala(3)	Cip-diAla(1)	Cip-diAla(2)	Cip-diAla(3)	Blank	
G	TFA(1)	TFA(2)	TFA(3)	Cip-Ala(1)	Cip-Ala(2)	Cip-Ala(3)	Cip-diAla(1)	Cip-diAla(2)	Cip-diAla(3)	Blank	
H											

Drug conc/ µM	Stock conc/ µM
0.0	0
2.0	10
4.0	20
6.0	30
8.0	40
10	50

Key:

TFA = Trifluroacetate

Cip-Ala = **46**

Cip-diAla = **38**

Table 2: 96 - well plate layout for *in vivo* plate reader assay with triple replicates of each antibiotic; cip-Ala **46** and cip-diAla **38** and trifluroacetate. Row B is a control with 0µM drug concentration; rows C-G are wells with increasing drug concentration, blank wells in column 11 and sterile water in the surrounding wells

E. coli was grown for 16 hours and absorbance (OD) was measured every 30 minutes to generate growth curves with trifluroacetate as a control. **Figure 40** shows that under control conditions; when no conjugate or trifluroacetate present, WT *E. coli* BW25113 strain reaches a peak OD_{650} of ~ 3 after about 11 hours.

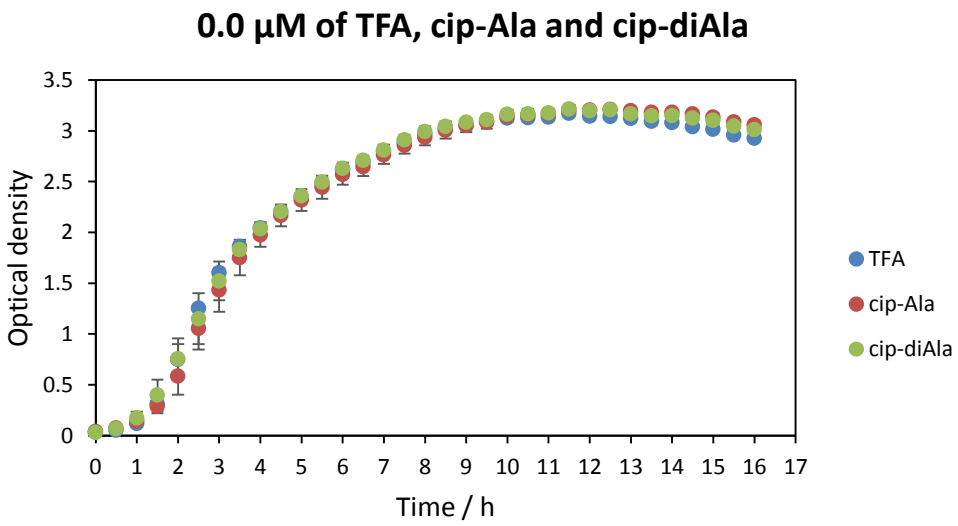

Figure 40: Control bacterial growth curve of BW25113 strain of *E. coli*. Error bars are ± standard deviation of three biological replicates

Adding 2.0 µM of trifluroacetate and cip-diAla **38** did not have any significant effect on the bacterial growth as a maximum OD_{650} of ~ 2.8 was reached after 8 hours (**Figure 41A**) which is not substantially different from the maximum OD_{650} ~ 3 reached under control conditions (**Figure 40**).

However, a difference in bacterial growth was observed with cip-Ala **46** at 2.0 µM, reaching a maximum OD_{650} of ~ 0.6 after 5 hours and almost complete bacterial growth inhibition after 12 hours (**Figure 41A**). This suggests that for **46** MIC > 0.0 µM but ≤ 2.0 µM, it also shows that the antimicrobial activity observed for **28**, the TFA salt of cip-Ala, was not due to the presence of trifluroacetate since no observable inhibition of bacterial growth was observed with trifluroacetate at this concentration.

These results indicate that **46** is a more effective bacterial growth inhibitor than **38**, suggesting that **38** is not being actively transported but probably entering the bacterial inner membrane by passive diffusion. The reduction in antimicrobial activity of **38** could also be due to the presence of the nutrient moiety as it has been suggested that a group on the piperazinyl nitrogen significantly reduces the ability of the fluoroquinolone to interact with DNA gyrase therefore leading to incomplete inhibition[30,29] and lower antimicrobial activity.

Increasing the concentration from 2.0 µM to 4.0 µM (**Figure 41B**) showed reduction in bacterial growth with **38** reaching a peak OD_{650} of ~ 2.0 after 5 hours and a

minimum OD_{650} of ~ 0.9 after 16 hours. This significant reduction in bacterial growth suggests that the MIC for **38** is between 2.0 µM and 4.0 µM. Cip-Ala **46** had increased antimicrobial activity at 4.0 µM with almost complete bacterial growth inhibition after 9 hours as opposed to after 12 hours at 2.0 µM.

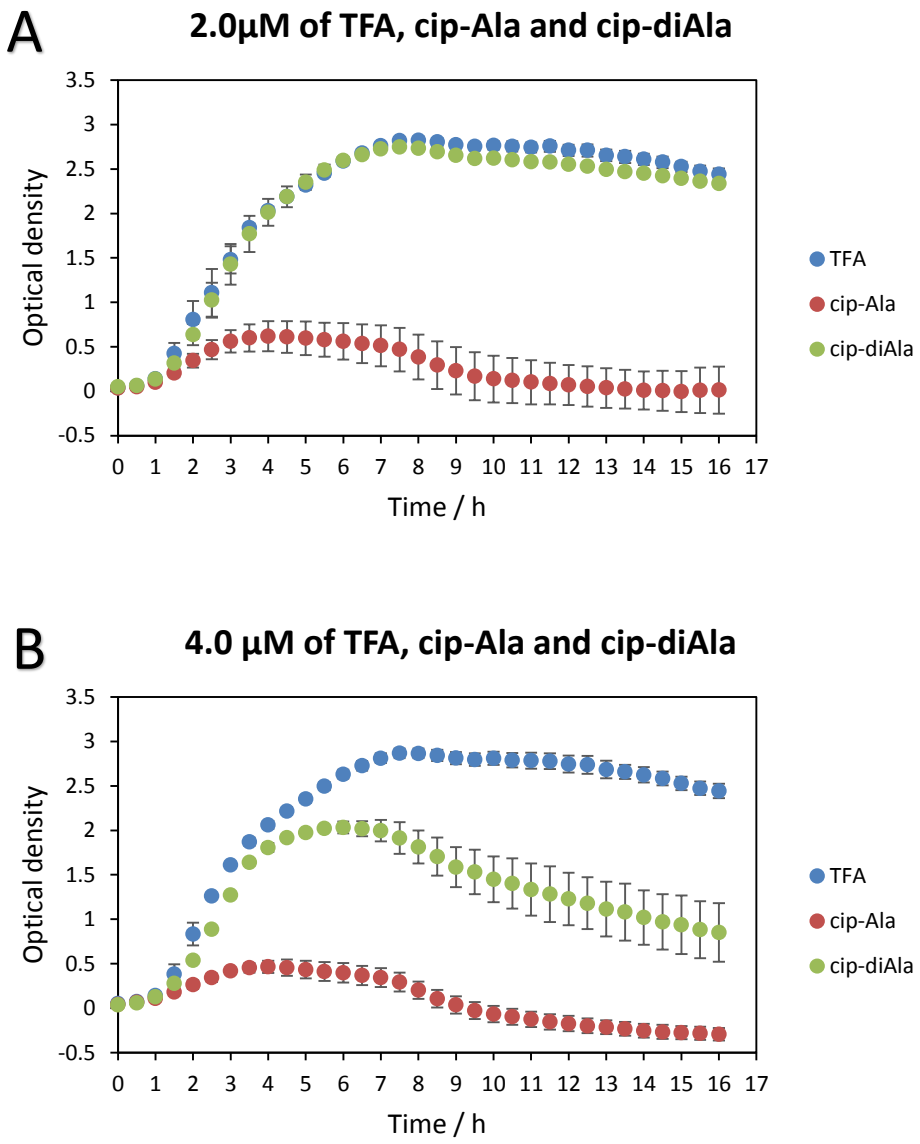

Figure 41: Bacterial growth curve of *E. coli* BW25113 with 2.0 µM (**A**) and 4.0 µM (**B**) additives. Error bars are ± standard deviation of three biological replicates

Further increase in concentration to 6.0 µM (**Figure 42A**), 8.0 µM (**Figure 42B**) and 10.0 µM (**Figure 42C**) had a significant increase on the antimicrobial activity of cip-diAla **38**, little effect on the antimicrobial activity of cip-Ala **46**.

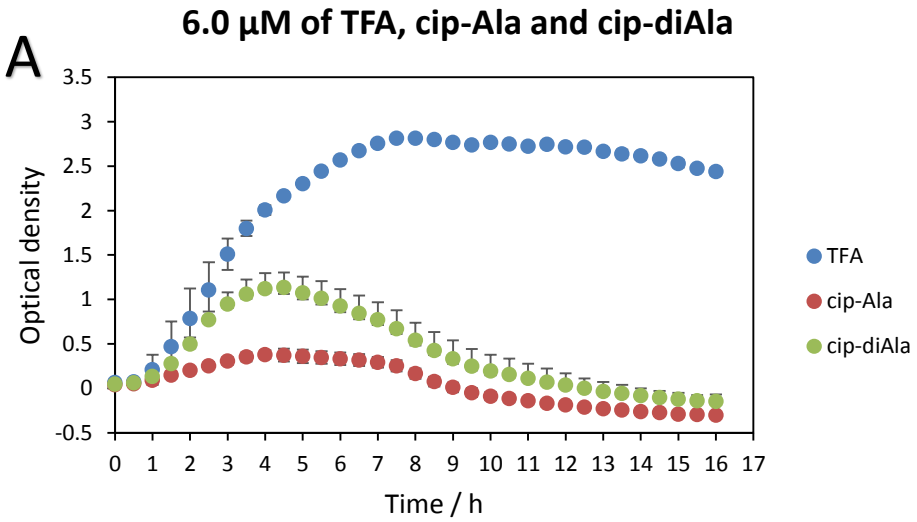

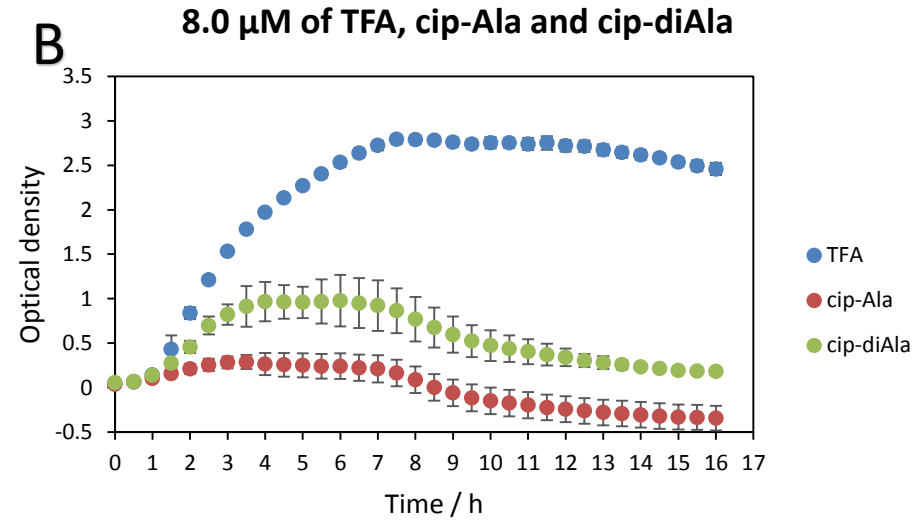

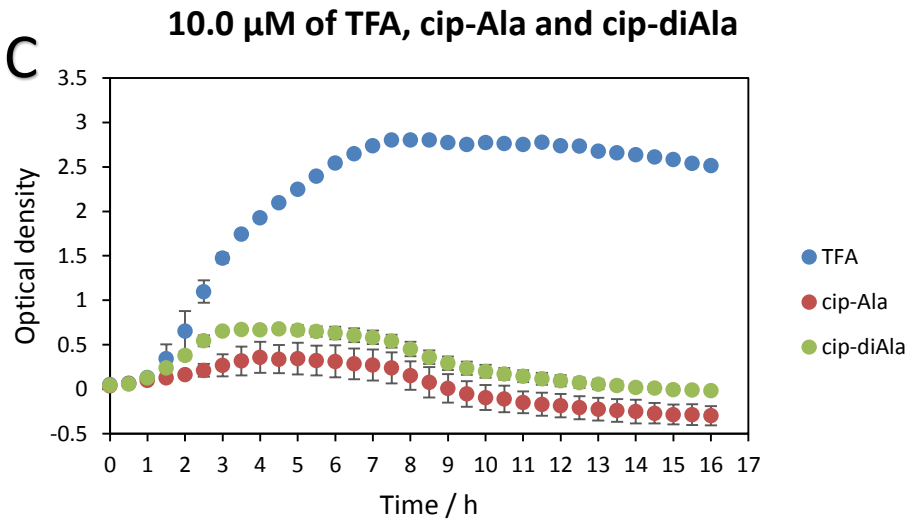

Figure 42: Bacterial growth curve of *E. coli* BW25113 grown with 6.0 µM (**A**), 8.0 µM (**B**) and 10.0 µM (**C**) additives. Error bars are ± standard deviation of three biological replicates

These results show that conjugate **38** has significantly reduced activity against *E. coli* BW25113 compared to **46** at the same concentration. This reduction has been suggested to be due to the nutrient moiety at the piperazinyl nitrogen which significantly reduces the ability of the fluoroquinolone to interact with DNA gyrase therefore leading to incomplete inhibition with diAla having a larger effect than Ala.

In-order to determine the effect of conjugating a di-peptide on the gyrase inhibitory activity of ciprofloxacin in-vitro DNA gyrase experiments were performed with ciprofloxacin as a control.

2.4.1. DNA gyrase assays

Gyrase assays show the DNA gyrase inhibition ability of the compounds, with the presence of relaxed plasmid on the gyrase indicating the inhibition of DNA gyrase whereas supercoiled plasmid indicates the activity of DNA gyrase therefore the compound has reduced activity or is inactive. Relaxed pBR322 open complex bacterial plasmid was incubated with *E. coli* DNA gyrase at variable concentrations of ciprofloxacin or cip-diAla **38** to investigate any changes in the DNA gyrase's ability to supercoil relaxed DNA at relatively low and high concentrations.

Ciprofloxacin	
Stock conc/ µM	Drug conc/ µM
3	0.1
6	0.2
9	0.3
12	0.4
15	0.5

Cip-diAla	
Stock conc/ µM	Drug conc/ µM
200	6
400	13
600	20
800	27
1000	33

Table 3: Tables showing the concentration of antibiotics used for each assay

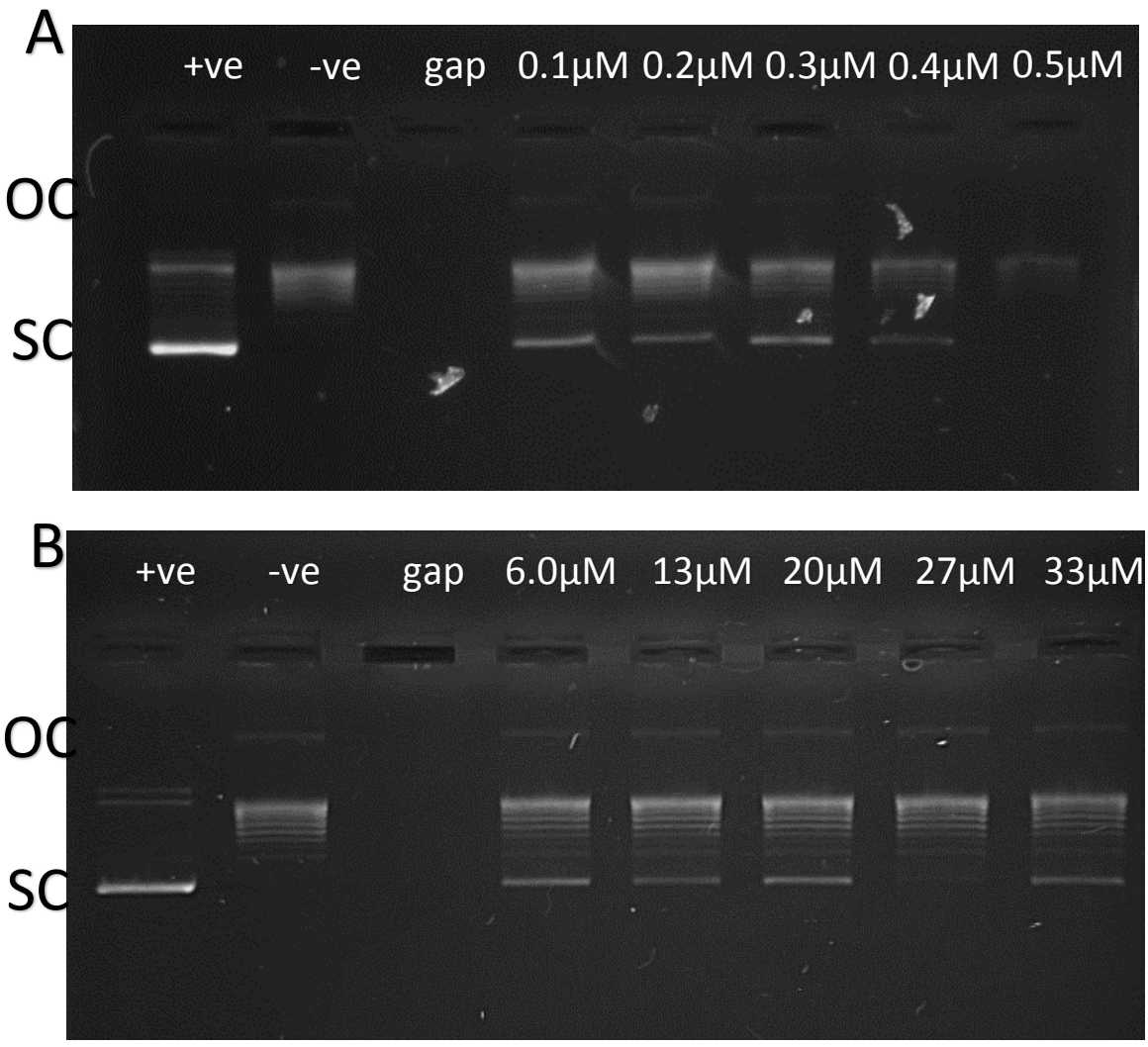

Figure 43: DNA gyrase assay of ciprofloxacin (**A**) and cip-diAla **38** (**B**) at different concentrations with positive control (+ve) – 2 µl DNA gyrase and 0.0 µM of drug, negative control (-ve) – no DNA gyrase and 0.0 µM of drug and an empty well (gap). OC- open circular and SC- supercoiled plasmid

Treatment of relaxed pBR322 with DNA gyrase converts the relaxed plasmid to the supercoiled plasmid which migrates faster on agarose gel as observed with the +ve control (**Figure 43**), an open circular plasmid is present in the relaxed plasmid and it co-migrates with some of the relaxed plasmid as observed with the –ve control (**Figure 43**).

Very little inhibition of DNA gyrase was observed between 0.1 µM and 0.3 µM of ciprofloxacin (**Figure 43A**) as the supercoiled bands were still present but also thick open complex bands were observed, as the concentration was increased to 0.4 µM significant inhibition of DNA gyrase was observed with more relaxed plasmid bands and a faint supercoiled band across the agarose gel. At 0.5 µM of ciprofloxacin, (**Figure 43A**) very faint relaxed plasmid bands were observed and no supercoil bands present, this could be due to pipetting error with not enough sample added to the well.

Cip-diAla **38** showed some gyrase inhibition between 6.0 µM and 20µM as both relaxed plasmid bands and supercoiled bands were observed (**Figure 43B**). However the intensity of the bands is similar at these three concentrations suggesting that the gyrase inhibitory activity of cip-diAla is not increasing with concentration. At 27µM no supercoiled band is observed but at 33 µM the band is present (**Figure 43B**) suggesting that the absence of the supercoiled band at 27 µM could have been due to pipetting error and not due to gyrase inhibition by cip-diAla.

Cip-diAla **38** has significantly reduced activity against *E. coli* DNA gyrase compared to that of ciprofloxacin, considering that at relatively high concentration of cip-diAla (20 µM) the supercoiled band is still present therefore cip-diAla does not completely inhibit DNA gyrase at this concentration. However, according to the *in vivo* assays of cip-diAla **38** (**Figure 42C**) cip-diAla almost completely inhibits bacterial growth of BW25113 strain of *E. coli* at 10.0 µM after about 15 hours. It has been reported that the MIC for intact bacteria can be much lower than the concentrations required to inhibit the gyrase from the same organism[15] therefore more gyrase assays at different concentrations of cip-diAla will need to be carried out in-order to compare the MIC and Ki (inhibition constant) of cip-diAla in *E. coli*.

It can be concluded from these results that the conjugate diAla significantly interferes with the inhibition of DNA gyrase therefore causing reduction in the activity of cip-diAla **38**. This may be due to the additional steric bulk which may be preventing the

effective formation of the DNA-enzyme-drug complex (**Figure 12**) which is critical for the activity of fluoroquinolones.[20] Therefore ciprofloxacin conjugates **39** and **40** with a bio-labile linker which allows the release of free ciprofloxacin within the bacterial inner membrane were synthesised.

2.5. Biological screening of conjugate 39 and 40

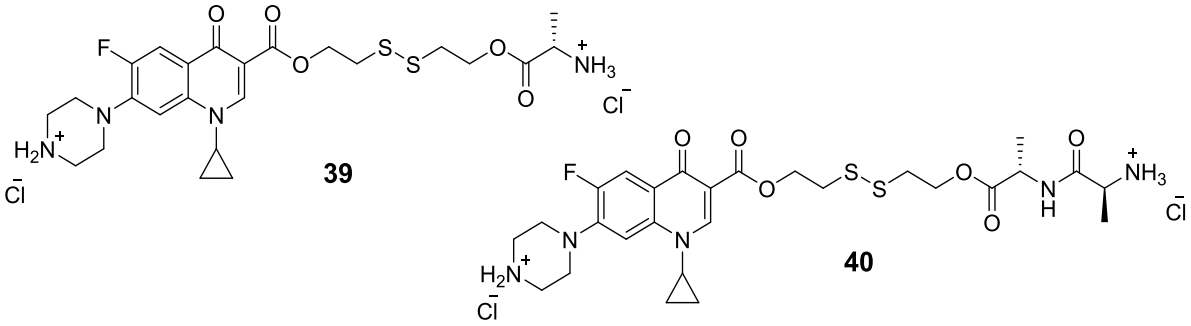

Figure 44: Structures of conjugate **39** and **40**

In vivo assays of conjugate **39** and **40** against *E. coli* BW25113 to test if the novel bio-labile linked compounds had increased antimicrobial activity compared to free ciprofloxacin as the conjugates are proposed to be actively transported by peptide transporters. The *in vivo* assays were carried out at different concentrations in LB using sterile techniques to prepare a 96 well plate with the layout outlined in **Table 4**.

1	2	3	4	5	6	7	8	9	10	11	12
A											
B	Cip(1)	Cip(2)	Cip(3)	Cip-link-Ala(1)	Cip-link-Ala(2)	Cip-link-Ala(3)	Cip-link-diAla(1)	Cip-link-diAla(2)	Cip-link-diAla(3)	Blank	
C	Cip(1)	Cip(2)	Cip(3)	Cip-link-Ala(1)	Cip-link-Ala(2)	Cip-link-Ala(3)	Cip-link-diAla(1)	Cip-link-diAla(2)	Cip-link-diAla(3)	Blank	
D	Cip(1)	Cip(2)	Cip(3)	Cip-link-Ala(1)	Cip-link-Ala(2)	Cip-link-Ala(3)	Cip-link-diAla(1)	Cip-link-diAla(2)	Cip-link-diAla(3)	Blank	
E	Cip(1)	Cip(2)	Cip(3)	Cip-link-Ala(1)	Cip-link-Ala(2)	Cip-link-Ala(3)	Cip-link-diAla(1)	Cip-link-diAla(2)	Cip-link-diAla(3)	Blank	
F	Cip(1)	Cip(2)	Cip(3)	Cip-link-Ala(1)	Cip-link-Ala(2)	Cip-link-Ala(3)	Cip-link-diAla(1)	Cip-link-diAla(2)	Cip-link-diAla(3)	Blank	
G	Cip(1)	Cip(2)	Cip(3)	Cip-link-Ala(1)	Cip-link-Ala(2)	Cip-link-Ala(3)	Cip-link-diAla(1)	Cip-link-diAla(2)	Cip-link-diAla(3)	Blank	
H											

Drug conc / µM	Stock conc / µM
0	0
0.01	1
0.1	10
0.5	50
1	100
10	1000 (1mM)

Key:

Cip = ciprofloxacin

Cip-link-Ala = **39**

Cip-link-diAla = **40**

Table 4: 96 - well plate layout for *in vivo* plate reader assay with triple replicates of each antibiotic; cip, cip-link-Ala **39** and cip-link-diAla **40**. Row B is a control with 0 µM drug concentration; rows C-G are wells with increasing drug concentration, blank wells in column 11 and sterile water in the surrounding wells

E. coli was grown for 16 hours and absorbance (OD) was measured every 30 minutes to generate growth curves with trifluroacetate as a control. **Figure 45** shows that under control conditions; when no conjugate or ciprofloxacin present, WT *E. coli* BW25113 strain reaches a peak OD_{650} of ~ 3 after about 11 hours.

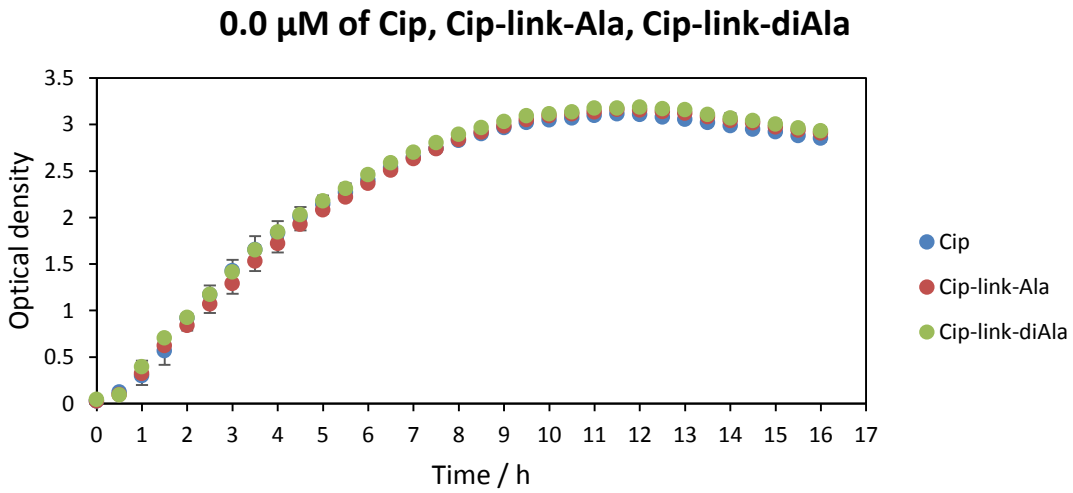

Figure 45: Control bacterial growth curve of BW25113 strain of *E. coli*. Error bars are ± standard deviation of three biological replicates

Adding 0.01 µM of each drug did not have any observable effect on the growth of the bacteria as a maximum OD_{650} of ~ 3 was reached after 11 hours as shown in **Figure 46A**.

A difference in bacterial growth was observed after increasing the concentration of ciprofloxacin from 0.01 µM to 0.1 µM (**Figure 46B**), reduction in bacterial growth with a peak OD of ~ 1, this suggests that the MIC of ciprofloxacin is in the range of 0.01 µM to 2.0 µM.

However, no difference in bacterial growth was observed with cip-link-Ala **39** and cip-link-diAla **40** (**Figure 46B**). This suggests that these conjugates are not effectively reaching their target at this concentration therefore no significant effect on bacterial growth is observed.

This result also rules out the hypothesis of the conjugates **39** and **40** being actively transported by primary or secondary peptide transporters as no bacterial growth inhibition was seen, whereas at the same concentration of 0.1 µM (**Figure 46B**), ciprofloxacin is showing significant inhibition and ciprofloxacin enters the cell through passive diffusion over a concentration gradient. This suggests that like ciprofloxacin the conjugates **39** and **40** are also transported by passive diffusion.

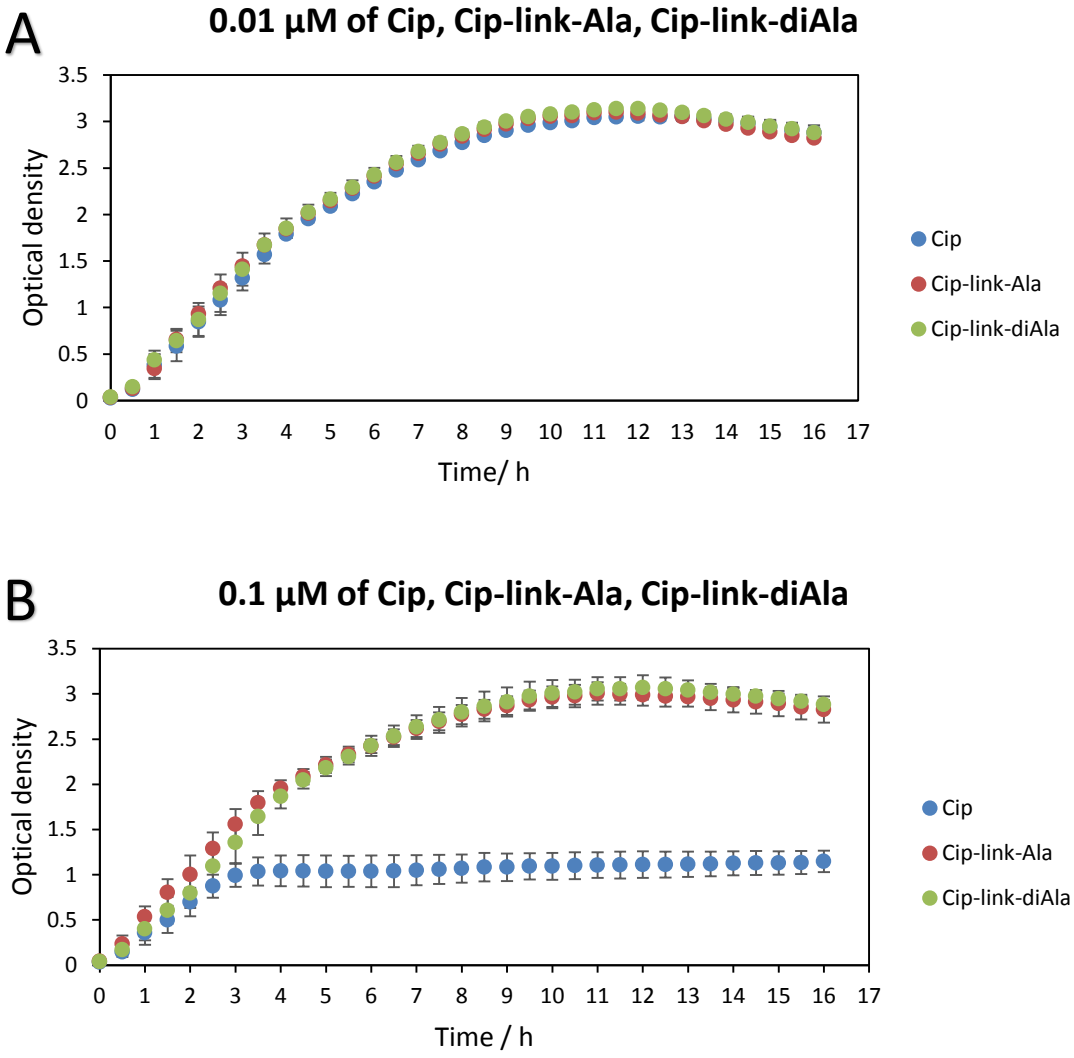

Figure 46: Bacterial growth curve of *E. coli* BW25113 grown with 0.01 µM (**A**) and 0.1 µM (**B**) additives. Error bars are ± standard deviation of three biological replicates

Reduction in bacterial growth was observed for all of the three drugs at 0.5 µM (**Figure 47**) with a significant reduction in bacterial growth observed for **39** and **40** reaching a maximum OD of ~ 0.7 compared to OD of 3.0 at 0.1 µM (**Figure 46B**). This shows that these conjugates retained their antimicrobial activity although it does not exceed that of ciprofloxacin as a higher concentration of the conjugates (x5 fold) is required to obtain similar results to those of ciprofloxacin. However, no significant difference between the activity of **39** and **40** was observed (**Figure 47**). This result suggests that no active transport of the conjugates by peptide transporters is occurring as further bacterial growth reduction was expected to be observed with **40** due to the

higher affinity of secondary peptide transporters for dipeptides than single amino acids.[44]

This result supports the hypothesised intracellular cleavage of the disulfide linker, which suggests that the disulfide is reduced within the bacterial cytoplasm either by glutathione or cysteine releasing free ciprofloxacin, the peptide and other non-toxic compounds like CO_2 (**Scheme 2**).

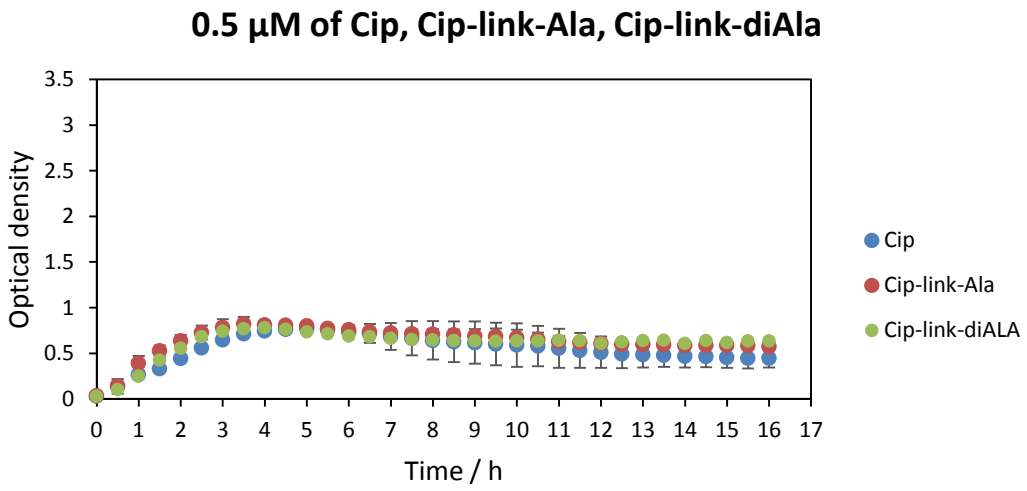

Figure 47: Bacterial growth curve of *E. coli* BW25113 grown with 0.5 µM additives. Error bars are ± standard deviation of three biological replicates

A further reduction in bacterial growth was observed as the concentration was increased to 1.0 µM (**Figure 48A**) and 10 µM (**Figure 48B**) with almost complete inhibition by ciprofloxacin at 10 µM. Although the conjugates, **39** and **40**, significantly inhibited growth at 10 µM, they did not completely inhibit it. This is thought to be due to inefficient thiol-induced cleavage of the disulfide bond in the bacterial cytoplasm and/or the disulfide bond can be cleaved but the formation of the 3-membered ring can be slow so mixed disulfides can be formed. The inefficient release of ciprofloxacin leads to reduced concentration of active ciprofloxacin accumulating in the cytoplasm, the disulfide was coupled at carboxylic group of ciprofloxacin, therefore cleaving the bond is essential for antimicrobial activity.

The inefficient release of ciprofloxacin could possibly be due to insufficient sulfhydryl concentration in the *E. coli* cytoplasm leading to slow kinetics of the reduction of the disulfide bond by sulfhydryl-containing species since the reduction rate is linearly dependent on the concentration of the reducing agent.[68]

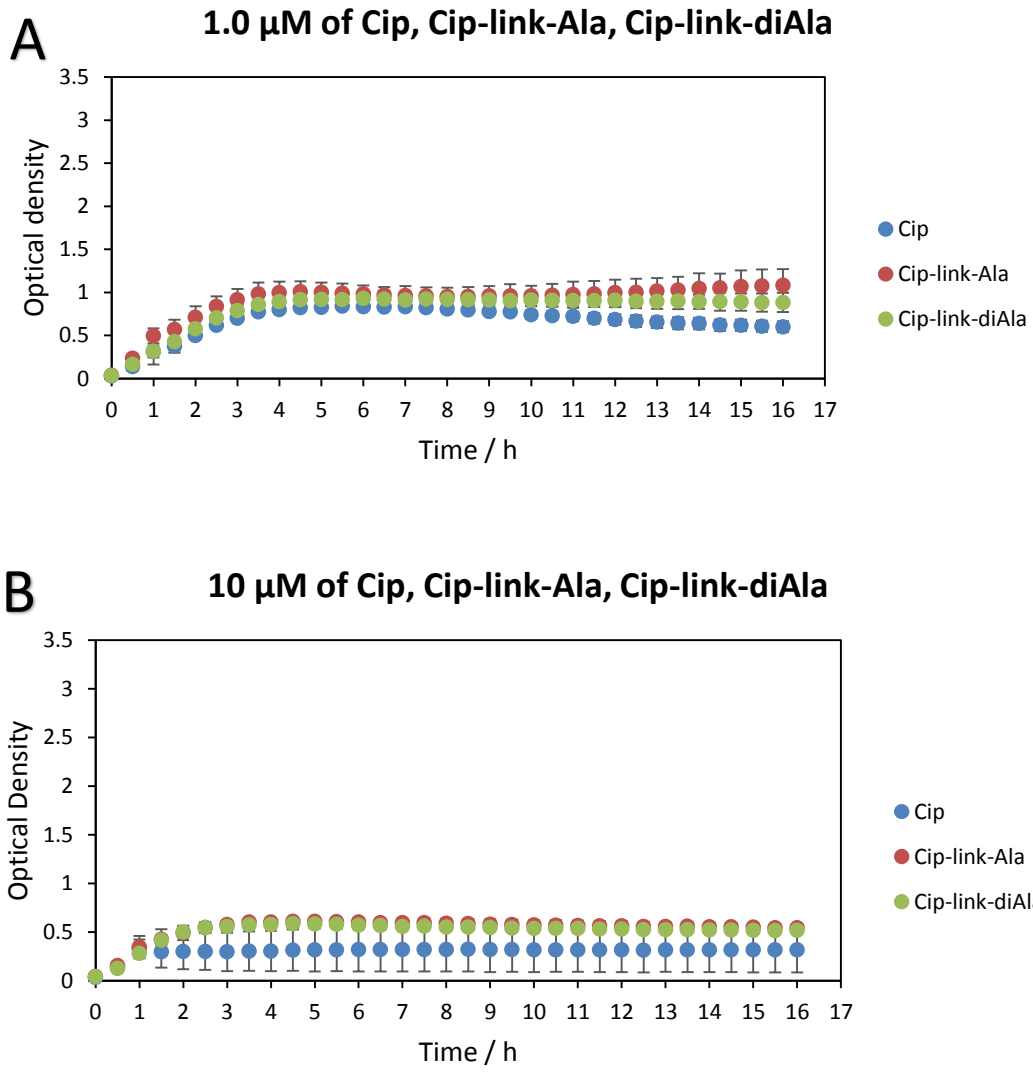

Figure 48: Bacterial growth curve of *E. coli* BW25113 grown with 1.0 µM (**A**) and 10 µM (**B**) additives. Error bars are ± standard deviation of three biological replicates

The hypothesis of intracellular disulfide bond cleavage was proven to be successful but no evidence of active transport of the conjugates by peptide transporters was observed. However, the possibility of active transport by peptide transporters cannot be ruled out without trying other peptides with hydrophobic or polar side chains such as serine.[41]

Chapter 3: Conclusions and future work

3.1. Conclusions

Trojan Horse conjugates were successfully prepared by connecting the fluoroquinolone ciprofloxacin to a single amino acid, Ala, and the dipeptide, Ala-Ala, through a non-biolabile amide bond and a biolabile disulfide linker. The conjugates were fully characterised and screened against the *E. coli* BW25113 bacterial strain.

Conjugate **38**, with a non-biolabile amide bond, was prepared by coupling Ala-Ala to the piperazinyl nitrogen of ciprofloxacin. Compound **38** was found to be significantly less active than the parent drug ciprofloxacin and also the single amino acid Ala conjugate **46**. DNA gyrase assay of **38** showed that the lack of activity of the conjugate is due to ciprofloxacin losing its activity, this suggests that the nutrient Ala-Ala significantly interferes with the inhibition of DNA gyrase and this could be due to steric bulk or electronic properties of the dipeptide preventing the effective formation of the DNA-enzyme-drug complex which is critical for the antimicrobial activity of fluoroquinolones.

Conjugates **39** and **40** were prepared by coupling Ala and Ala-Ala respectively to the carboxylic group of ciprofloxacin through a biolabile disulfide linker. Both conjugates, **39** and **40**, retained antimicrobial activity albeit lower than that of the parent drug, ciprofloxacin. This outcome supports the hypothesis of intracellular thiol-induced disulfide bond cleavage since the carboxylic group of ciprofloxacin is required for activity. However no significant difference was observed between the antimicrobial activity of **39** and **40**, with both conjugates found to be less active than ciprofloxacin, this suggests lack of active transport of the conjugates by peptide transporters as increased antimicrobial activity of **40** compared to **39** was expected since secondary peptide transporters have higher affinity for dipeptides than single amino acids. Therefore **39** and **40** could possibly be entering the bacterial inner membrane by passive diffusion.

The reduced antimicrobial activity of **39** and **40** is thought to either be due to inefficient thiol-induced cleavage of the disulfide bond or slow ciprofloxacin release after disulfide cleavage, however, these hypotheses have not been investigated.

3.2. Future work

As no active transport of the synthesised conjugates by peptide transporters across the bacterial inner membrane was observed, it would be advantageous to investigate other peptides possessing hydrophobic or polar side chains before ruling out the hypothesis.

Although the hypothesis of intracellular disulfide bond cleavage was confirmed, the cleavage of the disulfide bond was not monitored. Monitoring the cleavage process will allow investigation of the kinetics of the reduction process as well as reveal the fragments produced. It would also be advantageous to investigate the effect of the disulfide bond coupled at the piperazinyl nitrogen of ciprofloxacin as this will allow direct comparison with conjugates **39** and **40** which have the disulfide bond coupled at the carboxylic group of ciprofloxacin.

Chapter 4: Experimental

4.1. General

^{1}H NMR (400 MHz) and ^{13}C NMR (100 MHz) and ^{19}F NMR (376 MHz) spectra were recorded on a Jeol ECX-400 (400 MHz) spectrometer with chemical shifts quoted in parts per million relative to the stated deuterated solvents; $CHCl_3$ [δ_H 7.26 and δ_C 77.16], D_2O [δ_H 4.79] and CD_3OD [δ_H 3.31 and δ_C 49.00]. Coupling constant (J) are quoted in Hertz. Carbon NMR spectra were assigned using DEPT experiments. 1D spectra were processed using Bruker WinNMR software and 2D spectra using Jeol Delta software. Positive and negative electrospray (ESI) mass spectra were acquired on a Finnigan LCQ mass spectrometer or a Bruker MicroToF mass spectrometer. Infra-red spectra were recorded on an ATI Mattson Genesis FT-IR spectrometer. All samples were dried under vacuum before analysis. Melting points were recorded using a Bibby Stuart melting point apparatus and are uncorrected.

All solvents and chemical reagents were supplied by Aldrich or the Fischer Scientific. Solvents were used as received or dried over 4 Angstrom (Å) molecular sieves prior to use where necessary. Deionised water was used for all synthetic procedures. Analytical thin layer chromatography was performed using Merck F_{254} aluminium-backed plates using the specified solvent system and visualised through ultraviolet light (254 nm or 365 nm) with indicators such as iodine and potassium permanganate where necessary. Flash column chromatography was carried out using Davisil Flash Silica, 35-70 micron and the specified eluent. Dry-freezing was carried out by freezing the reaction mixture using liquid nitrogen (N_2).

4.2. Synthesis of Ala-Ala-ciprofloxacin conjugate 38

Compound 41

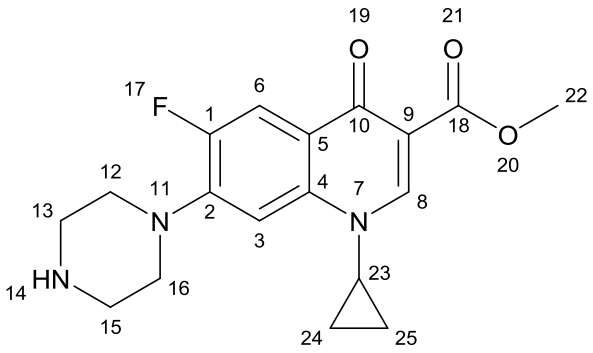

Chemical Formula: $C_{18}H_{20}FN_3O_3$
Molecular Weight: 345.37gmol^{-1}

Thionyl chloride (15.0 mL, 205.64 mmol) was added dropwise to a stirred solution of ciprofloxacin (3.36 g, 10.14 mmol) in dry methanol (100 mL) at 0-5^{0}C. The reaction mixture was heated under reflux for 17 hours. The reaction mixture was cooled to room temperature and concentrated *in vacuo* to yield a yellow oil.

The oil was taken up in aqueous potassium carbonate (25 mL) and extracted with DCM (4 x 40 mL). The organic layer was washed with deionised water (40 mL) and re-extracted with DCM (3 x 40 mL) then dried over $MgSO_4$, filtered and concentrated in vacuo to yield a white powder **41.**

Yield:

2.10 g, 60%

m.p. (^{O}C)

223.5 – 243.4

m/z (ESI):

346 ([M+H]$^+$, 100%)

HRMS (ESI):

Calc. for $C_{18}H_{21}FN_3O_3$ [M+H]$^+$ 346.1561, found 346.1547 (3.7 ppm mean error)

^{1}H NMR: (400 MHz, CD_3OD) δ_H (ppm):

8.64 (s, 1H, **H-8, CH**), 7.84 (d, $^{3}J_{H-F}$ = 13.3 Hz, 1H, **H-6, CH**), 7.48 (d, $^{4}J_{H-F}$ = 6.9 Hz, 1H, **H-3, CH**), 3.85 (s, 3H, **H-22**, **CH_3**), 3.63-3.65 (m, 1H, **cyclopropane**, **CH**), 3.26-3.28 (m, 4H, **piperazine**, **CH_2**), 3.03 (m, 4H, **piperazine**, **CH_2**), 1.33-1.39 (m, 2H, **cyclopropane**, **CH_2**), 1.16-1.18 (m, 2H, **cyclopropane**, **CH_2**)

^{13}C NMR: (100 MHz, CD_3OD) δ_c (ppm):

175.25 (d, $^{4}J_{C-F}$ = 3.0 Hz, **C-10**), 168.92 (**C-18**), 156.04 (d, $^{1}J_{C-F}$ = 249.0 Hz, **C-1**), 149.97 (**C-8**), 146.58 (d, $^{2}J_{C-F}$ = 10.7 Hz, **C-2**), 139.76 (**C-9**), 123.15 (d, $^{3}J_{C-F}$= 7.3 Hz, **C-5**), 113.01 (d, $^{2}J_{C-F}$ = 23.0 Hz, **C-6**), 110.30 (**C-4**), 106.89 (d,$^{3}J_{C-F}$= 2.3 Hz, **C-3**), 51.63 (**C-22**), 50.9 (C-**12/13/15/16**), 49.58 (**C-12/13/15/16**), 46.34 (C-**12/13/15/16**), 36.19 (**C-23**), 8.44 (**C-24, 25**)

IR (KBr cm^{-1}):

1724 (C=O), 1617 (C=O), 1311 (C-O), 1068 (C-O)

Compound 43

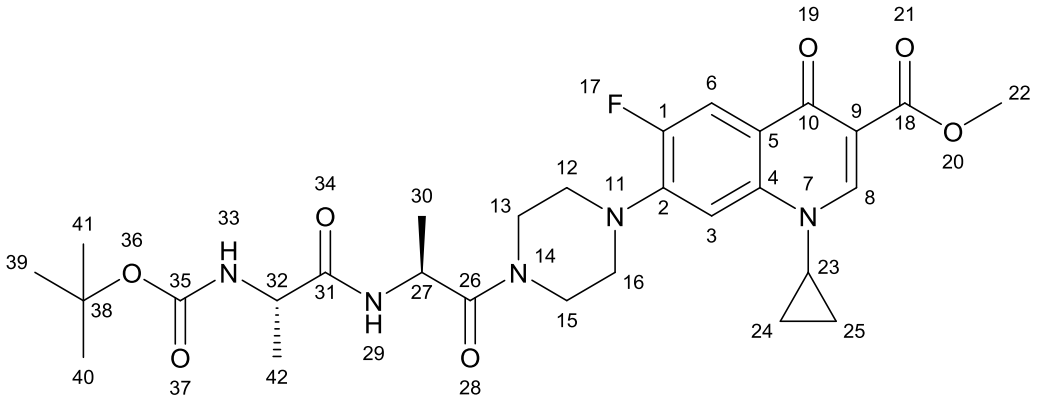

Chemical Formula: $C_{29}H_{38}FN_5O_7$
Molecular Weight: 587.65 $gmol^{-1}$

To stirred suspension of compound **41** (0.41 g, 1.20 mmol), compound **42** (0.25 g, 0.96 mmol) and HOBt.H_2O (0.21 g, 1.55 mmol) in dry DMF (25 mL) was added EDC.HCl (0.3 g, 1.56 mmol) and DIPEA (0.30 mL, 1.70 mmol). The reaction mixture was stirred at room temperature for 17 hours.

The reaction mixture was concentrated *in vacuo* to yield a yellow viscous oil. The oil was taken up in deionised water (50 mL) and extracted with DCM (3x70 mL). The organic extracts were combined and washed with deionised water (50 mL), 0.1M HCl (40 mL), aqueous $NaHCO_3$ (40 mL), brine (40 mL) and deionised water (50 mL). The organic layer was dried over $MgSO_4$ filtered then concentrated in vacuo to yield a viscous yellow oil. The crude product was purified by column chromatography on silica gel eluting with 7% propan-2-ol in $CHCl_3$ to obtain a yellowish solid **43**.

Rf: 0.40

Yield:

0.24 g, 43%

m.p. (^OC)

112.3 – 117.3

m/z (ESI):

610 ($[M+Na]^+$, 100%)

HRMS (ESI):

Calc. for $C_{29}H_{38}FN_5NaO_7$ $[M+Na]^+$ 610.2647, found 610.2662 (-2.1 ppm mean error)

^{1}H NMR: (400 MHz, $CDCl_3$) δ_H (ppm):

8.42 (s, 1H, **H-8, CH**), 7.85 (d, $^3J_{H-F}$ = 13.3 Hz, 1H, **H-6, CH**), 7.29(d, $^4J_{H-F}$ = 6.9 Hz, 1H, **H-3, CH**),7.21(m, 1H, **H-29/33, NH**), 5.31 (m,1H, **H-29/33, NH**), 4.90(m, 1H, **H-27/32, CH**), 4.18 (m, 1H, **H-27/32, CH**), 3.83 (s, 3H, **H-22**, **CH_3**), 3.64-3.77(m, 4H, **piperazine**, **CH_2**), 3.40-3.42(m, 1H, **cyclopropane**, **CH**), 3.13-3.24 (m, 4H, **piperazine**, **CH_2**), 1.38 (s, 9H, **H-39,40,41, CH_3**), 1.31-1.34 (m, 6H, **H-30,42, CH_3**), 1.26-1.29 (m, 2H, **cyclopropane**, **CH_2**), 1.08-1.12 (m, 2H, **cyclopropane**, **CH_2**)

^{13}C NMR: (100 MHz, $CDCl_3$) δ_c (ppm):

172.25 (d, $^4J_{C-F}$ = 3.0 Hz, **C-10**), 170.46 (**C-35**), 165.77 (**C-18**), 162.41 (**C-26,31**), 154.60 (d, $^1J_{C-F}$ = 249.0 Hz, **C-1**), 148.27 (**C-8**), 143.50 (d, $^2J_{C-F}$ = 10.7 Hz, **C-2**), 137.70 (**C-9**), 123.17 (d, $^3J_{C-F}$= 7.3 Hz, **C-5**), 113.07 (d, $^2J_{C-F}$ = 23.0 Hz, **C-6**), 109.63 (**C-4**), 105.25 (d,$^3J_{C-F}$= 2.3 Hz, **C-3**), 79.75 (**C-38**), 51.81 (**C-22**), 45.12 (C-**12/13/15/16**), 44.83 (**C-12/13/15/16**), 41.76 (C-**12/13/15/16**), 34.47 (**C-23**), 28.13 (**C-39, 40, 41**), 25.15 (**C-27, 32**), 18.52 (**C-30, 42**),7.97 (**C-24, 25**)

IR (KBr cm^{-1}):

3300 (N-H), 1620 (C=O), 1162 (C-O), 1021 (C-O)

Compound 44

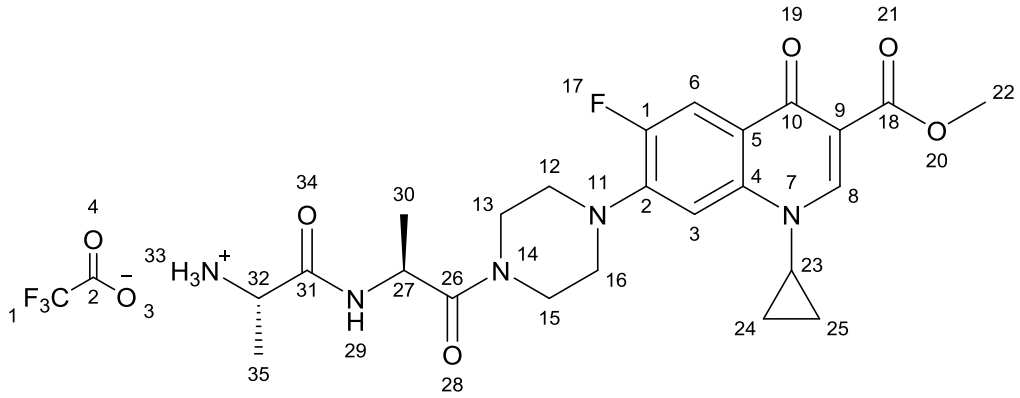

Chemical Formula: $C_{26}H_{31}F_4N_5O_7$
Molecular Weight: 601.56 $gmol^{-1}$

Compound **43** (0.10 g, 0.20 mmol) was taken up in 20% TFA in dry $CHCl_3$ (10 mL) and left stirring at room temperature for 24 hours. The reaction mixture was concentrated under vacuum to yield an orange residue. The residue as taken up in ethanol (5 x 10mL) and concentrated *in vacuo* to give a yellow oil **44**.

Yield:

0.10 g, 84%

m/z (ESI):

488 ($[M+H]^+$, 100%)

HRMS (ESI):

Calc. for $C_{24}H_{31}FN_5O_5$ $[M+H]^+$488.2304, found 488.2305 (-0.3 ppm mean error)

^{1}H NMR: (400 MHz, D_2O) δ_H (ppm):

8.39 (s, 1H, **H-8, CH**), 7.73 (d, $^3J_{H-F}$ = 13.3 Hz, 1H, **H-6, CH**), 7.23(d, $^4J_{H-F}$ = 6.9 Hz, 1H, **H-3, CH**), 4.65 (m, 1H, **H-27/32, CH**), 4.18 (m, 1H, **H-27/32, CH**), 3.65 (s, 3H, **H-22**, **CH_3**), 3.54-3.66(m, 4H, **piperazine**, **CH_2**), 3.40-3.42(m, 1H, **cyclopropane**, **CH**), 3.13-3.24 (m, 4H, **piperazine**, **CH_2**), 1.45-1.51 (m, 3H, **H-30/35, CH_3**), 1.28-1.30 (m, 3H, **H-30/35, CH_3**), 1.17 (m, 2H, **cyclopropane**, **CH_2**), 1.08 (m, 2H, **cyclopropane**, **CH_2**)

^{13}C NMR: (100 MHz, D_2O) δ_c (ppm):

171.99 (d, $^4J_{C-F}$ = 3.0 Hz, **C-10**), 168.34 (**C-18**), 162.58 (**C-26,31**), 157.99 (d, $^1J_{C-F}$ = 249.0 Hz, **C-1**), 149.60 (**C-8**), 142.40 (d, $^2J_{C-F}$ = 10.7 Hz, **C-2**), 136.24 (**C-9**), 122.36 (d, $^3J_{C-F}$= 7.3 Hz, **C-5**), 113.32 (d, $^2J_{C-F}$ = 23.0 Hz, **C-6**), 109.20 (**C-4**), 104.89 (d,$^3J_{C-F}$= 2.3 Hz, **C-3**), 55.75 (**C-22**), 47.46 (C-**12/13/15/16**), 47.17 (**C-12/13/15/16**), 44.55 (C-**12/13/15/16**), 40.39 (**C-23**), 33.86 (**C-27, 32**), 15.13 (**C-30, 35**), 5.60 (**C-24, 25**)

^{19}F NMR: (376 MHz, D_2O) δ_F (ppm):

-126.76 (dd, J_{H-F} = 13.0, 8.0 Hz, **F-17**), -76.76 (**F-1**)

IR (KBr cm^{-1}):

3300 (N-H), 1620 (C=O), 1162 (C-O), 1021 (C-O)

Compound 45

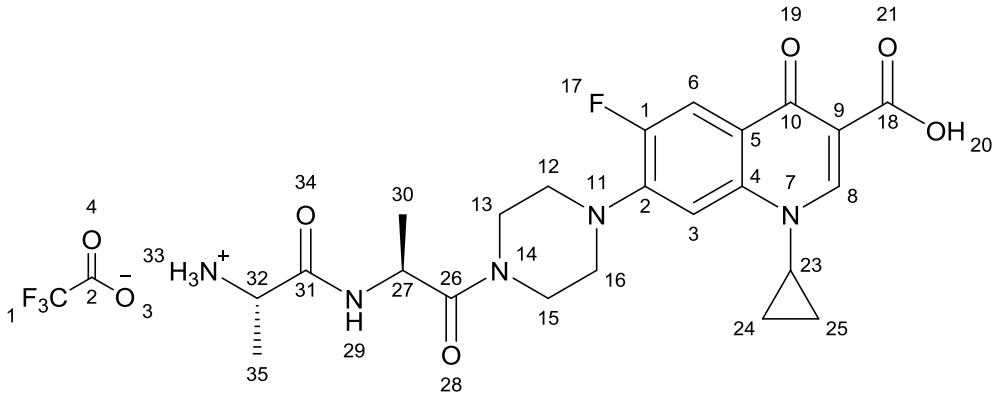

Chemical Formula: $C_{25}H_{29}F_4N_5O_7$
Molecular Weight: 587.53 $gmol^{-1}$

To a solution of compound **44** (0.08 g, 0.17 mmol) in 5:1 methanol: water (10 mL) was added 1M NaOH in methanol (1.3 mL) and the reaction mixture was left stirring for 26 hours. The reaction mixture was neutralised with 1M HCl to pH ~ 8 then concentrated under vacuum to give a yellow solid **45**.

Yield:

0.09 g, 93%

m.p. (^{O}C)

232 – 235.1

m/z (ESI):

474 ($[M+H]^+$, 100%)

HRMS (ESI):

Calc. for $C_{23}H_{29}FN_5O_5$ $[M+H]^+$ 474.2147, found 474.2134 (2.6 ppm mean error)

^{1}H NMR: (400 MHz, CD_3OD) δ_H (ppm):

8.37 (s, 1H, **H-8, CH**), 7.75 (d, $^3J_{H-F}$ = 13.3 Hz, 1H, **H-6, CH**), 7.23(d, $^4J_{H-F}$ = 6.9 Hz, 1H, **H-3, CH**), 4.60 (m, 1H, **H-27/32, CH**), 4.15 (m, 1H, **H-27/32, CH**), 3.45-3.53(m, 4H, **piperazine**, **CH_2**), 3.39-3.42(m, 1H, **cyclopropane**, **CH**), 3.13-3.24 (m, 4H, **piperazine**, **CH_2**), 1.45-1.51 (m, 3H, **H-30/35, CH_3**), 1.29 (m, 3H, **H-30/35, CH_3**), 1.17 (m, 2H, **cyclopropane**, **CH_2**), 1.05 (m, 2H, **cyclopropane**, **CH_2**)

^{13}C NMR: (100 MHz, CD_3OD) δ_c (ppm):

175.62 (d, $^4J_{C-F}$ = 3.0 Hz, **C-10**), 172.65 (**C-26, 31**), 163.21 (**C-18**), 154.0 (d, $^1J_{C-F}$ = 249.0 Hz, **C-1**), 146.97 (**C-8**), 143.64 (d, $^2J_{C-F}$ = 10.7 Hz, **C-2**), 138.54 (**C-9**), 122.06 (d, $^3J_{C-F}$= 7.3 Hz, **C-5**), 115.24 (d, $^2J_{C-F}$ = 23.0 Hz, **C-6**), 111.35 (**C-4**), 106.69 (d,$^3J_{C-F}$= 2.3 Hz, **C-3**), 49.45 (C-**12/13/15/16**), 46.04 (**C-12/13/15/16**), 45.30 (C-**12/13/15/16**), 34.93 (**C-23**), 18.95 (**C-27, 32**), 16.19 (**C-30, 35**), 7.49 (**C-24, 25**)

^{19}F NMR: (376 MHz, D_2O) δ_F (ppm):

-126.78 (dd, J_{H-F} = 13.0, 8.0 Hz, **F-17**), -76.76 (**F-1**)

IR (KBr cm^{-1}):

3374 (N-H), 1621 (C=O), 1238 (C-O), 1020 (C-O)

4.3. Synthesis of cip-link-Ala conjugate 39

Compound 50

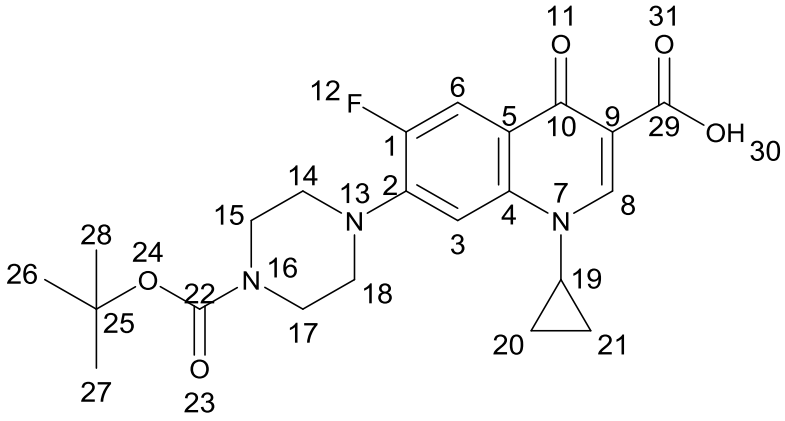

Chemical Formula: $C_{22}H_{26}FN_3O_5$
Molecular Weight: 431.46 g mol^{-1}

Ciprofloxacin (2.01 g, 6.07 mmol) was dissolved in water : dioxane (1:1, 20 mL) containing 1M NaOH (10 mL) and was left stirring for an hour. Di-tert-butylcarbonate (2.53 g, 11.59 mmol) was taken up in dioxane (2 mL) before adding it to the reaction mixture. The reaction was continued for 24 hours. Approximately three quarters of the solvent (15 mL) was removed *in vacuo*, and acetone (40 mL) was added to the residue. The solid white product was filtered, thoroughly washed with acetone and dried under vacuum to yield a white powder **50**.

Yield:

2.46g, 94%

Mp:

247.0 – 250.9^{o}C

m/z (ESI):

454.18 ($[M+Na]^+$, 100%)

HRMS (ESI):

Calc. for $C_{22}H_{26}FN_3NaO_5$ $[M+Na]^+$ 454.1749, found 454.1748 (-0.0 ppm mean error)

^{1}H NMR: (400 MHz, $CDCl_3$) δ_H (ppm):

8.74 (s, 1H, **H-8, CH**), 7.98 (d, $^{3}J_{H-F}$ = 13.3 Hz, 1H, **H-6, CH**), 7.36 (d, $^{4}J_{H-F}$ = 6.9 Hz, 1H, **H-3, CH**), 3.68-3.64 (m, 4H, **piperazine**, **CH_2**), 3.53 (m, 1H, **cyclopropane**, **CH**), 3.29-3.27 (m, 4H, **piperazine, CH_2**), 1.48 (s, 9H, **tert-butyl, CH_3**), 1.41-1.36 (m, 2H, **cyclopropane, CH_2**), 1.23-1.17 (m, 2H, **cyclopropane, CH_2**)

^{13}C NMR: (100 MHz, $CDCl_3$) δ_c (ppm):

177.03 (d, $^{4}J_{C-F}$ = 3.0 Hz, **C-10**), 169.98 (**C-22**), 166.89 (**C-29**), 154.54 (d, $^{1}J_{C-F}$ = 249.0 Hz, **C-1**), 147.47 (**C-8**), 145.77 (d, $^{2}J_{C-F}$ = 10.7 Hz, **C-2**), 139.01 (**C-9**), 123.48 (d, $^{3}J_{C-F}$= 7.3 Hz, **C-5**), 112.48 (d, $^{2}J_{C-F}$ = 23.0 Hz, **C-6**), 108.13 (**C-4**), 104.99 (d,$^{3}J_{C-F}$= 2.3 Hz, **C-3**), 80.34 (**C-25**), 70.01 (**C-14/15/17/18**), 69.66 (**C-14/15/17/18**), 49.77 (**C-14/15/17/18**), 49.81 (**C-14/15/17/18**) 35.28 (**C-19**), 28.37 (**C-26, 27, 28**), 8.22 (**C-20, 21**)

IR (KBr cm^{-1}):

1731.7 (C=O), 1688.3 (C=O), 1628.0 (C=O), 1247.9 (C-O)

Compound 54

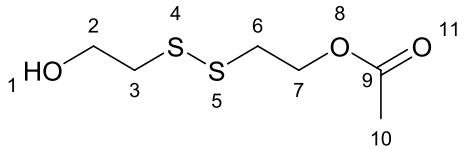

Chemical Formula: $C_6H_{12}O_3S_2$
Molecular Weight: 196.28 g mol^{-1}

To a solution of 2,2'-dithiodiethanol **48** (4.12 g, 26.71 mmol) dissolved in DCM (50 mL) was added acetic anhydride (1.40 mL, 14.81 mmol) and pyridine (10.50 mL, 129.82 mmol) and the mixture was stirred for 23 hours at room temperature. The reaction mixture was concentrated *in vacuo* yielding a yellow oil which was then partioned between ethyl acetate (30 mL) and 1M HCl (35 mL). The organic layer was washed with water (25 mL) and brine (25 mL), dried over anhydrous sodium sulphate (Na_2SO_4) filtered and concentrated *in vacuo* to yield a yellow viscous oil. The crude product was then purified by silica gel column chromatography using 40% EtOAc in petroleum ether to yield a pale yellow viscous oil **54**.

Yield:

0.76g , 26%

m/z (ESI):

219.01 ($[M+Na]^+$, 100%)

HRMS (ESI):

Calc. for $C_6H_{12}NaO_3S_2$ $[M+Na]^+$ 219.0120, found 219.0117 (1.6 ppm mean error)

^{1}H NMR: (400 MHz, $CDCl_3$) δ_H (ppm):

4.35 (t, J = 6.0 Hz, 2H, **H-2/7, CH_2**), 3.90 (t, J = 6.0 Hz, 2H, **H-2/7, CH_2**), 2.95-2.87 (m, 4H, **H-3, 6**), 2.09 (s, 3H, **H-10**),

^{13}C NMR: (100 MHz, $CDCl_3$) δ_c (ppm):

170.93 (**C-9**), 62.35 (**C-2/7**), 60.18 (**C-2/7**), 41.58 (**C-3/6**), 36.92 (**C-3/6**), 20.87 (**C-10**)

Compound 55

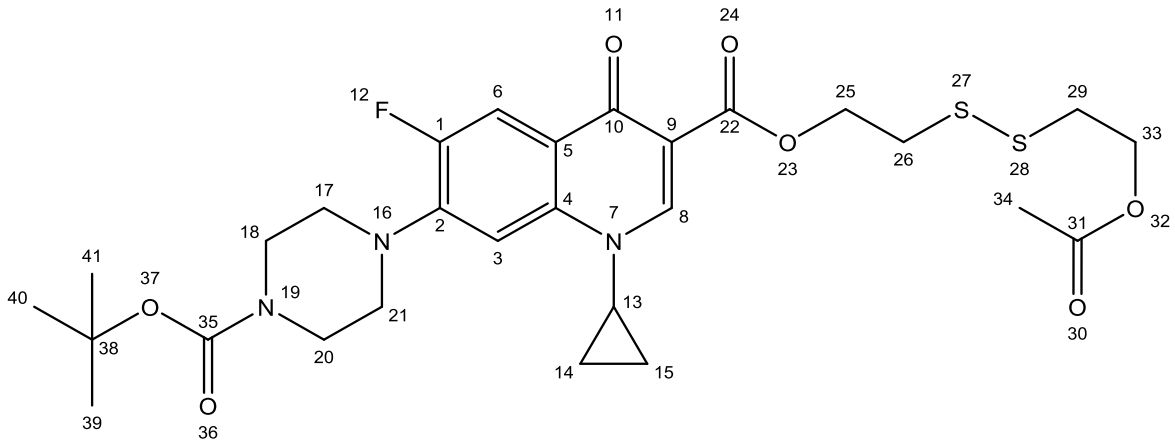

Chemical Formula: $C_{28}H_{36}FN_3O_7S_2$
Molecular Weight: 609.73 g mol^{-1}

Compound **50** (0.5 g, 1.16 mmol) was dissolved in dry DCM (50 mL) then DMAP (0.21 g, 1.73 mmol), HATU (0.66 g, 1.74 mmol) was added with continuous stirring at room temperature forming a yellow suspension. Shortly after DIPEA (0.45 mL, 2.60 mmol) was added to the mixture followed by compound **54** (0.26 g, 1.33 mmol) taken up in approx. 2 mL dry DCM. The reaction mixture was left stirring at room temperature for 72 hours and a clear yellow solution was observed. DCM (30 mL) was added to the reaction mixture and extracted with water (30 mL). The organic layer was washed with saturated Na_2CO_3 and water (30 mL each) then dried over $MgSO_4$ filtered and concentrated *in vacuo* yielding the crude product. The crude product was purified by column chromatography on silica gel eluting with 5% MeOH in $CHCl_3$ to obtain a pale yellow oil **55**.

Rf:

0.30

Yield:

0.24g, 34%

m/z (ESI):

632.19 ($[M+Na]^+$, 100%)

HRMS (ESI):

Calc. for $C_{28}H_{36}FN_3NaO_7S_2$ $[M+Na]^+$ 632.1871, found 632.1859 (1.9 ppm mean error)

^{1}H NMR: (400 MHz, $CDCl_3$) δ_H (ppm):

8.34 (s, 1H, **H-8, CH**), 7.74 (d, $^{3}J_{H-F}$ = 13.3 Hz, 1H, **H-6, CH**), 7.15 (d, $^{4}J_{H-F}$ = 6.9 Hz, 1H, **H-3, CH**), 4.45-4.42 (m, 2H, **H-25/33, CH_2**), 4.25-4.23 (m, 2H, **H-25/33, CH_2**), 3.56 (m, 4H**, piperazine, CH_2**), 3.41-3.38 (m, 1H, **cyclopropane**, **CH**), 3.12 (m, 4H, **piperazine, CH_2**), 2.99-2.96 (m, 2H, **H-26/29, CH_2**), 2.89-2.85 (m, 2H, **H-26/29, CH_2**), 1.98 (s, 3H, **H-34, CH_3**), 1.41 (s, 9H, **tert-butyl, CH_3**), 1.25 (m, 2H, **cyclopropane, CH_2**), 1.08 (m, 2H, **cyclopropane, CH_2**)

^{13}C NMR: (100 MHz, $CDCl_3$) δ_c (ppm):

172.25 (d, $^{4}J_{C-F}$ = 3.0 Hz, **C-10**), 170.28 (**C-35**), 165.21 (**C-22**), 164.17 (**C-31**), 154.04 (d, $^{1}J_{C-F}$ = 249 Hz, **C-1**), 147.83 (**C-8**), 143.84 (d, $^{2}J_{C-F}$ = 10.7 Hz, **C-2**), 137.36 (**C-9**), 122.35 (d, $^{3}J_{C-F}$ = 7.3 Hz, **C-5**), 112.35 (d, $^{2}J_{C,F}$ = 23.0 Hz, **C-6**), 108.80 (**C-4**), 104.80 (d, $^{3}J_{C-F}$ = 2.3Hz, **C-3**), 79.65 (**C-38**), 61.91(**C-17/18/20/21**) 61.80 (**C-17/18/20/21**), 49.37 (**C-17/18/20/21**), 49.30 (**C-17/18/20/21**), 38.11 (**C-25, 33**), 36.65 (**C-26, 29**), 34.22 (**C-13**), 27.93 (**C-39, 40, 41**), 20.39 (**C-34**) 7.64 (**C-14, 15**)

IR (KBr cm^{-1}):

1735.03 (C=O), 1720.18 (C=O), 1689.05 (C=O), 1242.74 (C-O), 1159.96 (C-O)

Compound 57

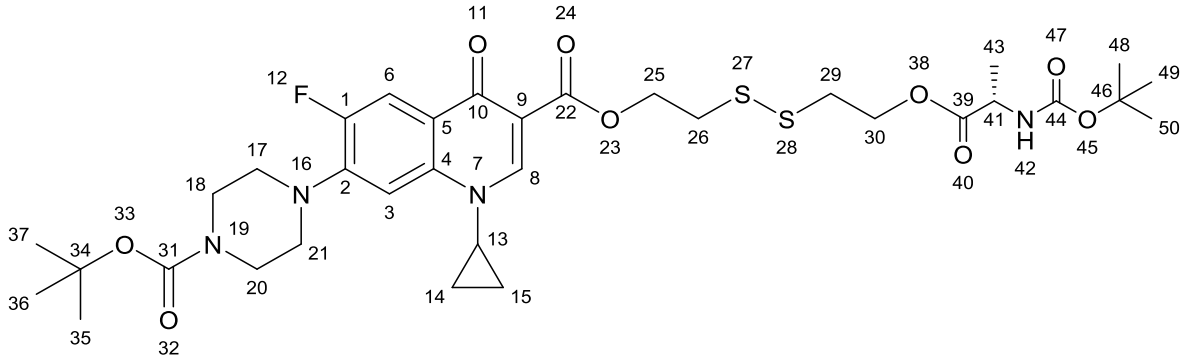

Chemical Formula: $C_{34}H_{47}FN_4O_9S_2$
Molecular Weight: 738.89 g mol^{-1}

Compound **50** (0.49 g, 1.15 mmol) was dissolved in dry DCM (50 mL) then DMAP (0.22 g, 1.76 mmol), HATU (0.66 g, 1.75 mmol) was added with continuous stirring at room temperature forming a yellow suspension. Shortly after DIPEA (0.45 mL, 2.60 mmol) was added to the mixture followed by 2,2'-dithiodiethanol **48** (0.26 g, 1.33 mmol) taken up in approx. 2 mL dry DCM. The reaction mixture was left stirring at room temperature for 23 hours and a clear yellow solution was observed. DCM (30 mL) was added to the reaction mixture and extracted with water (30 mL). The organic layer was washed with saturated Na_2CO_3 and water (30 mL each) then dried over $MgSO_4$ filtered and concentrated *in vacuo* yielding an off white paste-like crude product compound **51** which was used without further purification.

Approx. 0.40mmol of the crude product **51** was dissolved in dry DCM (30 mL) with stirring and compound **56** (0.08 g, 0.45 mmol) was added to the solution. DMAP (0.08 g, 0.65 mmol), DIPEA (0.14 mL, 0.80 mmol) and EDC (0.13 g, 0.66 mmol) were added to the reaction mixture and this was allowed to stir at room temperature for 19 hours. The reaction mixture was concentrated under vacuum and a yellow oil was obtained. The oil was then taken up in DCM (15 mL) and extracted with water (10 mL). The organic layer was separated, washed with Na_2CO_3 (2 x 10 mL) and water (2 x 10 mL) then dried over Na_2SO_4 filtered and concentrated *in vacuo* yielding a yellowish oil. The crude product was purified by silica gel column chromatography using 25% acetone in DCM to yield a pale yellow oil **57**.

<u>Rf:</u>

0.37

Yield:

0.10g, 35%

m/z (ESI):

761.27 ($[M+Na]^+$, 100%)

HRMS (ESI):

Calc. for $C_{34}H_{47}FN_4NaO_9S_2$ $[M+Na]^+$ 761.2661, found 761.2651 (1.0ppm mean error)

^{1}H NMR: (400 MHz, $CDCl_3$) δ_H (ppm):

8.23 (s, 1H, **H-8, CH**), 7.58 (d, $^3J_{H-F}$ = 13Hz, 1H, **H-6, CH**), 7.07 (d, $^3J_{H-F}$ = 6.9Hz, 1H, **H-3, CH**), 4.12-4.36 (m, 5H, **H-25, 30, 41, CH_2, CH**), 3.49 (m, 4H**, piperazine, CH_2**), 3.33 (m, 1H, **cyclopropane, CH**), 3.05 (m, 4H, **piperazine, CH_2**), 2,90 (m, 2H, **H-26/29, CH_2**), 2.82 (m, 2H, **H-26/29, CH_2**), 1.34 (s, 9H, **tert-butyl, CH_3**), 1.27 (m, 12H, **tert-butyl, H-43, CH_3**), 1.16 (m, 2H, **cyclopropane, CH_2**), 1.02 (m, 2H, **cyclopropane, CH_2**)

^{13}C NMR: (100 MHz, $CDCl_3$) δ_c (ppm):

172.80 (**C-10**), 172.57 (**C-31, 44**), 164.81 (**C-22, 39**), 154.21 (d, $^1J_{C-F}$ = 249 Hz, **C-1**), 148.04 (**C-8**), 144.10 (d, $^2J_{C-F}$ = 10 Hz, **C-2**), 137.57(**C-9**), 122.85 (d, $^3Jc_{-F}$ = 6 Hz, **C-5**), 113.12 (d, $^2J_{C-F}$ = 23 Hz, **C-6**), 109.37 (**C-4**), 104.70 (d, $^3J_{C-F}$ = 3.0 Hz, **C-3**), 79.82 (**C-34, 46**), 62.53 (**C-17/18/20/21**), 62.41(**C-17/18/20/21**) 62.16 (**C-17/18/20/ 21**), 60.50 (**C-17/18/20/21**), 36.68 (**C-25, 30**), 36.58 (**C-26, 29**), 34.23 (**C-13/41**), 30.55 (**C-13/41**), 28.02 (**C-35, 36,37/48, 49, 50**), 27.94 (**C-35, 36, 37/ 48, 49,50**), 18.14 (**C-43**), 7.80 (**C-14, 15**)

IR (KBr cm^{-1}):

3300.81 (N-H), 1694.04 (C=O), 1621.02 (C=O), 1245.13 (C-O), 1160.16 (C-O)

Compound 58

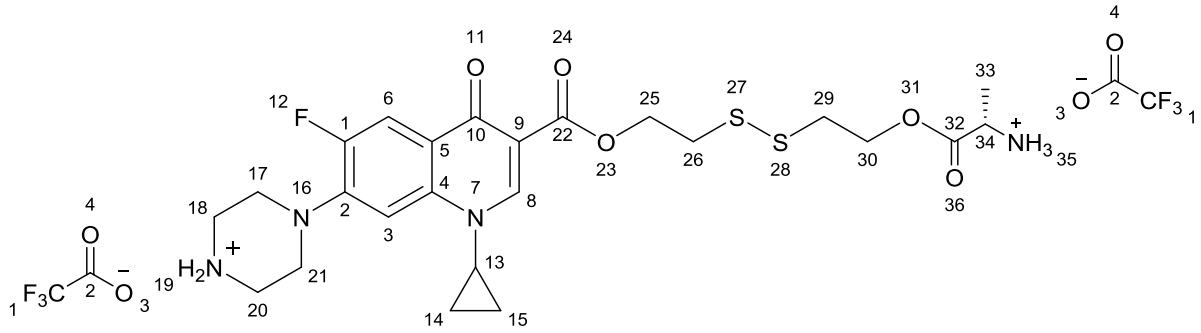

Chemical Formula: $C_{28}H_{33}F_7N_4O_9S_2$
Molecular Weight: 766.70 g mol^{-1}

Compound **57** (0.17 g, 0.23 mmol) was taken up in 20% TFA in dry DCM (10 mL) to give a yellow solution which was left stirring at room temperature for 23 hours. The reaction mixture was concentrated under vacuum yielding a dark orange residue. The residue was taken up in ethanol (5 x 10 mL) and concentrated under vacuum, yielding a yellowish oil **58**.

Yield:

0.16g, 91%

m/z (ESI):

270.09 ($[M]^{2+}$,100%)

HRMS (ESI):

Calc. for $C_{24}H_{33}FN_4O_5S_2$ $[M]^{2+}$ 270.0933, found 270.0920 (4.4ppm mean error)

^{1}H NMR: (400 MHz, CD_3OD) δ_H (ppm):

8.65 (s, 1H, **H-8, CH**), 7.77 (d, $^3J_{H-F}$ = 13Hz, 1H, **H-6, CH**), 7.52 (d, $^3J_{H-F}$ = 6.9Hz, 1H, **H-3, CH**), 4.45-4.56 (m, 4H, **H-25,30, CH_2**), 4.14-4.20 (m, 1H, **H-34, CH**), 3.68 (m, 1H, **cyclopropane, CH**), 3.59(m, 4H, **piperazine, CH_2**), 3.50 (m, 4H, **piperazine, CH_2**), 3.10-3.03 (m, 4H, **H-26,29, CH_2**), 1.59 (m, 3H, **H-33, CH_3**), 1.39 (m, 2H, **cyclopropane, CH_2**), 1.20 (m, 2H, **cyclopropane, CH_2**)

^{13}C NMR: (100 MHz, CD_3OD) δ_c (ppm):

171.10 (**C-10**), 167.35 (**C-22, 32**), 155.81 ($^1J_{C,F}$ = 249 Hz, **C-1**), 150.34 (**C-8**), 145.01 ($^2J_{C,F}$ = 10 Hz, **C-2**), 139.64 (**C-9**), 128.86 (**C-5**), 113.24 ($^2J_{C,F}$ = 23 Hz, **C-6**), 109.32 (**C-4**), 107.89 (**C-3**), 64.52(**C-17/18/20/21**) 63.71 (**C-17/18/20/21**), 44.58 (**C-13/34**), 37.99 (**C-25, 30**), 37.53 (**C-26, 29**), 36.43 (**C-13/34**), 16.19 (**C-33**), 8.59 (**C-14, 15**)

^{19}F NMR: (376 MHz, D_2O) δ_F (ppm):

-124.56 (dd, J_{H-F} = 13.0, 8.0 Hz, **F-17**), -76.94 (**F-1**)

IR (KBr cm^{-1}):

3375.00 (N-H), 1750.48 (C=O), 1673.57 (C=O), 1621.44 (C=O), 1171.06 (C-O)

4.4. Synthesis of cip-link-Ala-Ala conjugate 40

Compound 60

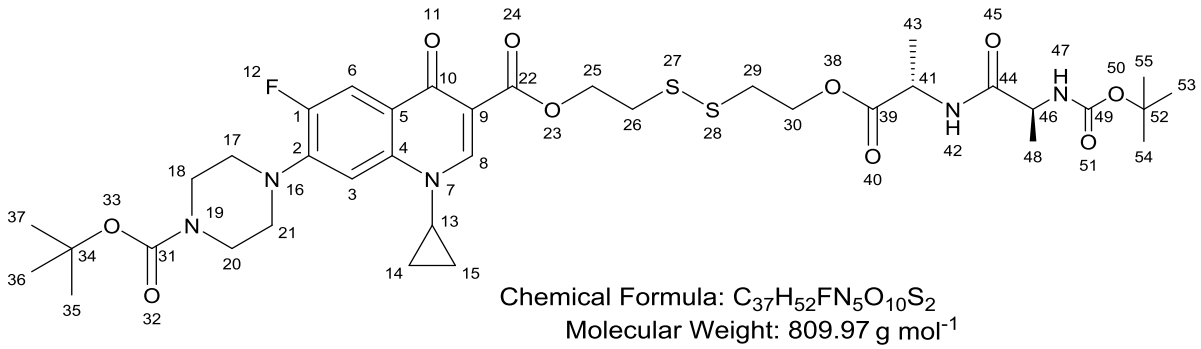

Approx. 0.70 mmol of compound **51** was dissolved in dry DCM (30 mL) with stirring and compound **59** (0.16 g, 0.61 mmol) was added to the solution. DMAP (0.10 g, 0.86 mmol), DIPEA (0.17 mL, 1.00 mmol) and EDC (0.17 g, 0.89 mmol) were added to the reaction mixture and this was allowed to stir at room temperature for 19 hours. The pale yellow reaction mixture was then taken up in water (25 mL) and extracted with DCM (2 x 25 mL). The organic layers were combined and washed with $NaHCO_3$ (2 x 25 mL), Brine (2 x 25 mL) and water (2 x 25 mL) then dried over Na_2SO_4 filtered and concentrated *in vacuo* yielding a yellow oil. The crude product was purified by silica gel column chromatography using 25% acetone in DCM to yield a pale yellow oil **60**.

Rf:

0.57

Yield:

0.15g, 30%

m/z (ESI):

832.30 ($[M+Na]^+$, 100%)

HRMS (ESI):

Calc. for $C_{37}H_{52}FN_5NaO_{10}S_2$ $[M+Na]^+$ 832.3032, found 832.3050 (-2.6ppm mean error)

^{1}H NMR: (400 MHz, $CDCl_3$) δ_H (ppm):

8.50 (s, 1H, **H-8, CH**), 7.96 (d, $^{3}J_{H-F}$ = 13Hz, 1H, **H-6, CH**), 7.25 (d, $^{3}J_{H-F}$ = 6.9Hz, 1H, **H-3, CH**), 4.35-4.54 (m, 5H, **H-25, 30, CH_2, 41/46, CH**), 4.21 (m, 1H, **H-41/46, CH**), 3.63 (m, 4H**, piperazine, CH_2**), 3.44 (m, 1H, **cyclopropane, CH**), 3.20 (m, 4H, **piperazine, CH_2**), 3.04-3.02 (m, 2H, **H-26/29, CH_2**), 2.95-2.93 (m, 2H, **H-26/29, CH_2**), 1.47 (s, 9H, **tert-butyl, CH_3**), 1.41 (s, 10H, **tert-butyl, H-43/48, CH_3**), 1.33 (m, 5H, **H-43, 48**), 1.23 (m, 2H, **cyclopropane, CH_2**), 1.13 (m, 2H, **cyclopropane, CH_2**)

^{13}C NMR: (100 MHz, $CDCl_3$) δ_c (ppm):

172.63 (**C-10**), 170.15 (**C-31, 49**), 172.09 (**C-44**), 164.60 (**C-22, 39**), 154.22 (d, $^{1}J_{C,F}$ = 249 Hz, **C-1**), 148.03 (**C-8**), 144.13 (d, $^{2}J_{C,F}$ = 10 Hz, **C-2**), 137.58(**C-9**), 122.72 (d, $^{3}J_{C-F}$ = 6 Hz, **C-5**), 112.94 (d, $^{2}J_{C,F}$ = 23 Hz, **C-6**), 109.21 (**C-4**), 104.70 (d, $^{3}J_{C-F}$ = 3.0 Hz, **C-3**), 79.81 (**C-34, 52**), 62.27(**C-17/18/20/21**) 62.18 (**C-17/18/20/21**), 36.70 (**C-25, 30**), 36.58 (**C-26, 29**), 34.27 (**C-13/41/46**), 29.28 (**C-13/41/46**), 28.01 (**C-35, 36, 37/53, 54, 55**), 27.91 (**C-35, 36, 37/53, 54, 55**), 17.63 (**C-43, 48**), 7.79 (**C-14, 15**)

IR (KBr cm^{-1}):

3314.16 (N-H), 1689.41 (C=O), 1620.33(C=O), 1245.41 (C-O), 1161.30 (C-O)

Compound 61

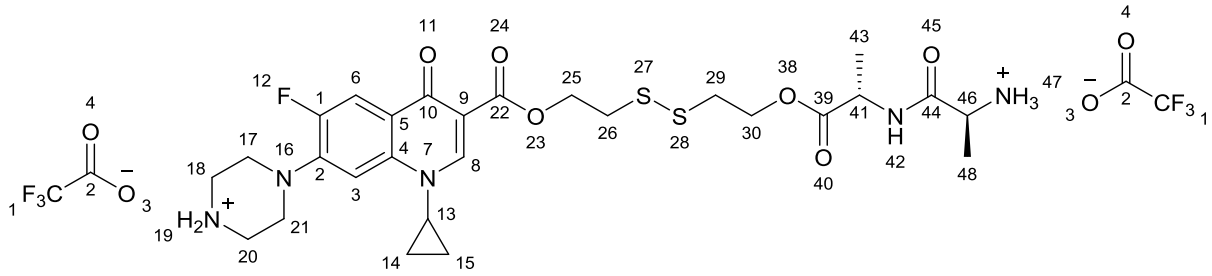

Chemical Formula: $C_{31}H_{38}F_7N_5O_{10}S_2$
Molecular Weight: 837.78 g mol^{-1}

Compound **60** (0.11 g, 0.14 mmol) was taken up in 20% TFA in dry DCM (10 mL) to give a yellow solution which was left stirring at room temperature for 23 hours. An orange solution was observed and this was concentrated under vacuum yielding a dark orange residue. The residue was taken up in ethanol (5 x 10 mL) and concentrated *in vacuo*, yielding a yellowish oil **61**.

Yield:

0.10 g, 87%

m/z (ESI):

305.61 ($[M]^{2+}$,100%)

HRMS (ESI):

Calc. for $C_{27}H_{38}FN_5O_6S_2$ $[M]^{2+}$ 305.6118, found 305.6110 (1.6 ppm mean error)

^{1}H NMR: (400 MHz, CD_3OD) δ_H (ppm):

8.70 (s, 1H, **H-8, CH**), 7.83 (d, $^3J_{H\text{-}F}$ = 13Hz, 1H, **H-6, CH**), 7.55 (d, $^3J_{H\text{-}F}$ = 6.9Hz, 1H, **H-3, CH**), 4.38-4.46 (m, 4H, **H-25, 30**), 3.98-4.02 (m, 1H, **H-41/46, CH**), 3.79 (m, 1H, **H-41/46, CH**), 3.69 (m, 1H, **cyclopropane, CH**), 3.60 (m, 4H**, piperazine, CH_2**), 3.51 (m, 4H, **piperazine, CH_2**), 2.82-3.02 (m, 4H, **H-26, 29, CH_2**), 1.54 (m, 3H, **H-43/48**, **CH_3**), 1.39-1.41 (m, 5H, **H-43/48, CH_3, cyclopropane, CH_2**), 1.18 (m, 2H, **cyclopropane, CH_2**)

^{13}C NMR: (100 MHz, CD_3OD) δ_c (ppm):

174.00 (**C-10**), 170.60 (**C-44**), 163.23 (**C-22, 39**), 154.22 (d, $^{1}J_{C,F}$ = 249 Hz, **C-1**), 148.03 (**C-8**), 144.13 (d, $^{2}J_{C,F}$ = 10 Hz, **C-2**), 137.58(**C-9**), 122.72 (d, $^{3}J_{c\text{-}F}$ = 6 Hz, **C-5**), 117.87 (d, $^{2}J_{C,F}$ = 23 Hz, **C-6**), 109.21 (**C-4**), 105.51 (d, $^{3}J_{C\text{-}F}$ = 3.0 Hz, **C-3**), 63.49(**C-17/18/20/21**) 59.21 (**C-17/18/20/21**), 49.02 (**C-25, 30**), 40.01 (**C-26, 29**), 38.04 (**C-13/41/46**), 36.20 (**C-13/41/46**), 16.50 (**C-43/48**), 15.88 (**C-43/48**), 7.43 (**C-14, 15**)

^{19}F NMR: (376 MHz, D_2O) δ_F (ppm):

-124.50 (dd, $J_{H\text{-}F}$ = 13.0, 8.0 Hz, **F-17**), -76.87 (**F-1**)

IR (KBr cm^{-1}):

3385.87 (N-H), 1667.57 (C=O), 1628.93(C=O), 1269.14 (C-O), 1198.95 (C-O), 1180.19 (C-O)

4.5. Biological procedures

4.5.1. Plate reader assay

In vivo assay of BW25113 strain of wild type (WT) E. *coli* was carried out using sterile techniques, three liquid cultures of BW25113 were inoculated in 5ml of lysogenic broth (LB) each at 37^{o}C overnight. 1 in 10 dilution of each culture was prepared in LB and normalised to OD_{650} = 2 with LB used as a blank.

A 96 well plate was prepared by adding sterile water (200 µl) into all perimeter wells to prevent evaporation, LB (198 µl) into blank wells (column 11), LB (193 µl) into all other wells except blank wells, antibiotic of specific concentrations (2 µl) into all wells (columns 2-10), specific normalised bacterial strain (5 µl) into all wells apart from water wells and blank columns, 0.1M acetic acid (2 µl) into blank wells and row B with 0 µM drug concentration. Row B was used as a control for all experiments with no conjugate or ciprofloxacin present, only normalised LB (a nutritionally rich medium) and 0.1M acetic acid, therefore measuring the OD_{650} of wild type E. coli BW25113.

The 96 well plate was placed into a BMG LabTech FLUOstar Omega plate reader and OD_{650} was measured every 30 minutes for 16 hours. The plate was shaken at 200RPm in between measurements to keep aerobic bacterial growth. Optical densities from blank wells was subtracted from sample wells to obtain normalised OD measurements which was used for data analysis. Growth curves were plotted with error bars calculated as ± standard deviation of the three biological replicates for each experiment.

4.5.2. Gyrase assay

In vitro assay of cip-diAla conjugate **38** was carried to test if the antibiotic was still active against DNA gyrase, a control experiment was performed using ciprofloxacin. E. coli gyrase supercoiling assay kit from Inspiralis was used to carry out the experiments.

1 U of DNA gyrase was prepared by diluting the stock of 5 U/µl DNA gyrase solution with the provided dilution buffer. Samples of diluted DNA gyrase (2 µl) with relaxed pBR322

open complex bacterial plasmid (0.5 µl), assay buffer (6 µl), desired antibiotic concentration (1 µl) and sterile water to make up the reaction volume of 30µl were incubated at 37^{o}C for 30 minutes. The conditions for each reaction are shown in **Table 5** below.

Sample	Antibiotic/ µl	Dulited gyrase/µl	Assay buffer/µl	pBR322/µl	Water/µl
Positive control	0	2	6	0.5	21.5
Negative control	0	0	6	0.5	23.5
Antibiotic assay	1	2	6	0.5	20.5

Table 5. Table showing the reaction conditions for each sample.

Chapter 5: Appendices

Appendix 1. ^{1}H NMR of protected Ala-Ala-ciprofloxacin 43

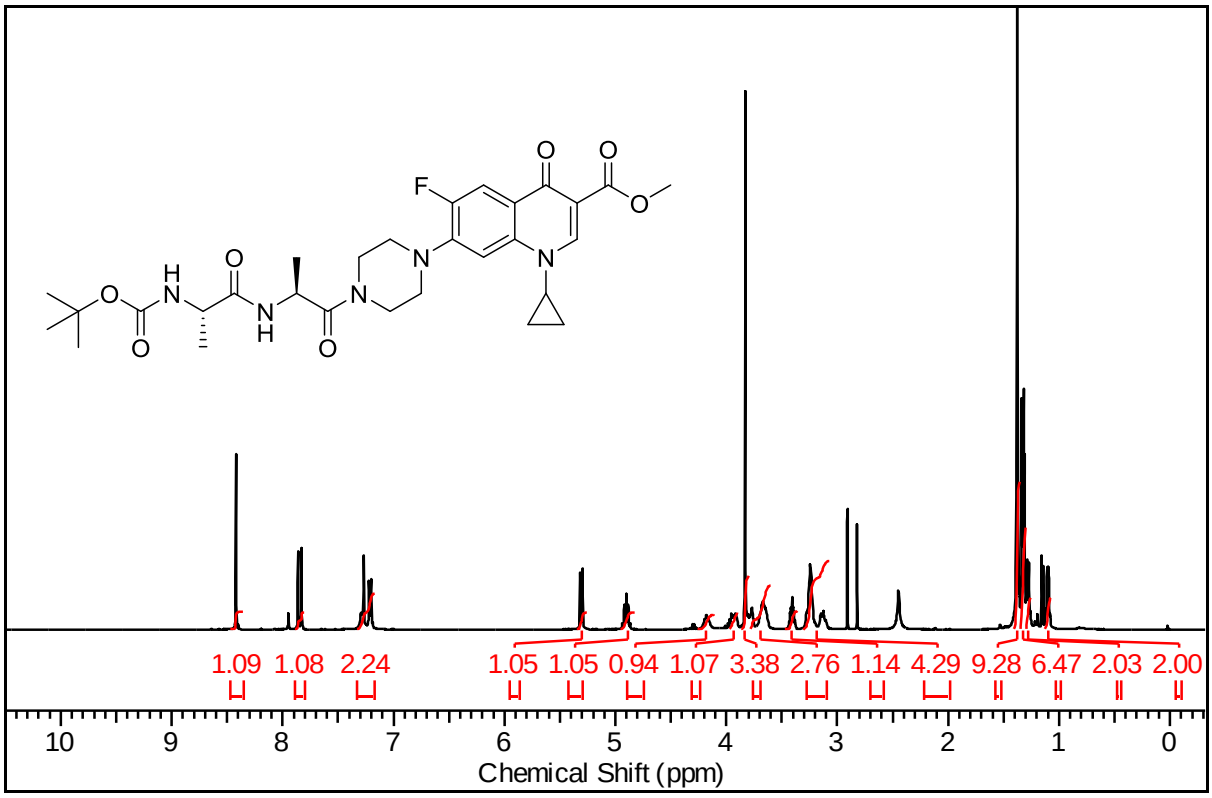

Appendix 2. ^{13}C NMR of protected Ala-Ala-ciprofloxacin 43

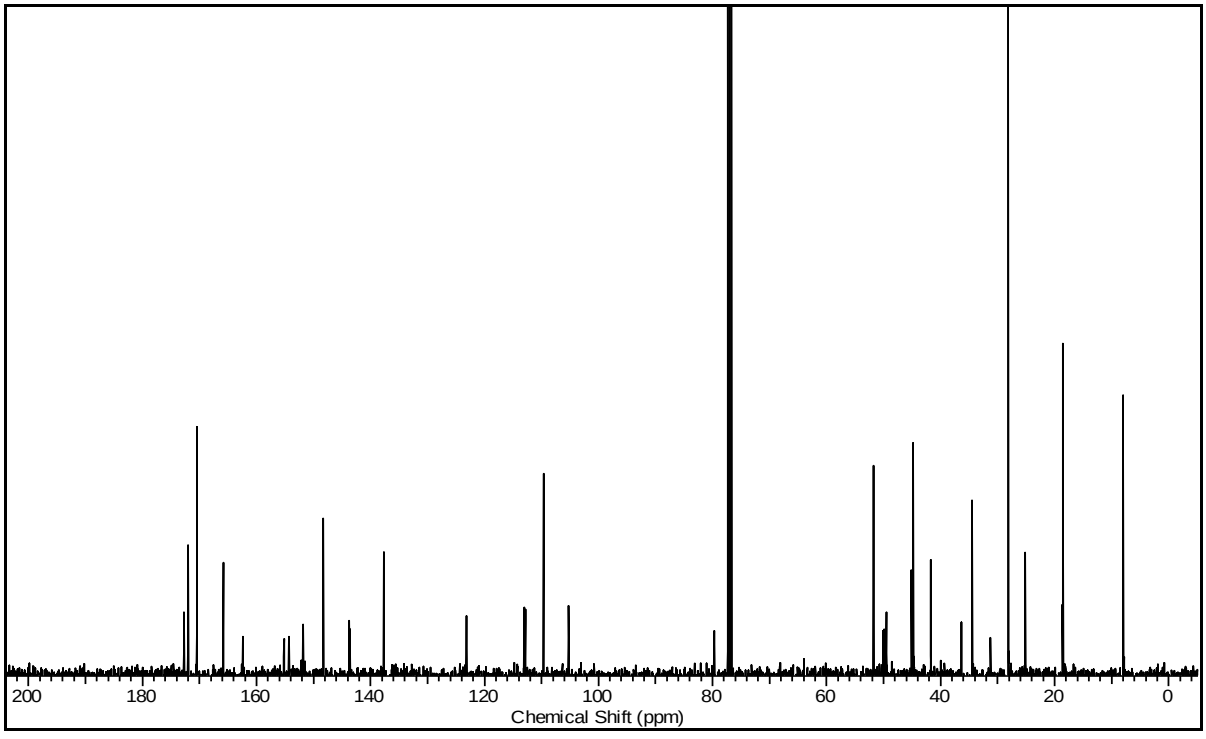

Appendix 3. ^{1}H NMR of protected ciprofloxacin-disulfide-Ala 57

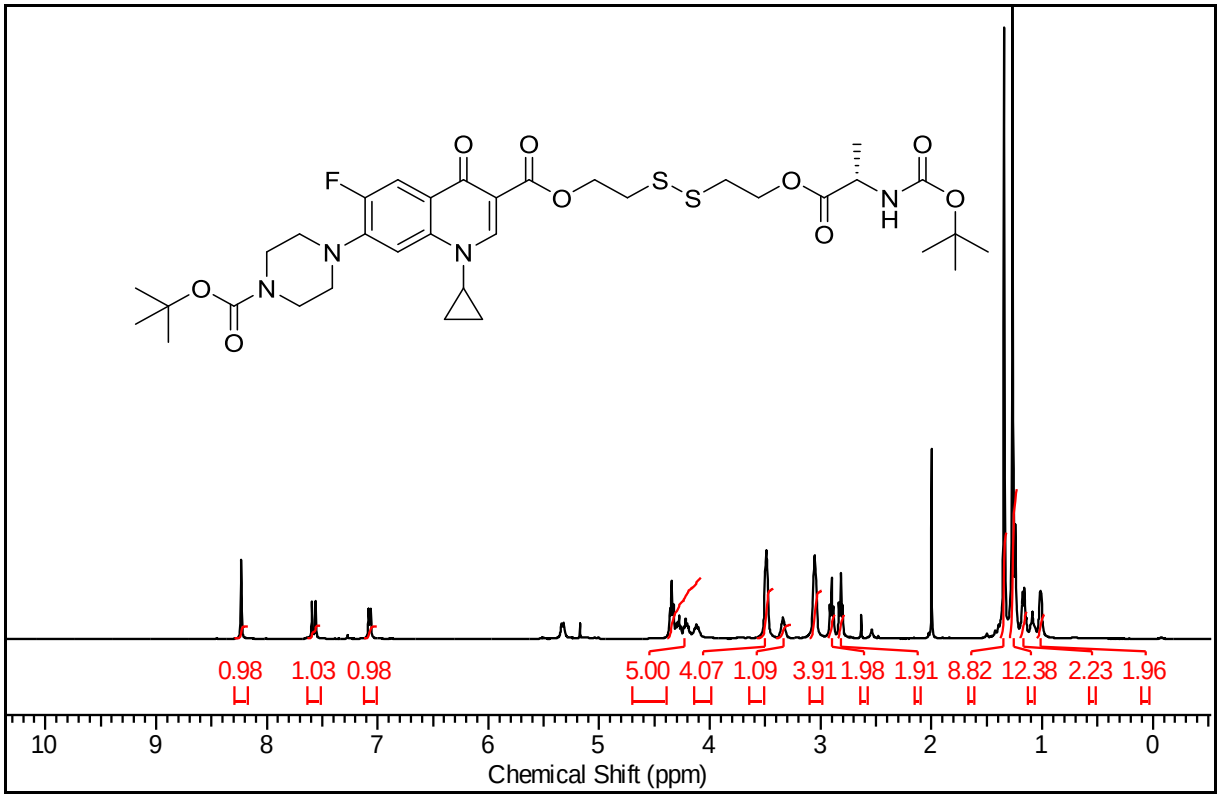

Appendix 4. ^{13}C NMR of protected ciprofloxacin-disulfide-Ala 57

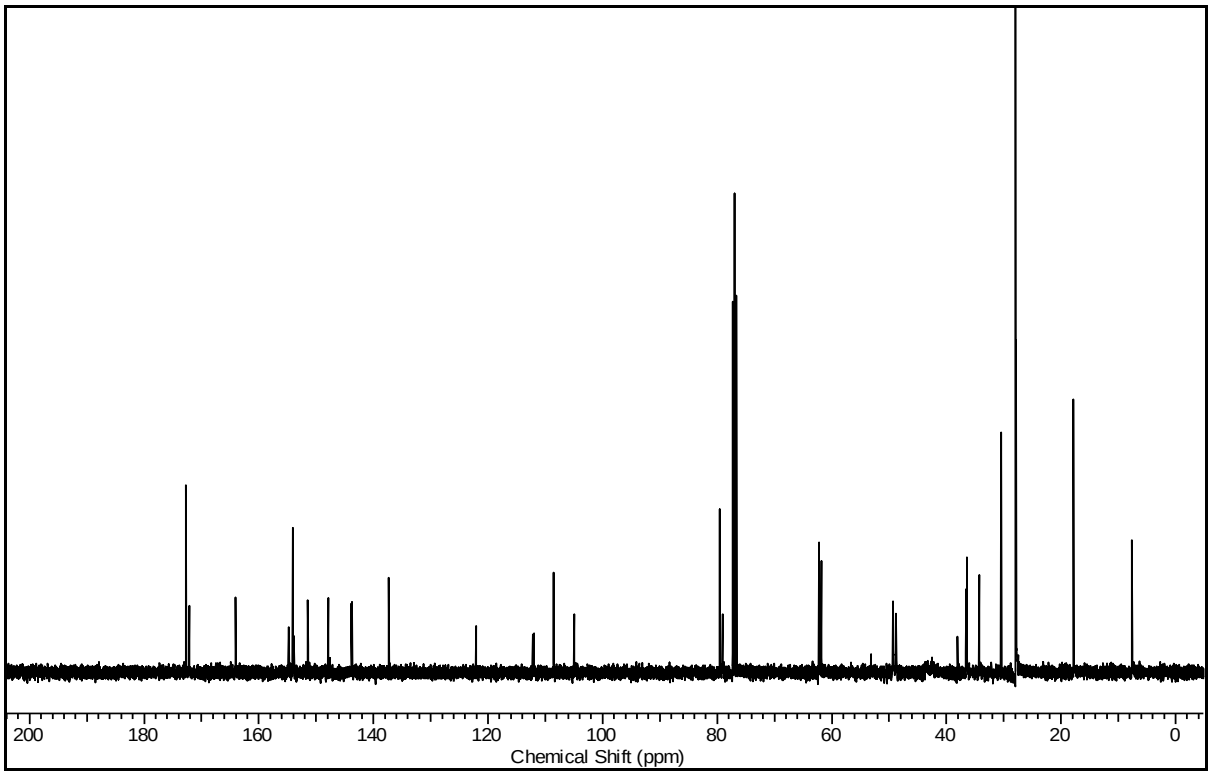

Appendix 5. ^{1}H NMR of ciprofloxacin-disulfide-Ala 39

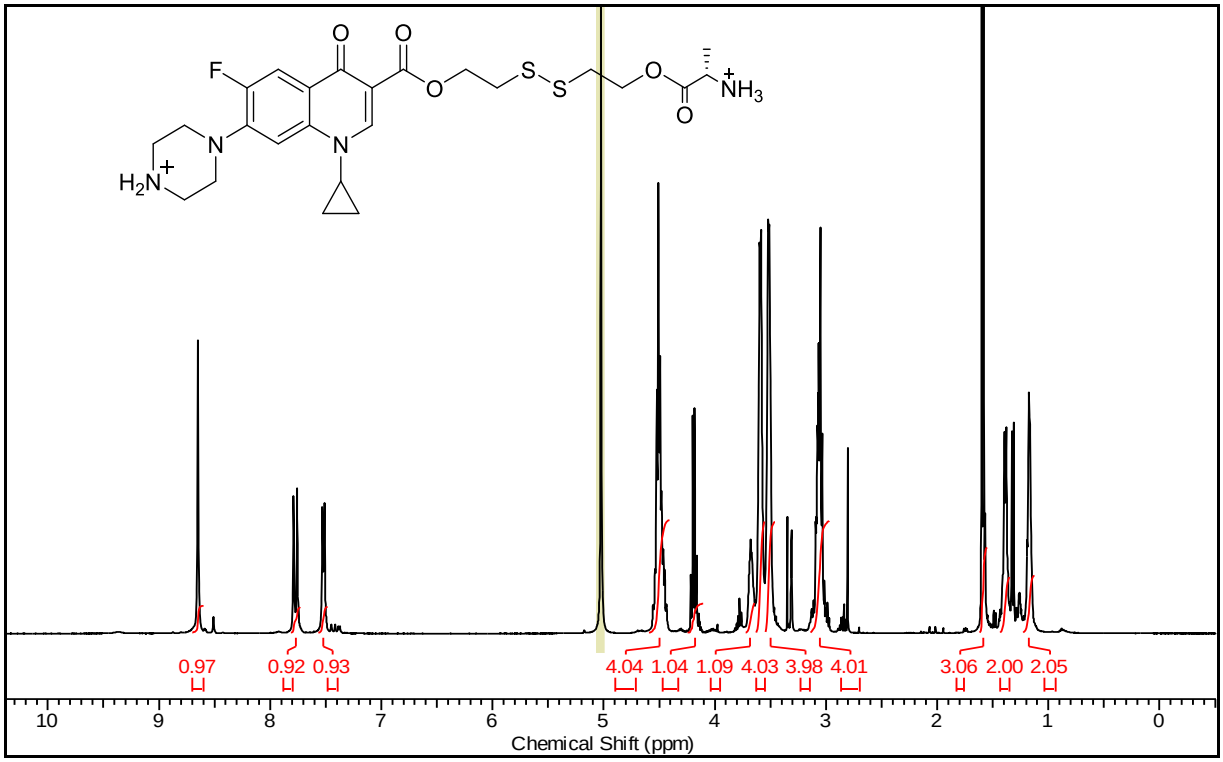

Appendix 6. ^{13}C NMR of ciprofloxacin-disulfide-Ala 39

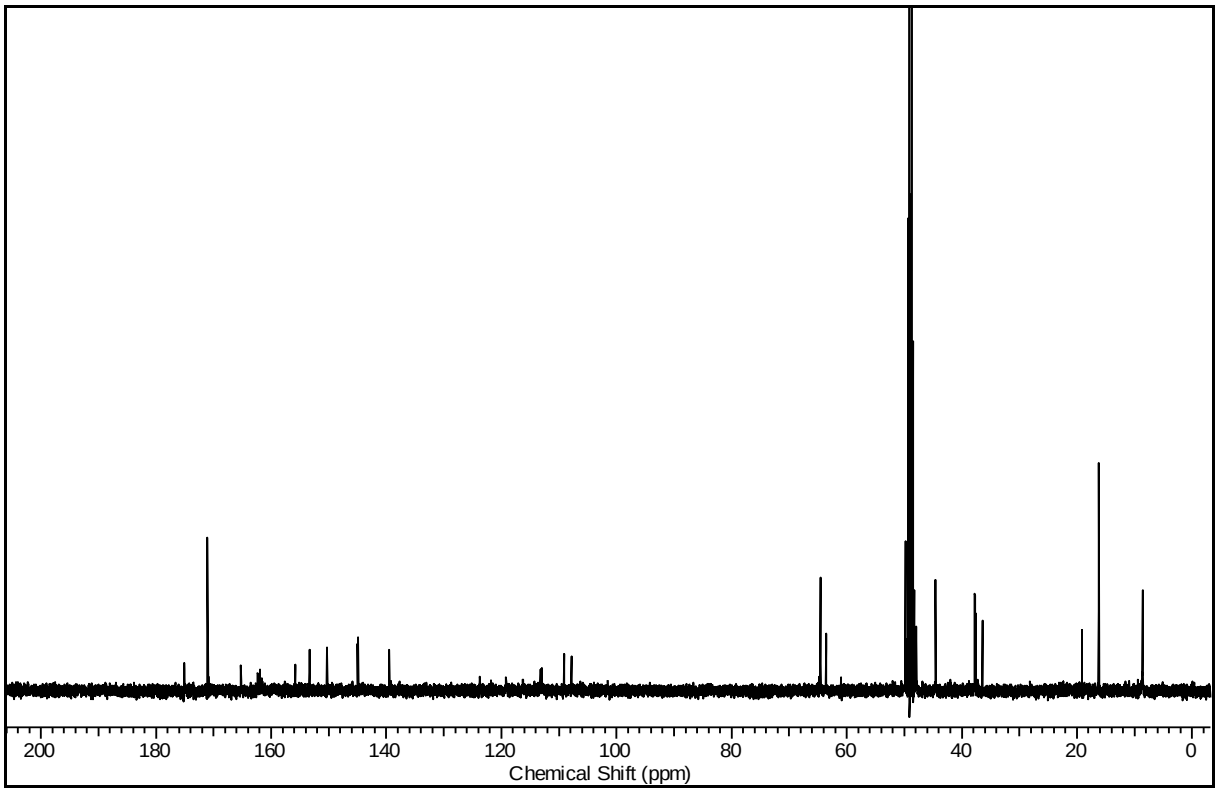

Appendix 7. ^{1}H NMR of protected ciprofloxacin-disulfide-Ala-Ala 60

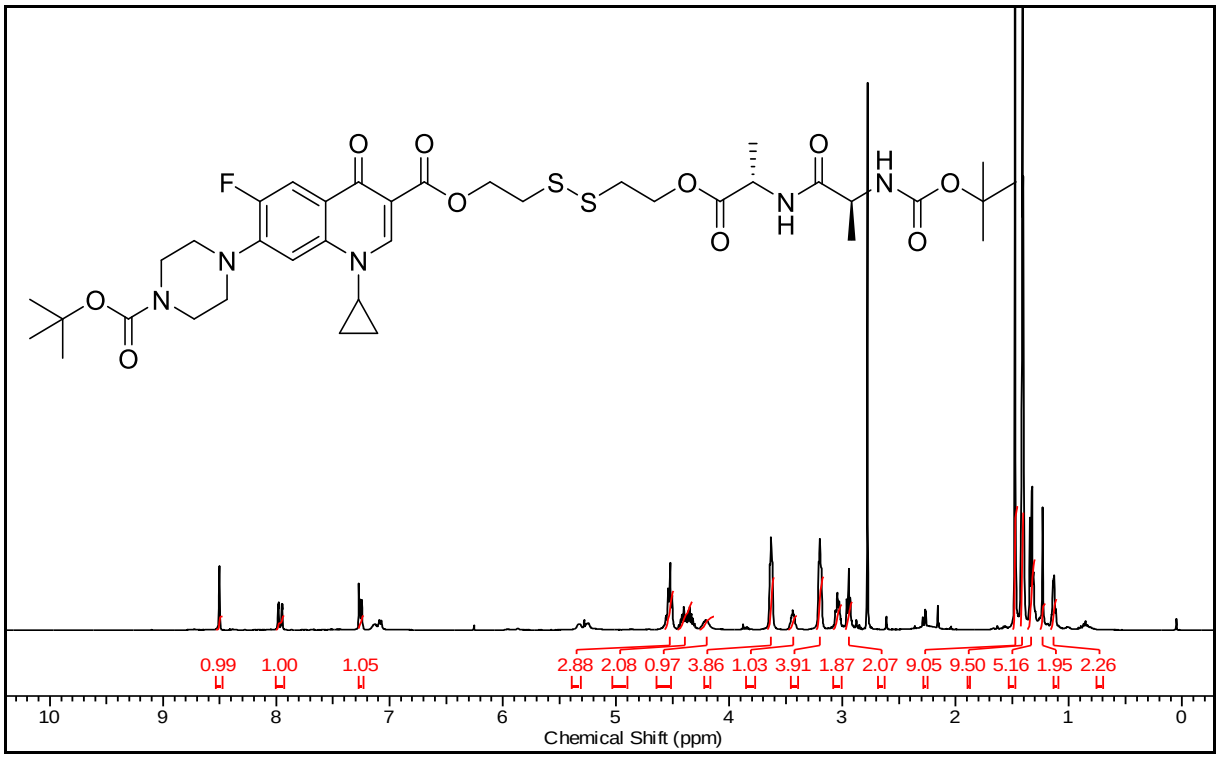

Appendix 8. ^{13}C NMR of protected ciprofloxacin-disulfide-Ala-Ala 60

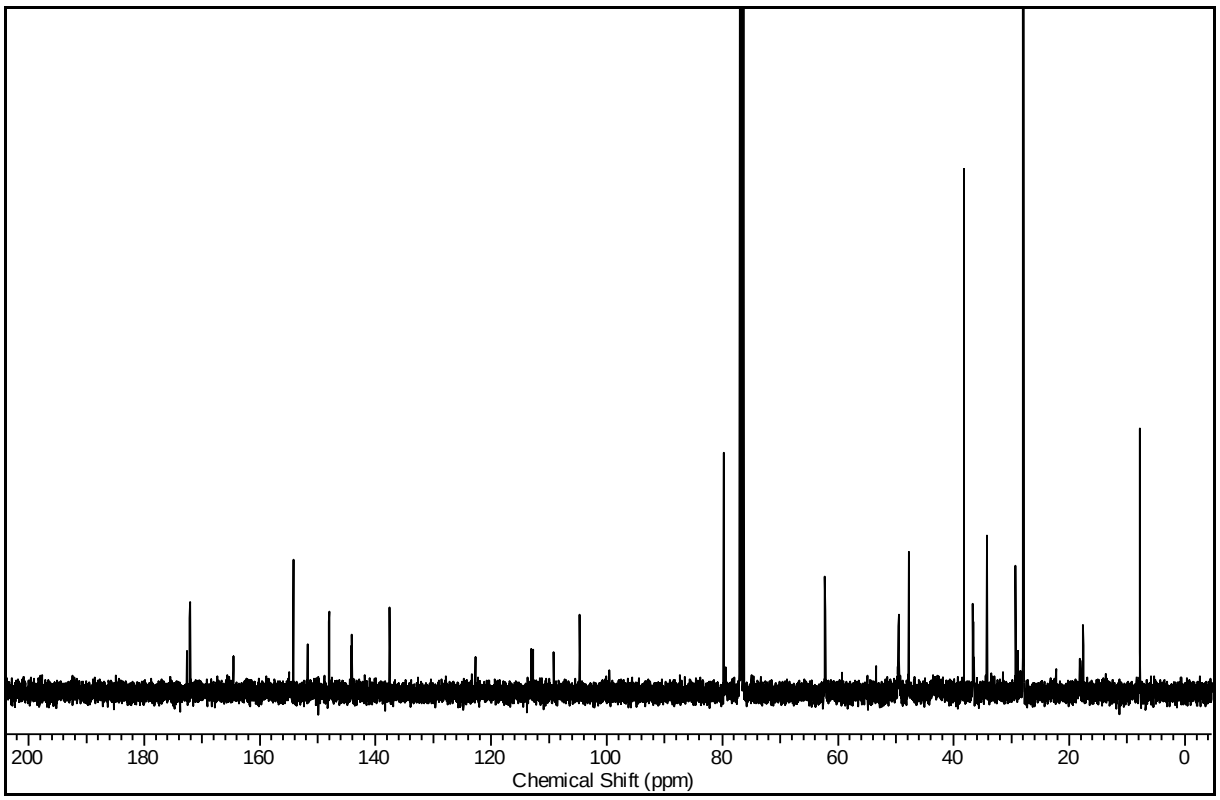

Appendix 9. ^{1}H NMR of ciprofloxacin-disulfide-Ala-Ala 40

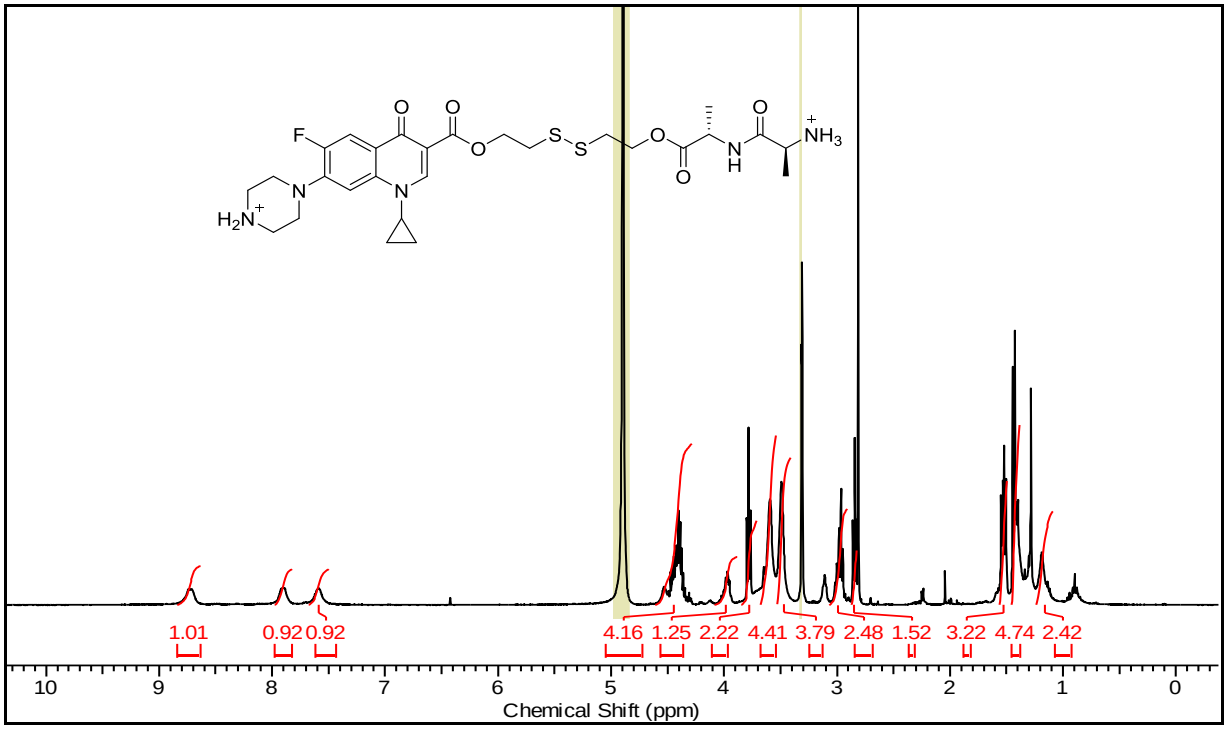

Appendix 10. ^{13}C NMR of ciprofloxacin-disulfide-Ala-Ala 40

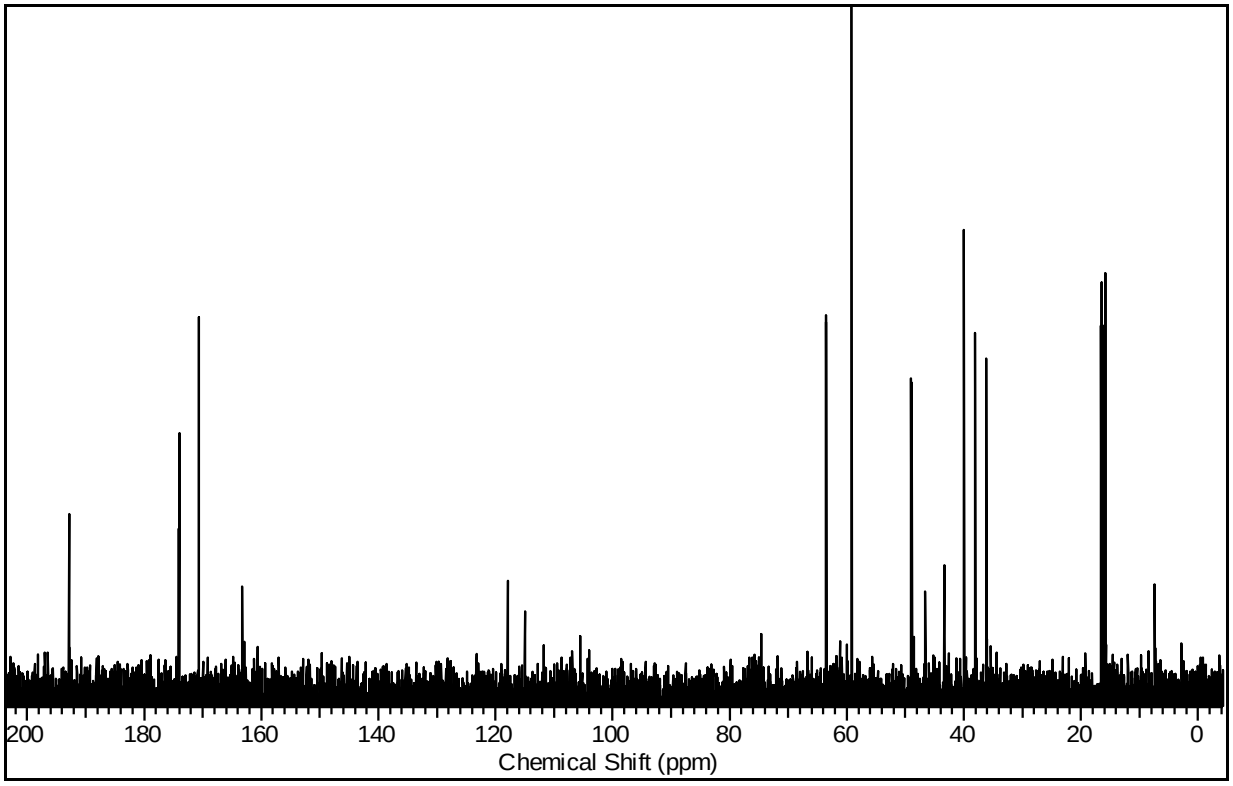

6. Glossary

Biological

ABC	ATP Binding Cassette
ADP	Adenosine Diphosphate
Ala	Alanine
Arg	Arginine
ATP	Adenosine Triphosphate
DNA	Deoxyribosenucleic acid
Glu	Glutamic acid
GSH	Glutathione
GSSG	Glutathione disulfide
LB	Lysogenic Broth
LPS	Lipopolysaccharide
Lys	Lysine
MDR	Multi-drug resistance
MFS	Major Facilitator Superfamily
MIC	Minimal Inhibitory Concentration
NADPH	Nicotinamide adenine dinucleotide phosphate
PBP	Penicillin Binding Protein
PepT	Peptide Transporter
$PepT_{st}$	Peptide Transporter from Shewanella aneidensis
$PepT_{so}$	Peptide Transporter from Streptococcus thermophiles
PEP-PTS	Phosphoenolpyruvate-dependent sugar phosphotransferase system
P^i	Inorganic phosphate
PTR / POT	Proton-dependent Oligopeptide Transporter
RNA	Ribonucleic acid

Chemistry

α	Alpha
β	Beta
Boc	tert-Butyloxycarbonyl
CD_3OD	Deuterated methanol
$CDCl_3$	Deuterated chloroform
$CHCl_3$	Chloroform
Cip	Ciprofloxacin
Conc	Concentration
Dan	Desferridanoxamine
D_2O	Deuterated water
DCC	N,N'-Dicyclohexylcarbodiimide
DCM	Dichloromethane
DIPEA	N,N'-Diisopropylethylamine
DMAP	4-Dimethylaminopyridine
DMF	Dimethylformamide
EDC.HCl	1-Ethyl-3-(3'-dimethylaminopropyl)carbodiimide hydrochloride
EtOAc	Ethyl acetate
H_2SO_4	Sulfuric acid
HATU	1-[Bis(dimethylamino)methylene]-1H-1,2,3-triazolo[4,5-b]pyridinium 3-oxid hexafluorophosphate
HBTU	N,N,N',N'-Tetramethyl-O-(1H-benzotriazol-1-yl)uronium hexafluorophosphate
HCl	Hydrochloric acid
$HOBt.H_2O$	N-Hydroxybenzotriazolee hydrate
Lor	Lorabid®
m.p.	Melting point
MeOH	Methanol
$MgSO_4$	Magnesium Sulphate
Na_2CO_3	Sodium Carbonate
$NaHCO_3$	Sodium Hydrogen Carbonate
NaOH	Sodium Hydroxide
NHS	N-Hydroxy Succinimide

NMR	Nuclear Magnetic Resonance
NO	Nitric Oxide
rt	Room Temperature
$SOCl_2$	Thionyl Chloride
TFA	Trifuoroacetic acid
Tri	Trisclosan
TLC	Thin Layer Chromatography
^{o}C	Degrees Centigrade
µM	Micromolar
cm^{-1}	Wavenumber
g	Grams
g mol^{-1}	Grams per mole
hrs	Hours
Hz	Hertz
mM	millimolar
M	Molar
mol	Moles

Spectroscopy

^{1}H	Proton
^{13}C	Carbon
^{19}F	Fluorine
Calc	Calculated
COSY	Correlation Spectroscopy
δ	Chemical Shift
d	doublet
DEPT	Distortionless Enhancement of Polarisation Transfer
ESI	Electronspray Ionisation
m	Multiplet
m/z	Mass to charge ratio
ppm	Parts per million
Rf	Retention factor
s	Singlet

References

1. S. R. Norrby, C. E. Nord and R. Finch, *Lancet Infect. Dis*. 2005, **5**, 115-119.
2. A. Kumar and H. P. Schweizer, *Adv. Drug. Deliv. Rev*. 2005, **57**, 1486-1513.
3. S. B. Levy and B. Marshall, *Nat. Med*. 2004.
4. P. A. Lambert, *Adv. Drug. Deliv. Rev*. 2005, **57**, 1471-1485.
5. G. De Pascale and G. D. Wright, *Chem. Biochem*. 2010, **11**, 1325-1334.
6. R. E. W. Hancock, *Trends in Microbiol*. 1997, **5**, 37-42.
7. E. Dé, A. Baslé, M. Jaquinod, N. Saint, M. Malléa and G. Molle, *Mol. Microbiol*. 2001, **41**, 189-198.
8. C. Hubschwerlen, J.-L. Specklin, D. K. Baeschlin, Y. Borer, S. Haefeli, C. Sigwalt, S. Schroeder and H. H. Locher, *Bioorg. Med. Chem. Lett*. 2003, **13**, 4229-4233.
9. U. Möllmann, L. Heinisch, A. Bauernfeind, T. Köhler and D. Ankel-Fuchs, *BioMetals*. 2009, **22**, 615-624.
10. G. Y. Lesher, E. J. Froelich, M. D. Gruett, J. H. Bailey and R. P. Brundage, *J. Med. Pharm. Chem*. 1962, **5**, 1063-1065.
11. L. A. Mitscher, *Chem. Rev*. 2005, **105**, 559-592.
12. R. A. Bonomo, *Clin. Microbiol. Newsl*, 1998, **20**, 197-201.
13. A. M. Emmerson and A. M. Jones, *J. Antimicrob. Chemother*. 2003, **51**, 13-20.
14. K. J. Aldred, R. J. Kerns and N. Osheroff, *Biochem*. 2014, **53**, 1565-1574.
15. K. E. Brighty and T. D. Gootz, *J. Antimicrob. Chemother*. 1997, **39**, 1-14.
16. H. J. L. Chen, K. J. Bloch and J. A. Maclean, *N. Engl. J. Med*. 2000, **342**, 359-360.
17. D. M. Barnes, A. C. Christesen, K. M. Engstrom, A. R. Haight, M. C. Hsu, E. C. Lee, M. J. Peterson, D. J. Plata, P. S. Raje, E. J. Stoner, J. S. Tedrow and S. Wagaw, *Org. Process Res. Dev*. 2006, **10**, 803-807.
18. H. Gmünder, K. Kuratli and W. Keck, *Nucleic Acids Res*. 1997, **25**, 604-611.
19. I. Laponogov, M. K. Sohi, D. A. Veselkov, X.-S. Pan, R. Sawhney, A. W. Thompson, K. E. McAuley, L. M. Fisher and M. R. Sanderson, *Nat. Struct. Mol. Biol*. 2009, **16**, 667-669.
20. L. L. Shen, L. A. Mitscher, P. N. Sharma, T. J. O'Donnell, D. W. T. Chu, C. S. Cooper, T. Rosen and A. G. Pernet, *Biochem*. 1989, **28**, 3886-3894.
21. X. Xiong, E. H. C. Bromley, P. Oelschlaeger, D. N. Woolfson and J. Spencer, *Nucleic Acids Res*. 2011, **39**, 3917-3927.
22. T. Guillard, E. Cambau, F. Chau, L. Massias, C. De Champs and B. Fantin, *Antimicrob. Agents Chemother*. 2013, **57**, 5830-5835.
23. G. A. Jacoby, *Clin. Infect. Dis*. 2005, **41**, S120-S126.
24. G. Benz, T. Schröder, J. Kurz, C. Wünsche, W. Karl, G. Steffens, J. Pfitzner and D. Schmidt, *Angew. Chem. Int. Ed. Engl*. 1982, **21**, 527-528.
25. L. Vértesy, W. Aretz, H. W. Fehlhaber and H. Kogler, *Helvetica Chimica. Acta*. 1995, **78**, 46-60.
26. H. Zahner, H. Diddens, W. Keller-Schierlein and H. U. Nageli, *Jpn. J. Antibiot*. 1977, **30 Suppl**, 201-206.
27. T. Zheng and E. M. Nolan, *J. Am. Chem. Soc*. 2014, **136**, 9677-9691.
28. T. A. Wencewicz, U. Möllmann, T. E. Long and M. J. Miller, *BioMetals*. 2009, **22**, 633-648.
29. S. J. Milner, C. T. Carrick, K. G. Kerr, A. M. Snelling, G. H. Thomas, A.-K. Duhme-Klair and A. Routledge, *Chem. Biochem*. 2014, **15**, 466-471.
30. F. Rivault, C. Liébert, A. Burger, F. Hoegy, M. A. Abdallah, I. J. Schalk and G. L. A. Mislin, *Bioorg. Med. Chem. Lett*. 2007, **17**, 640-644.
31. S. J. Milner, A. M. Snelling, K. G. Kerr, A. Abd-El-Aziz, G. H. Thomas, R. E. Hubbard, A. Routledge and A.-K. Duhme-Klair, *Bioorg. Med. Chem.* 2014, **22**, 4499-4505.
32. S. J. Milner, A. Seve, A. M. Snelling, G. H. Thomas, K. G. Kerr, A. Routledge and A.-K. Duhme-Klair, *Org. Biomol. Chem.* 2013, **11**, 3461-3468.
33. M. E. Jung, E. C. Yang, B. T. Vu, M. Kiankarimi, E. Spyrou and J. Kaunitz, *J. Med. Chem.* 1999, **42**, 3899-3909.

34. V. Zsoldos-Mády, P. Sohár, J. Kovács, I. Pintér and Z. Szakács, *J. Carbohyd. Chem.* 2005, **24**, 19-39.
35. H. Zheng, J. Taraska, A. J. Merz and T. Gonen, *J. Mol. Biol.* 2010, **396**, 593-601.
36. M. Cai, D. C. Williams, G. Wang, B. R. Lee, A. Peterkofsky and G. M. Clore, *J. Biol. Chem.* 2003, **278**, 25191-25206.
37. S. Agarwal, S. H. S. Boddu, R. Jain, S. Samanta, D. Pal and A. K. Mitra, *Int. J. Pharm.* 2008, **359**, 7-14.
38. G. N. Kumar, V. K. Jayanti, M. K. Johnson, J. Uchic, S. Thomas, R. D. Lee, B. A. Grabowski, H. L. Sham, D. J. Kempf and J. F. Denissen, *Pharm. Res.* 2004, **21**, 1622-1630.
39. S. Agarwal, D. Pal and A. K. Mitra, *Int. J. Pharm.* 2007, **339**, 139-147.
40. D. Foley, P. Bailey, M. Pieri and D. Meredith, *Org. Biomol. Chem.* 2009, **7**, 1064-1067.
41. C. F. Higgins, *Annu. Rev. Cell. Biol.* 1992, **8**, 67-113.
42. C. A. Guyer, D. G. Morgan and J. V. Staros, *J. Bacteriol.* 1986, **168**, 775-779.
43. N. Solcan, J. Kwok, P. W. Fowler, A. D. Cameron, D. Drew, S. Iwata and S. Newstead, *EMBO J*. 2012, **31**, 3411-3421.
44. F. Guettou, E. M. Quistgaard, M. Raba, P. Moberg, C. Löw and P. Nordlund, *Nat. Struct. Mol. Biol.* 2014, **21**, 728-731.
45. S. Newstead, D. Drew, A. D. Cameron, V. L. Postis, X. Xia, P. W. Fowler, J. C. Ingram, E. P. Carpenter, M. S. Sansom and M. J. McPherson, *EMBO J.* 2011, **30**, 417-426.
46. O. Boudker and G. Verdon, *Trends in Pharmacol. Sci.* 2010, **31**, 418-426.
47. M. Brandsch, *Curr. Opin. Pharmacol.* 2013, **13**, 881-887.
48. B. Baltzer, E. Binderup, W. V. Daehne, W. Godtfredsen, K. Hansen, B. Nielsen, H. Sorensen and S. Vangedal, *J. Antibiot.* 1980, **33**, 1183-1192.
49. M. H. Lee, Z. Yang, C. W. Lim, Y. H. Lee, S. Dongbang, C. Kang and J. S. Kim, *Chem. Rev.* 2013, **113**, 5071-5109.
50. K. V. S. Nemmani, S. V. Mali, N. Borhade, A. R. Pathan, M. Karwa, V. Pamidiboina, S. P. Senthilkumar, M. Gund, A. K. Jain, N. K. Mangu, N. P. Dubash, D. C. Desai, S. Sharma and A. Satyam, *Bioorg. Med. Chem. Lett.* 2009, **19**, 5297-5301.
51. M. H. Lee, J. Y. Kim, J. H. Han, S. Bhuniya, J. L. Sessler, C. Kang and J. S. Kim, *J. Am. Chem. Soc.* 2012, **134**, 12668-12674.
52. S. Ohlan, S. Nanda, D. P. Pathak and M. Jagia, *IJPSR*, 2011, **2**, 719-729.
53. A. K. Jain, M. G. Gund, D. C. Desai, N. Borhade, S. P. Senthilkumar, M. Dhiman, N. K. Mangu, S. V. Mali, N. P. Dubash, S. Halder and A. Satyam, *Bioorg. Chem.* 2013, **49**, 40-48.
54. H. S. Kim, W. Y. Song and H. J. Kim, *Org. Biomol. Chem.* 2015, **13**, 73-76.
55. W. H. Miller, M. A. Seefeld, K. A. Newlander, I. N. Uzinskas, W. J. Burgess, D. A. Heerding, C. C. K. Yuan, M. S. Head, D. J. Payne, S. F. Rittenhouse, T. D. Moore, S. C. Pearson, V. Berry, W. E. DeWolf, P. M. Keller, B. J. Polizzi, X. Qiu, C. A. Janson and W. F. Huffman, *J. Med. Chem.* 2002, **45**, 3246-3256.
56. N. Nakajima and Y. Ikada, *Bioconjugate Chem.* 1995, **6**, 123-130.
57. D. M. Shendage, R. Fröhlich and G. Haufe, *Org. Lett.* 2004, **6**, 3675-3678.
58. J. Cornish, K. E. Callon, C. Q.-X. Lin, C. L. Xiao, T. B. Mulvey, G. J. S. Cooper and I. R. Reid, *Am. J. Physiol. Endocrinol. Metab.* 1999, **277**, E779-E783.
59. V. V. Andrushchenko, H. J. Vogel and E. J. Prenner, *J. Pept. Sci.* 2007, **13**, 37-43.
60. H. Koga, A. Itoh, S. Murayama, S. Suzue and T. Irikura, *J. Med. Chem.* 1980, **23**, 1358-1363.
61. A. P. Rajput and R. P. Gore, *Der. Pharma. Chemica*. 2011, **3**.
62. C. A. G. N. Montalbetti and V. Falque, *Tetrahedron Lett*. 2005, **61**, 10827-10852.
63. R. Bruckner, *Advanced Organic Chemistry, Reaction Mechanisms*, Elsevier, 2002.
64. B. Neises and W. Steglich, *Angew. Chemie. Int. Ed. Engl.* 1978, **17**, 522-524.
65. D. Kakkar, A. K. Tiwari, J. Verma and A. K. Mishra, *Int. J. Chem. Kinet.* 2009, **41**, 349-356.
66. L. A. Carpino, *J. Am. Chem. Soc.* 1993, **115**, 4397-4398.
67. M. K. Dhaon, R. K. Olsen and K. Ramasamy, *J. Org. Chem*. 1982, **47**, 1962-1965.

68. A. P. Wiita, S. R. K. Ainavarapu, H. H. Huang and J. M. Fernandez, *Proc. Natl. Acad. Sci.* 2006, **103**, 7222-7227.